# JOURNAL OF THE Electrochemical Society

LIBRARY
UNIVERSITY OF UTAH
DEC 14 1950
SALT LAKE CITY

Vol. 97, No. 12 December, 1950

Engineering Library

*Published Monthly by*

THE ELECTROCHEMICAL SOCIETY

UMI

# Electrochemistry at Dow

## 2,190,000,000 KWH?

Yes, that's the total power consumed each year by the Dow magnesium cells shown above, the chlorine cells at Dow plants across the country, and the other electrochemical operations of The Dow Chemical Company.

Two billion, one hundred and ninety million kilowatt hours is a lot of power! In fact, this power would supply the approximate annual requirements of a city of one million people according to national averages. It demonstrates the magnitude of electrochemical operations at Dow.

Even more important than the size of Dow electrochemical operations are the research and development programs that lie behind them. These programs are responsible for the present Dow products, and from these programs will come new and better "Chemicals Indispensable to Industry and Agriculture."

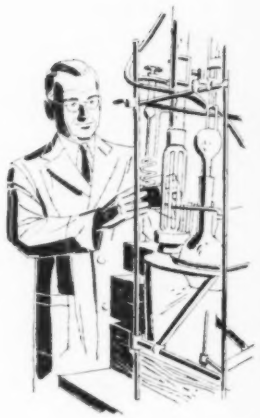

THE DOW CHEMICAL COMPANY
MIDLAND, MICHIGAN

**DOW**

**CHEMICALS**

INDISPENSABLE TO INDUSTRY
AND AGRICULTURE

UMI

The
pound
in the
other
tivate
structu
give o
acteris
surrou
from t
which
interac

The
earth
phates
are pa
matrix
fluores

EUROP

Hab
extens
ring s
ride c
charac
was d
earth
other
2CaO·
rescent
Pure e
in the
togeth
and a

In c
alkalin

[1] Ma
pared f
to 22, 1

UMI

# Some Rare Earth Activated Phosphors[1]

H. G. Jenkins and A. H. McKeag

*Communication from the Staff of the Research Laboratories of The General Electric Company, Limited, Wembley, England*

ABSTRACT

Two classes of rare earth activated phosphors having interesting and unusual properties are described. The first series, consisting of alkaline earth silicates activated by divalent europium, shows a wide range of fluorescent colors when excited by 3650 Å radiation. Some of these compounds are characterized by the stability of their fluorescence at comparatively high temperatures.

The second class of phosphors, consisting of alkaline earth pyrophosphates activated by dysprosium and samarium, has unusual phosphorescent characteristics when excited by cathode rays.

## Introduction

The spectral characteristics of rare earth compounds have been studied by various workers, both in the form of the pure salts or when dispersed in other matrices. The fluorescence spectra of such activated matrices frequently show narrow banded structures in contrast to most other phosphors which give only diffuse structureless bands which are characteristic not only of the activator but also of the surrounding matrix. The narrow banded spectra arise from transitions of the 4*f* (incomplete shell) electrons which are shielded by the completed outer shells from interactions with the crystal environment.

The present paper describes some interesting rare earth activated alkaline earth silicates and phosphates, some of which show diffuse spectra which are particularly sensitive to the nature of the crystal matrix, while one or two give almost monochromatic fluorescence and phosphorescence.

## Europium Activated Alkaline Earth Silicates

Haberlandt, Karlik, and Przibram (1) have studied extensively the fluorescence of both naturally occurring samples of fluorite and synthetic calcium fluoride containing europium. They showed that the characteristic blue-violet fluorescence of this mineral was due to extremely small quantities of this rare earth present in the divalent form. A number of other minerals such as potash feldspar and datolite $2CaO \cdot B_2O_3 \cdot 2SiO_2 \cdot H_2O$ also give a blue-violet fluorescent band which can be ascribed to $Eu^{++}$ ions (2). Pure europous chloride likewise gives a broad band in the blue-violet, closely similar to the fluorite band, together with a narrow band in the red at 6900 Å and a more diffuse band at 6300 Å (3).

In contrast to the above compounds, the range of alkaline earth silicates activated by europium (4), described in this paper, shows a wide variety of colors depending on the composition of the matrix and on the conditions of preparation.

Table I gives the fluorescent color under 3650 Å radiation of a number of europium activated alkaline earth silicates with different oxide-silica ratios and fired at different temperatures. The fluorescent brightness of the samples marked with an asterisk is comparable to that of zinc and zinc cadmium sulfide phosphors of similar color. The remainder might be described as of weak or moderate intensity. The color of the fluorescence is, in general, more saturated than that of the sulfides.

### *Preparation*

A very pure form of silica, obtained in the gelatinous form by the hydrolysis of redistilled silicon tetrachloride, is mixed with the appropriate alkaline earth carbonate or oxide to form a smooth paste. The europium is added to this as a solution of the chloride to give 0.1 per cent by weight in the fired powder. The paste is dried at 150°C and after thorough remixing the powder is fired for one hour in silica tubes in a slow stream of hydrogen at temperatures ranging from 800° to 1150°C.

### *Excitation and Emission Characteristics*

The phosphors in Table I are excited most strongly by long wavelength ultraviolet radiation (3650 Å) and show no perceptible afterglow. The brightness is considerably reduced when they are excited by short ultraviolet (2537 Å) but a feeble and, in some cases, persistent phosphorescence is then produced. Under 6000-volt cathode ray bombardment the fluorescent intensity is usually of the same order as under 2537 Å radiation.

It is evident from the results given in Table I that these luminescent materials are not characteristic of most rare earth activated compounds, in that a wide variety and range of colors is obtained by comparatively small changes in the lattice surroundings.

[1] Manuscript received April 17, 1950. This paper prepared for delivery before the Cleveland Meeting, April 19 to 22, 1950.

Neither do the spectra of these compounds reveal the narrow banded type of structure associated with many rare earth ions embedded in a foreign matrix.

Fig. 1 shows spectral energy curves of a number of the phosphors described in Table I. Curve A refers to the well-known synthetic fluorite and is included for comparison. It will be seen that although curves B and C give relatively narrow structureless bands similar to fluorite, curves D and E are much broader and extend further into the red. The latter curves clearly show the presence of at least two overlapping bands. The measurements suggest the presence of a series of common bands due to the $Eu^{++}$ ion modified in each case by the nature of the matrix, and some support for this is given by the similarity in color of a number of the samples.

TABLE I. *Fluorescence of Eu activated alkaline earth silicates excited by 3650 Å*

| Me | $MeO/SiO_2$ | Firing temperatures | | |
|---|---|---|---|---|
| | | 800°C | 1000°C | 1150°C |
| Ca | 3 | Green* | Yellow-green | Green |
| Ca | 2 | Green* | Yellow-green | Blue |
| Ca | 1½ | Green | Green | Blue |
| Ca | 1 | Blue | Blue | Blue* |
| Ca | ⅔ | Violet-blue* | Violet-blue | Blue |
| Ca | ½ | Violet-blue | Blue | Blue |
| Sr | 3 | Yellow* | Yellow | Yellow |
| Sr | 2 | Yellow | Yellow | Yellow |
| Sr | 1½ | Yellow | Violet | Violet |
| Sr | 1 | Yellow-green | Blue | Violet |
| Sr | ⅔ | Green-blue* | Violet | Violet |
| Sr | ½ | Green | Green | Green |
| Ba | 3 | Green | Green | Green |
| Ba | 2 | Green* | Green* | Green* |
| Ba | 1½ | Green* | Yellow | Yellow |
| Ba | 1 | Green | Blue | Green |
| Ba | ⅔ | Green | Blue* | Blue |
| Ba | ½ | Blue | Blue | Blue |

It may be assumed that the changes in color of fluorescence of different members are associated with structural changes in the basic material corresponding to the formation of either new chemical phases or polymorphic forms of the same compound. Complete x-ray diffraction evidence for this assumption is not available, but a general similarity to phase diagrams of the various systems lends support to the assumption.

### *Temperature Characteristics*

Some of the phosphors discussed exhibit quite unusual stability of fluorescence at high temperatures. Fig. 2 shows temperature response curves of typical europium activated silicates. Curves for ZnS (Cu) and ZnS (Ag) are included for comparison. Although there is a considerable variation in the temperature response characteristics within the various members of the group, certain phosphors, e.g., $2SrO \cdot 3SiO_2$ prepared at 900°C (curve A), show outstanding temperature stability. This phosphor continues to fluoresce even at temperatures as high as 500°C. The technical importance of this type of material for color correction of light sources which operate at a high temperature is unfortunately nullified by the extreme rarity of europium compounds.

A comprehensive study of the three systems (Ca, Sr, and Ba) is made difficult for the same reason since this would involve the preparation of a large number of samples prepared at different temperatures with varying proportions of the component oxides. Mixed silicates of two or more alkaline earth

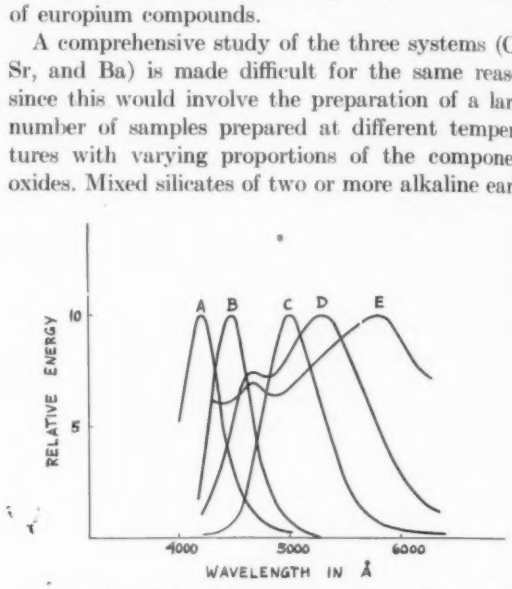


FIG. 1. Spectral energy curves of europium activated alkaline earth compounds.
A. $CaF_2$ (1100°C)
B. $1CaO \cdot 2SiO_2$ (900°C)
C. $2BaO \cdot 1SiO_2$ (900°C)
D. $3SrO \cdot 1SiO_2$ (1100°C)
E. $1SrO \cdot 3SiO_2$ (900°C)

elements have not been investigated extensively, but certain compounds, e.g., $1SrO \cdot 1BaO \cdot 1SiO_2$ · (0.1% Eu), fired at 900°C give phosphors which are strongly excited by 3650 Å radiation.

### Dysprosium Activated Alkaline Earth Pyrophosphate Phosphors

An interesting example of a rare earth activated phosphor having pronounced phosphorescence is $Ca_2P_2O_7$ (Dy) (5) which, although not appreciably excited by ultraviolet radiation, exhibits strong fluorescence and phosphorescence under cathode rays and x-rays. Unlike the compounds discussed above, the luminescence is characteristic of the $Dy^{+++}$ ion.

If the calcium in this compound is replaced by strontium and barium, the general characteristics of the phosphors remain unchanged but the phosphorescence progressively decreases. If the dysprosium is replaced by samarium the characteristic $Sm^{+++}$ spectrum results, as do the same general luminescent characteristics (6). The phosphors described in this

paper are, therefore, of interest in extending the range of known phosphors having long persistence of afterglow excited by cathode rays. A brief note on the preparation of $Ca_2P_2O_7$ (Dy) phosphors is given below, before discussing their main characteristics. The preparation of the other members follows similar lines.

### *Preparation*

A very pure form of calcium pyrophosphate, $Ca_2P_2O_7$, may be prepared by conventional chemical methods either by heating calcium hydrogen phosphate ($CaHPO_4$) or by firing together in the required proportions calcium carbonate and diammonium hydrogen phosphate. Pure dysprosium oxide is added before heating in an amount calculated to give about 0.1 per cent by weight in the final product. The mixture is heated to a temperature of 1080°C for periods of the order of one hour depending on

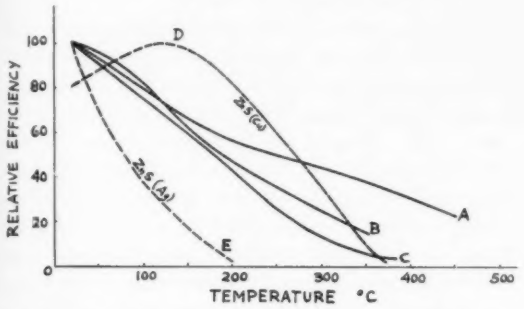


FIG. 2. Temperature response curves of europium activated silicates compared with ZnS (Cu) and ZnS (Ag).

A. $2SrO \cdot 3SiO_2$ (900°C)
B. $1SrO \cdot 3SiO_2$ (900°C)
C. $1SrO \cdot 1BaO \cdot 1SiO_2$ (900°C)
D. ZnS (Cu)
E. ZnS (Ag)

the mass of material. To achieve the optimum phosphorescence experience has shown that it is important to pay attention to the following points:

1. The exact composition of the pyrophosphate base material is important. A range of compositions centering on the stoichiometric ratio $2CaO \cdot 1P_2O_5$ shows that a slight excess or deficiency of calcium oxide leads to a diminution in intensity of afterglow.

2. The temperature and duration of firing is important and indicates that a certain degree of sintering must be reached, but not exceeded.

3. The presence of a small amount of certain other rare earths in the dysprosium oxide, notably terbium, produces a diminution in luminescence.

X-ray diffraction photographs indicate that the pure calcium pyrophosphate gives the best results. Both samarium and dysprosium give phosphors with similar characteristics, the former giving an orange luminescence and the latter a pale yellow color.

### *Excitation and Emission Characteristics*

As already mentioned, the phosphors are strongly excited by 6000-volt cathode rays and show little or no response to short ultraviolet radiation and only a weak fluorescence under long ultraviolet, with no perceptible afterglow; both fluorescence and phosphorescence are strongly excited by relatively soft x-rays. Fig. 3 is a spectrum photograph of the fluorescence of $Ca_2P_2O_7$ (Dy) excited by 6000-volt cathode rays and clearly shows the strong narrow band in the yellow (Fig. 3*a*). With longer exposures of the plate, the well-defined structure in the faint blue band and an additional weak band in the red can be observed (Fig. 3*b*). The characteristics of this

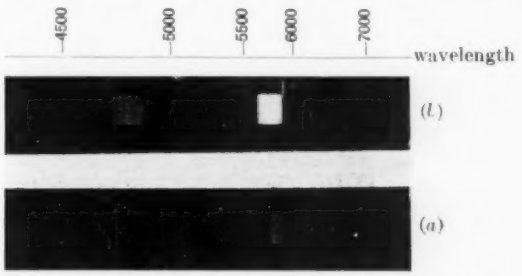


FIG. 3. Spectrum photograph of the fluorescence of $Ca_2P_2O_7$ (Dy) excited by 6000-volt cathode rays. (*a*) Spectrum photograph of $Ca_2P_2O_7$ (Dy)—30 min exposure; (*b*) spectrum photograph of $Ca_2P_2O_7$ (Dy)—60 min exposure.

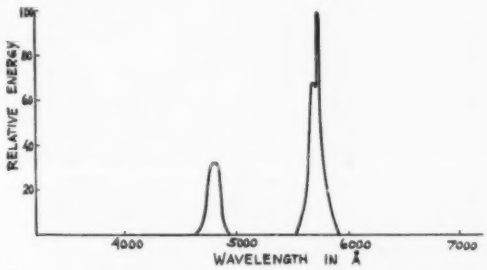


FIG. 4. Approximate spectral energy curve of $Ca_2P_2O_7$ (Dy).

spectrum resemble closely those described by Deutschbein and Tomaschek (7) for $Dy(NO_3)_3$ dissolved in water, and by Gobrecht (8) for dysprosium salts dispersed in a borax bead. It seems probable, therefore, that the three main bands are characteristic of the $Dy^{+++}$ ion. Fig. 4 shows an approximate spectral energy curve of the fluorescent radiation. The spectral characteristic of the phosphorescence is almost the same as that of the fluorescence. The emission of the samarium activated material also shows fine structure in the orange-red.

The unusual decay characteristics after cathode ray excitation of the dysprosium activated phosphor which have found considerable use in certain radar applications are evident from Fig. 5. Although starting at a much lower initial brightness than the yellow

copper activated zinc-cadmium sulfide phosphor (88% ZnS, 12% CdS by weight), the dysprosium activated phosphor is appreciably brighter after one second and thereafter continues to decay at a much slower rate. This property renders the material particularly suitable for normal oscillographic applications where a persistent trace is needed. The shape of the curve does not conform to a simple power law relationship but is probably a combination of an exponential and a logarithmic component. The color of the light emitted shows no appreciable change during the decay indicating that the three band systems, shown in Fig. 3, occur during phosphorescence.

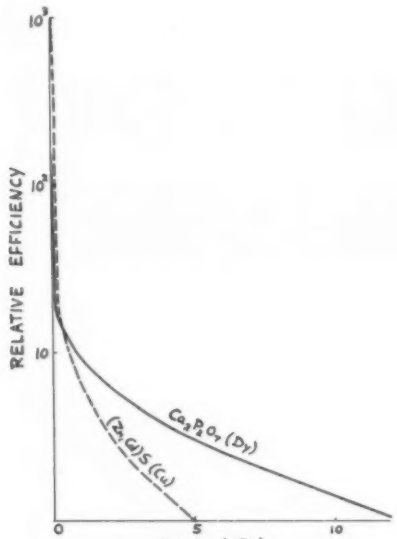


FIG. 5. Decay characteristic of $Ca_2P_2O_7$ (Dy) compared with (Zn,Cd)S(Cu) (cathode ray excitation).

## DISCUSSION

Discrete absorption and emission spectra of rare earth compounds arise from electronic transitions involving rearrangements of the 4*f* electrons (incomplete shell) which are shielded from external field effects by the completed 5*s* and 5*p* shells. An electron from the 4*f* shell can, however, be activated into the outer shells with certain rare earths ($Ce^{+++}$, $Yb^{+++}$) and diffuse absorption spectra are then obtained (9). Divalent europium salts show similar diffuse absorption spectra at wavelengths less than 4480 Å and it is believed that in the activated state an electron is raised "across" the closed shells into the outer shells (10).

The fluorescence of europium ($Eu^{++}$) salts has also been found to consist mainly of a strong broad diffuse band in the blue-violet region of the spectrum. The europium activated phosphors described support previous results and show in addition that the color of the fluorescence can be made to vary over almost the complete visible spectrum by varying the composition of the matrix. The influence of the surrounding lattice on the emission of the $Eu^{++}$ atoms is obviously much greater than for most other rare earths. There is some evidence to suggest the existence of a system of discrete bands common to the various alkaline earth silicates investigated although these are profoundly modified by changes in the nature of the matrix.

The comparative insensitivity of certain of the alkaline earth silicate compounds to temperature is somewhat surprising since it might reasonably be expected that good temperature stability would be associated with a protected transition, as in the case of luminescent ruby ($Al_2O_3$:Cr).

The second class of phosphors described are of interest because of the unusual phosphorescence characteristics shown under cathode ray excitation and of the fine structure exhibited by the fluorescent spectra. The shape of the decay curve does not conform to a simple law but suggests that an exponential process, due to metastable activator states, may exist in combination with the formation of "trapping states" in the crystal lattice. The formation of both these conditions seems to be dependent on certain critical factors in the preparation of the phosphors such as composition and firing conditions.

Any discussion of this paper will appear in a Discussion Section, to be published in the June 1951 issue of the JOURNAL.

## REFERENCES

1. H. HABERLANDT, B. KARLIK, AND K. PRZIBRAM, *Sitzber. Akad. Wiss. Wien Math.-naturw. Klasse, Abt. IIa*, **143,** 151 (1934).
2. H. HABERLANDT AND A. KÖHLER, *Naturwissenschaften*, **27,** 257 (1939).
3. K. PRZIBRAM, *Nature*, **135,** 100 (1935).
4. A. H. MCKEAG AND P. W. RANBY, British Pat. 544,160, Aug. 27, 1940.
5. H. G. JENKINS, A. H. MCKEAG, AND P. W. RANBY, British Pat. 582,122, April 10, 1941.
6. A. H. MCKEAG AND P. W. RANBY, British Pat. 578,272, June 17, 1942.
7. O. DEUTSCHBEIN AND R. TOMASCHEK, *Ann. Physik*, **29,** 311 (1937).
8. H. GOBRECHT, *Ann. Physik*, **31,** 181 (1938).
9. S. FREED, *Phys. Rev.*, **38,** 2122 (1938).
10. S. FREED AND S. KATCOFF, *Physica*, **14,** 17 (1948).

# Refining of Magnesium by Vaporization at Extremely Low Pressure[1]

R. R. Rogers and G. E. Viens

*Division of Mineral Dressing and Process Metallurgy, Mines Branch, Department of Mines and Technical Surveys Ottawa, Canada*

ABSTRACT

The experiments described indicate that magnesium alloy scrap may be refined by vaporization of the magnesium at pressures less than 0.05 micron. The refined metal contains no manganese and only small traces of aluminum, silicon, copper, and iron. The zinc is vaporized also, but the zinc content of the refined magnesium is substantially lower than that of the original charge.

## Introduction

As the use of magnesium alloys increases, the tonnage of scrap metal of this type doubtless will increase. Scrap of known composition, such as that from fabricating processes, machine shops, and foundries, can be blended with new metal or melted and cast into ingots which may not be greatly different from ingots of new metal. Grinding and blasting dust and sand, if present in appreciable quantities, make the recovery of this type of scrap difficult. Obviously, metals such as aluminum, copper, brass, bronze, and plated parts must be absent (4). Accordingly, a process in which some or all of the alloying metals are removed from the magnesium may prove to be the simplest and cheapest method of recovery. The presence in the scrap of grinding and blasting dust, sand, and metals such as those mentioned above might not be particularly inconvenient in such a process. It is possible that the data presented in this paper will contribute to the development of such a process.

Work described in this paper was carried out to investigate the possibility of refining magnesium alloys by vaporization at an extremely low pressure. It was hoped that, in this way, a contribution to the knowledge of both magnesium metallurgy and the increasingly important field of metal vaporization might be made. In 1929 Bakken (1) described a process which was primarily for the purpose of refining magnesium produced by electrolysis. The pressure used was in the range 150 to 500 microns. Van Arkel (7) mentioned the subject, but he apparently was interested only in pressures as low as 10 microns in the case of magnesium. During World War II one plant of the German I. G. Farbenindustrie refined aluminum scrap by a process which included volatilizing certain of the impurities in an atmosphere of hydrogen at a pressure of 2 mm (2). In 1944 Pidgeon (5) discussed a new process for the manufacture of magnesium which involved vaporization of the metal at a pressure in the order of 50 to 150 microns and a temperature of 1100° to 1200°C. It is understood that a pressure somewhat below 50 microns is used at present in this process. In 1945 Kroll (3) published an excellent general article on the melting and vaporization of metals in "vacuum." Practically all reference was to pressures of one micron or higher, although many of his statements doubtlessly would apply to the lower pressures. In 1947 Stauffer (6) reported using a pressure of 25 microns and a temperature of 1100°C in the experiments in which he produced a lithium-magnesium alloy from spodumene.

In view of the fact that the pressure immediately above an evaporating metal is very difficult to determine, it may be assumed that the above values were of residual pressure within the retort and did not include the vapor pressure of the vaporized metal. Residual pressures of less than 0.05 micron and temperatures between 400° and 750°C were used in the experiments which are described in the present paper.

The more common magnesium alloys contain up to about 10 per cent aluminum, 3 per cent zinc, and 1.5 per cent manganese. Since the zinc content of a number of these alloys is well below 1 per cent, the actual zinc content of any given batch of scrap probably would be much less than 3 per cent. With this in mind it was decided to use samples of the standard AZ63x and AZ61x alloys in the first experiments which are described in this paper. The compositions of these alloys are given in Table I. The aluminum and zinc contents were determined chemically and the others spectrographically.

As it was found, in the first experiments, that the refined magnesium always contained a certain amount of zinc, it was thought that the separation of the constituents of these magnesium-zinc alloys

[1] Manuscript received February 6, 1950. This paper prepared for delivery before the Cleveland Meeting, April 19 to 22, 1950. Published by permission of the Director-General of Scientific Services, Department of Mines and Technical Surveys, Ottawa, Canada.

by evaporation at a still lower temperature might be feasible. An alloy containing 90 per cent of commercially pure magnesium and 10 per cent of commercially pure zinc was made up in the laboratory for use in this part of the investigation.

TABLE I. *Compositions of original alloys*

| Alloy | Element, % | | | | | |
|---|---|---|---|---|---|---|
| | Al | Zn | Mn | Si | Fe | Cu |
| AZ63x | 5.93 | 2.98 | 0.28 | 0.009 | <0.001 | 0.004 |
| AZ61x | 5.98 | 0.95 | 0.34 | 0.011 | <0.001 | 0.005 |

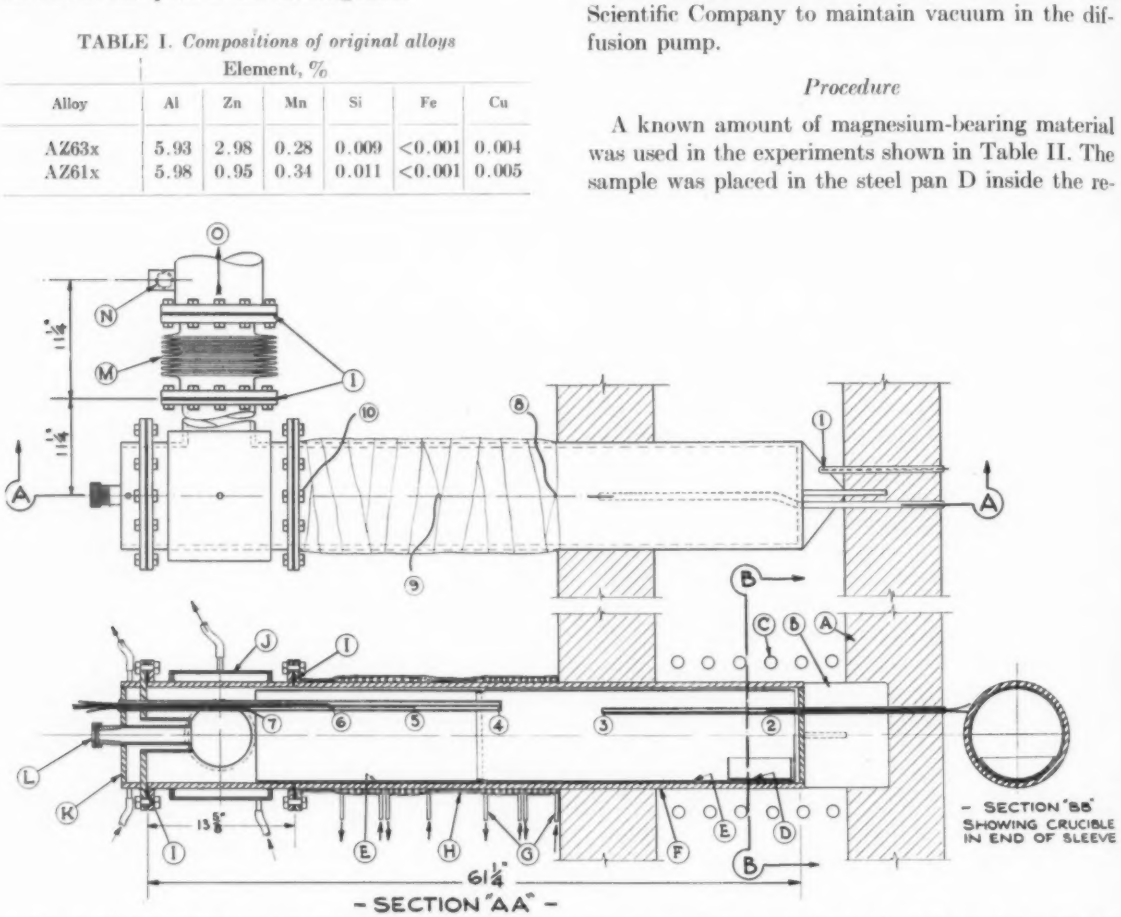


FIG. 1. Unit for refining metals by low pressure distillation. A - furnace wall, B - support for hot end of retort, C - Globars, D - steel pan for charge, E - sheet steel sleeves, F - low carbon steel retort, 10 in. OD, G - copper coils for cooling with water, H - asbestos wrapping, I - gaskets, J - chamber for water-cooling T section, K - water-cooled retort head, L - sight glass, M - flexible connector, N - Philips ionization pressure gauge tube (the accompanying indicator has the two scales, 0 to 25 microns and 0 to 0.2 micron), O - to pumps, 1 - thermocouple in the interior of the furnace, 2 to 7, inclusive—thermocouples in the interior of the retort, 8 to 10 inclusive—thermocouples on the external surface of the cold end of the retort. All temperatures and pressures were recorded on Minneapolis-Honeywell Electronik strip chart potentiometers.

## EXPERIMENTAL

### *Equipment*

The equipment used in all of these experiments consisted of a retort of low carbon steel 61¼ inches (155 cm) long and 9¼ inches (23.5 cm) inside diameter. One end of the retort was placed in a Globar-heated furnace and the other end was connected to a pumping system. The details of the retort drawn to scale are given in Fig. 1. The pumping system included an MC-500 vertical metal diffusion pump manufactured by Distillation Products, Inc., a VSD 5-5-6 mechanical pump manufactured by the Kinney Manufacturing Company to produce the primary vacuum in the system, and a No. 1403 auxiliary mechanical pump manufactured by the W. M. Welch Scientific Company to maintain vacuum in the diffusion pump.

### *Procedure*

A known amount of magnesium-bearing material was used in the experiments shown in Table II. The sample was placed in the steel pan D inside the retort and then the head K was bolted tightly to the end of the retort. After the air had been pumped out down to a pressure of about 0.05 micron, the retort was filled with sufficient argon to bring the pressure back to that of the atmosphere. A rapid flow of cooling water was passed through the copper coil G which was nearest to the head of the retort. The power was turned on in the Globar furnace and the retort was heated until pan D and its contents were at the desired temperature, as indicated by means of thermocouple 2. Slow heating was continued, without per-

mitting the temperature of the pan to change materially from the desired value, until the temperatures indicated by means of thermocouples 3 to 10 had become stationary. During this heating period the pressure of the argon was maintained at approximately that of the atmosphere. When constant temperatures were reached in the various parts of the retort the argon was pumped out until a pressure of approximately 0.01 micron was indicated at gauge N. Metal vaporized from pan D and condensed inside sleeves E and elsewhere in the cold end of the furnace. After maintaining these conditions for a

contents of the residues in Experiments I, II, and IV also are included in the table.

It will be noted that the aluminum content of the residues from Experiments I, II, and IV was very high. In Experiment III a large part of the charge was not volatilized and in Experiment V almost none was volatilized.

Early in the experiments, before the sight glass became covered with condensed metal, the actual metal vapors could be observed. It was noted that the rate of vaporization was much greater at 735°C than at the lower temperatures.

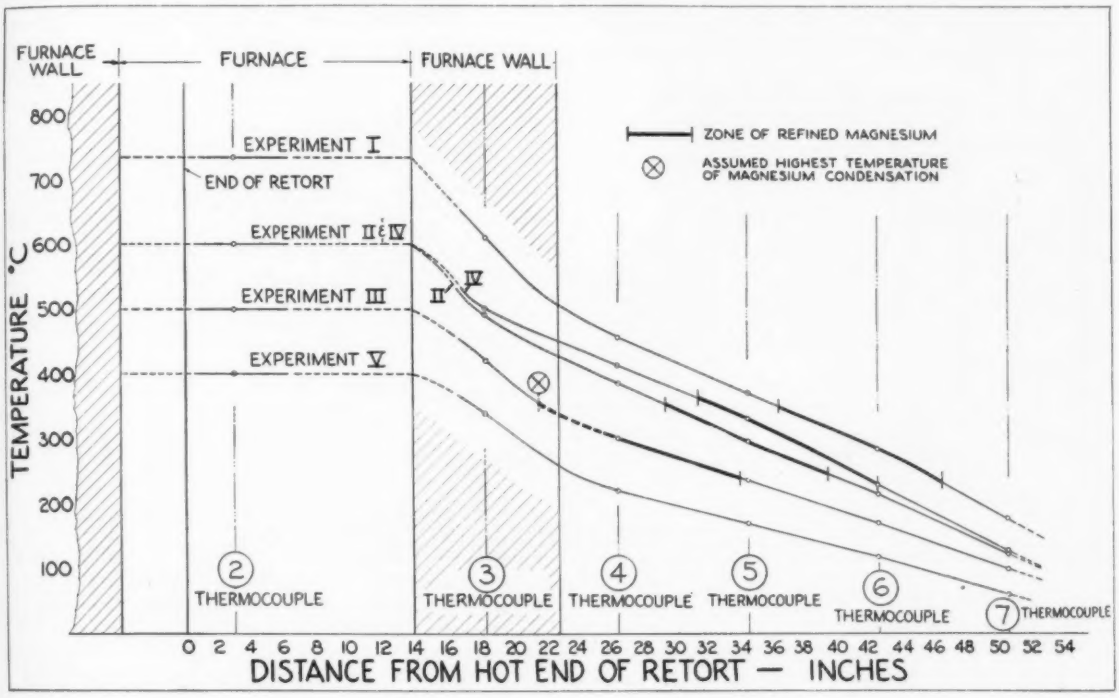


FIG. 2. Interior retort temperatures

determined time the power was turned off. The retort was filled with argon and its temperature was allowed to decrease until it had almost reached that of the laboratory before the head was removed and the results of the experiment examined.

*Results*

The temperatures at the different points in the two thermocouple tubes are shown for each experiment in Fig. 2. The temperatures at different points on the sleeves may be estimated by comparing those inside the thermocouple tubes with those on the exterior of the retort. The latter are given in Fig. 3. The weight of metal in pan D before and after each experiment is given in Table II. The aluminum

Spectrographic examination of the metals which had condensed in the sleeves in Experiments I to IV showed only faint traces of aluminum, iron, copper and silicon, and manganese was absent entirely. The metals consisted substantially of magnesium and zinc in different ratios. The values of the ratio $\frac{\text{magnesium}}{\text{zinc}}$ (by weight) for typical samples from different parts of the sleeves are given in Table III. Where the ratio in the case of the product exceeded the ratio in the case of the original alloy (either AZ63x or AZ61x), then the magnesium was refined with respect to zinc.

In Experiments I to IV the metal had condensed in two fairly well-defined zones, both on the colder of the two thermocouple tubes and on the sleeves.

The metal in the zone nearer to the hot end of the retort was fairly bright and coarse grained, and that in the zone farther from the hot end was dull and comparatively fine grained. By far the greater proportion of the metal condensed was in the first of these two zones.

The ratio $\frac{\text{magnesium}}{\text{zinc}}$ was much higher in the metal in the hotter zone than it was in the original standard alloys. In other words, the metal in this zone had been refined with respect to zinc. The metal in the colder zone had a much lower ratio than did the original alloys.

The maximum and minimum temperatures at which refined magnesium was condensed on the colder thermocouple tube in the various experiments are shown in Fig. 2. It will be noted that in all cases these maximum and minimum temperatures were in the neighborhood of 360° and 240°C, respectively. Although it was impossible to determine the temperature range in which refined magnesium condensed on the sleeves it is suspected that it was fairly similar to that in the case of the thermocouple tube.

In the AZ63x alloy the ratio was found to have increased from 30 to as much as 103. In other words, the zinc content was decreased from about 3 per cent to about 1 per cent. If more samples had been analyzed it is possible that an even greater degree of refinement would have been noted.

In the AZ61x alloy the ratio was found to have increased from 97 to as much as 1615, indicating a decrease in zinc content from about 1 per cent to well below 0.1 per cent.

It will be noted in Table III that the refined magnesium at the top of the sleeve tended to be

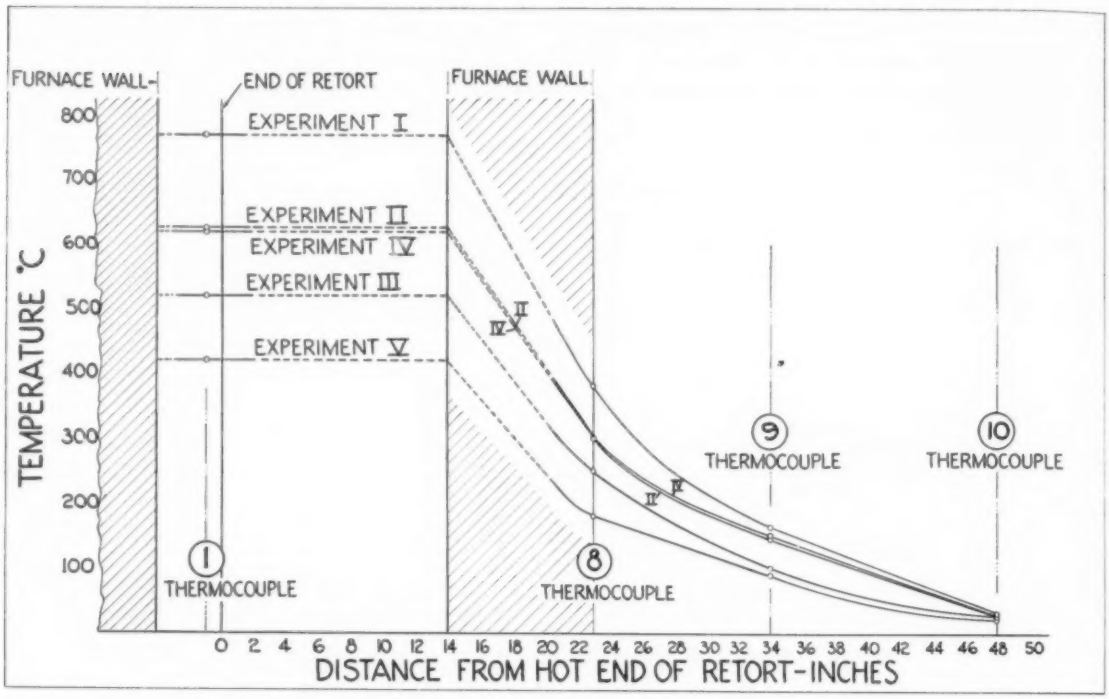


FIG. 3. Exterior retort temperatures

TABLE II. *Changes in weight and composition of original metal during experiments*

| Expt. No. | Material, charged | Time at low pressure, min | Temperature of test °C | Wt of charge in pan, g | | Calculated orig. wt of aluminum in pan, g | Aluminum content, % | |
|---|---|---|---|---|---|---|---|---|
| | | | | Original | Final | | Original alloy | Residue |
| I | AZ63x | 250 | 735 | 582.5 | 35.6 | 34.5 | 5.93 | 96.8 |
| II | AZ63x | 303 | 600 | 524.5 | 39.0 | 31.1 | 5.93 | 88.4 |
| III | AZ63x | 315 | 500 | 555.5 | 325.0 | 32.9 | 5.93 | |
| IV | AZ61x | 312 | 600 | 637.5 | 54.0 | 38.1 | 5.98 | 89.9 |
| V | 90% Mg 10% Zn | 323 | 400 | 631.5 | 627.5 | none | none | none |

considerably more highly refined than that at the bottom of the sleeve. Also, the small crystalline trees, which were observed only in Experiment IV, were more highly refined than the metal to which they were attached.

By far the greatest degree of refinement was found in the magnesium which condensed at the highest temperature in Experiment IV.

### *Safety Precautions*

Considerable care was used in opening the retort after each experiment in view of the fact that magnesium is quite active chemically and there was a possibility that at least part of the product might have been in very finely divided form. The cold retort was evacuated to remove the argon and then air was permitted to enter it slowly. This procedure was repeated until there was no evidence of oxygen being absorbed inside the retort. Then the retort was filled with argon again and the head was removed while argon continued to enter through the side tube. The head was immediately placed in a large metal trough which had been filled with argon. The two sleeves E, with their films of condensed metal, were removed from the retort and deposited in the trough. Finally the pan D was removed and placed in the trough. Only after it definitely had been ascertained that no danger existed were the various parts examined in order to obtain the results of the experiment.

TABLE III. *Typical values of ratio* $\frac{magnesium}{zinc}$ *by weight*

| Expt. No. | Original alloy | Ratio in original charge* | Ratio in condensed metal | | | | | | | |
|---|---|---|---|---|---|---|---|---|---|---|
| | | | In hot sleeve | | In colder sleeve | | | | Cold end of retort | Side arm |
| | | | Cold end | | Hot end | | Middle | Cold end | | |
| I | AZ63x | 30 | 103 (top) | — | 86 (top)<br>45 (bottom) | — | 8 (top)<br>9 (bottom) | 8 (top)<br>8 (bottom) | 7 | — |
| II | AZ63x | 30 | 83 | — | 15 | — | 8 | — | 10 | 8 |
| III | AZ63x | 30 | 87 | 28 | 7 | — | — | — | — | — |
| IV | AZ61x | 97 | 1615 | 475 (top)<br>99 (bottom)<br>770 (trees) | 108 | 61<br>78 (trees) | — | — | — | — |

* Ratios higher than these values indicate refinement of the magnesium with respect to zinc.
*Note:* Ratios of 1000, 200, 100, and 10 are approximately equivalent to 0.1, 0.5, 1.0, and 10% of zinc, respectively.

## Discussion and Conclusions

A considerable number of conclusions may be reached on the basis of the above experimental results. Perhaps the one of most immediate practical value is that it should be possible to refine magnesium alloy scrap by volatilization under extremely low pressures such as those used in these experiments. Metals such as aluminum and manganese may be removed from the magnesium practically quantitatively. It is probable that other metals such as silicon, copper, and iron may be removed equally well, although these metals were not fully investigated in the experiments. Although zinc was not completely eliminated from the magnesium, a considerable amount of refinement took place with regard to that metal. A higher degree of refinement probably could be obtained by using a retort of somewhat different design.

It would appear that heating the scrap at a temperature much lower than 600°C would give unsatisfactory results. At temperatures above this value the rate of the refining process is much greater and the final aluminum content of the residue is considerably higher.

At the pressures used in these experiments it is not feasible to volatilize magnesium containing about 10 per cent zinc at a temperature as low as 400°C.

The magnesium which underwent refinement with respect to zinc was condensed at temperatures between about 240° and 360°C.

It is hoped that the operating data and the information regarding equipment which have been included in this paper will be of service to others who are or may become interested in the volatilization of metals at extremely low pressures.

## Acknowledgments

The writers wish to express their appreciation to Mr. R. J. Traill, Chief of the Division of Mineral

Dressing and Process Metallurgy at the Mines Branch, for his interest in this research. Thanks also are due for the cooperation which was received from the Chemical and Spectrographic Sections of the Mines Branch. The excellent work of the Mechanical Section in constructing and maintaining the experimental equipment was particularly noteworthy.

Any discussion of this paper will appear in a Discussion Section, to be published in the June 1951 issue of the JOURNAL.

## REFERENCES

1. H. E. BAKKEN, *Chem. & Met. Eng.*, **36**, 345 (1929).
2. I. E. C. Report, "Scrapped Scrappers," *Ind. Eng. Chem.*, **40**, 16A (January 1948).
3. W. J. KROLL, *Trans. Electrochem. Soc.*, **87**, 571 (1945).
4. C. E. NELSON, *Am. Inst. Mining Met. Engrs. Metals Technol., Tech. Pub.* 1642 (October 1943).
5. L. M. PIDGEON, *Trans. Can. Inst. Mining Met.*, **47**, 16 (1944).
6. R. A. STAUFFER, *Am. Inst. Mining Met. Engrs. Metals Technol., Tech. Pub.* 2268 (September 1947).
7. A. E. VAN ARKEL, "Reine Metalle," Edwards Bros., Inc., Ann Arbor, Mich. (1943).

# The Relative Reliability of Aluminum and Zinc Starting Sheets for the Electrodeposition of Zinc[1,2]

GLEN C. WARE AND KENNETH B. HIGBIE

*Bureau of Mines, U. S. Department of the Interior, Albany, Oregon*

ABSTRACT

Zinc sheet from three different sources and aluminum sheet have been compared to determine their relative reliability as starting-sheet material for the electrodeposition of zinc from acid solutions. The aluminum sheet was used with edge strips, as required by present commercial practice, and without edge strips. The materials were tested in electrolytes with a wide range of impurity contents. Average residence period was used as the measure of reliability.

## INTRODUCTION

The use of zinc starting sheets for the electrodeposition of zinc met discouraging failures early in the development of processes to produce zinc electrolytically, and subsequently the position of aluminum has not been challenged seriously, despite obvious advantages to be gained if zinc could be used. Ralston (1) has shown that if solution-level corrosion were controlled by a protective coating on the cathode at the solution level, the residence periods of zinc cathodes could be prolonged to three to five times the duration of aluminum cathodes under the same conditions. Earlier work at this laboratory (2) developed a design of starting sheet that eliminated solution-level corrosion by completely immersing the cathode, except for a shank that protruded above the electrolyte to make contact with the conductor bar. This shank was of such dimensions that normal solution-level corrosion did not seriously impair its functions. The general corrosion of the cathode surface was mitigated by using zinc sheet of high purity and by highly purifying the solution that was fed to the cell. Application of these refinements led to the development of cathodes up to 2.6 inches (6.7 cm) thick after residence periods as long as 39 days. Owing to the special conditions employed, this work did not compare zinc starting sheets directly with aluminum under the same conditions. For this reason, the work reported herein was undertaken to determine the relative length of residence and the thickness of the deposit to be expected from aluminum and zinc starting sheets operating in the same cell.

[1] Manuscript received March 1, 1950. This paper prepared for delivery before the Buffalo Meeting, October 11 to 13, 1950.

[2] Published by permission of the Director, Bureau of Mines, U. S. Department of the Interior. Not subject to copyright.

## EXPERIMENTAL

### *Materials*

Soft, annealed, aluminum sheet was compared with Horse Head Special strip zinc from the New Jersey Zinc Sales Company, zinc sheet rolled at the Albany station, and zinc sheet stripped from aluminum cathodes. All three types of zinc were four-nines grade. The aluminum sheet was used both with and without edge strips. Calcined zinc concentrates and zinc dust were obtained from the Electrolytic Zinc Plant of the Sullivan Mining Company at Kellogg, Idaho. Acid losses were made up with C. P. sulfuric acid.

Stock solutions for these tests were prepared by leaching calcined zinc concentrates with return electrolyte from the cells. Manganese dioxide or potassium permanganate was used to oxidize the ferrous iron leached from the calcine. The manganese dioxide was always added to the leach before the slurry was neutralized. The potassium permanganate was added sometimes to the neutral leach and sometimes to the filtered leach solution. It oxidized manganese as well as iron to an insoluble oxide. All stock solutions were given four zinc-dust treatments subsequent to oxidation. It has been observed that, when solutions of high purity are fed to the cell, the quality of the deposit cannot be predicted accurately from the analysis of the feed. Since the oxidation treatment to precipitate manganese and iron may also remove other undetected contamination, it is given in Table I along with the impurity analysis.

### *Apparatus*

A cell with three cathodes and four anodes was used for all tests. It was put into operation with electrolyte made by combining stock solution with sulfuric acid and water to bring its composition to 50 grams of zinc and 112 grams of acid per liter. The anodes were made of a lead alloy containing 1

per cent silver. They were spaced 2.25 inches (5.7 cm) apart on centers. The rectangular glass cell vessel was fitted with a siphon overflow which caused the height of the solution level to fluctuate. The cathodes were 5.75 inches (14.6 cm) wide, and were immersed an average of 6 inches (15.24 cm). An air lift was installed to recycle return electrolyte at the rate of 13 liters per hour to simulate the rate of flow of solution in commercial cells. The cathode current density was 30 amperes per square foot (3.23 amp/dm²). Feed solution was supplied at the rate required to maintain the zinc content of the electrolyte at about 50 grams and the acid content at about 112 grams per liter. An ammeter was placed in the circuit of each cathode, and the ampere hours of operation for each were calculated from time and current readings. The sum for the three cathodes was checked by an ampere-hour meter. This meter was checked against a copper coulometer and found to agree within ½ per cent. Fig. 1 shows the cell in operation.

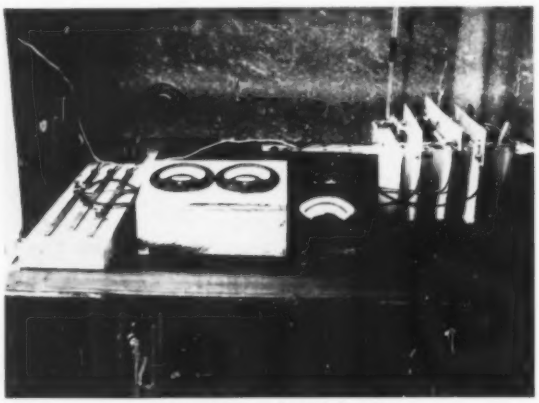

FIG. 1. Experimental cell

Three separate tests were made, each consisting of two or more trials of the same three materials. The only difference between trials was the feed solution. The selection of cathode materials for trial in each test overlapped that of other tests, so that the performance of each type of starting sheet could be compared with all the others. The cathodes were continued in residence in the cell until their current efficiency dropped below 90 per cent, or until their appearance indicated the onset of re-solution. When a cathode failed according to these standards it was replaced by a duplicate. When the cathode longest in residence failed, the trial was terminated.

## RESULTS

Table II gives the experimental results of all three tests. In the first column the letter in the letter-number designation refers to the position of the cathode in the cell: "A" referring to the position near the feed end, "B" to the center position, and "C" to the discharge end of the cell. The number gives the position of the cathode in the sequence of cathodes used in a trial. For example, A-1 refers to the first cathode operated near the feed end of the cell and B-3 to the third of a series of three in the center position. In column 2, "Aluminum" refers to aluminum sheet operated with edge strips and "Aluminum*" to the same but operated without edge strips. "Albany" refers to zinc sheet rolled at the Albany Station, "Stripped" to zinc stripped from an aluminum cathode, and "Horse Head" to Horse Head Special strip supplied by the New Jersey Zinc Sales Company. The solution number in column 3 refers to the same solution as in Table I. A change in solution number within a test indicates a separate trial.

TABLE I. *Analysis of impurities in the feed solutions*

| Soln. | Oxidation method | | Impurities, milligrams per liter | | | | | | | |
|---|---|---|---|---|---|---|---|---|---|---|
| | Agent | Where applied | Ni | Co | Cu | Cd | Fe | Mn | Pb | Sb |
| 1 | $KMnO_4$ | Leach | 0.29 | 0.03 | 0.19 | 0.13 | 0.28 | 1.2 | 0.23 | —* |
| 2 | $KMnO_4$ | Stock | 0.12 | 0.22 | 2.9 | 0.03 | 1.04 | 2.0 | 0.47 | 0.003 |
| 3 | $KMnO_4$ | Stock | 0.26 | 0.10 | 7.56 | 0.01 | 0.97 | 1.78 | 0.09 | 0.001 |
| 4 | $KMnO_4$ | Stock | 0.07 | 0.08 | 1.40 | 0.03 | 15.0 | 7.0 | 1.05 | 0.002 |
| 5 | $KMnO_4$ | Stock | 0.18 | 0.11 | 0.05 | 0.03 | 0.83 | 1.5 | 0.47 | 0.003 |
| 6 | $KMnO_4$ | Leach | 0.58 | 0.12 | 0.64 | 9.88 | 0.53 | 3.5 | 4.5 | 0.001 |
| 7 | $KMnO_4$ | Leach | 0.05 | 0.32 | 2.10 | 0.04 | 0.88 | 4.24 | 1.98 | 0.001 |
| 8 | None | | 0.14 | 3.36 | 0.21 | 0.13 | 3.9 | 223 | 0.50 | 0.025 |
| 9 | $MnO_2$ | Leach | 0.02 | 3.9 | 0.17 | 0.05 | 53.2 | 266 | 0.51 | 0.001 |
| 10 | $KMnO_4$ | Stock | 0.07 | 1.18 | 0.86 | 0.19 | 8.48 | 3.58 | 1.04 | 0.123‡ |
| 11 | $MnO_2$ | Leach | 0.08 | 4.82 | 0.26 | 0.13 | 0.45 | 292 | 1.59 | 0.001 |

* Sample depleted before this value was determined.
‡ This value is obviously in error, probably by two decimal places.

## DISCUSSION

It is necessary to understand certain cell characteristics and operating conditions to appraise ac-

curately the relative dependability of the various starting sheets. The cells were operated without attention at night and during other off-hour periods. Such unattended operation amounted to 75 per cent of the total operating time. Current efficiency, as a general rule, decreases at an accelerated rate as time passes with the result that a cathode which failed during the night might suffer serious re-solution before it received attention; while one that showed evidence of failure during work hours would be replaced before serious loss of current efficiency occurred. Short-lived cathodes were most affected because the loss in current efficiency was averaged over a shorter residence time. Deterioration of the deposit could be detected earliest on aluminum starting sheets with edge strips, because re-solution was localized along the edges of the deposit. Since it was possible to detect re-solution early in its progress, these cathodes could be replaced promptly after its onset, and thus compensate for greater damage suffered when the cell was unattended. This explains why their average current efficiency compared favorably with longer-lived cathodes in the same cell. On the other four starting sheets the re-solution of the deposit was less accelerated with time, and their condition could be appraised more accurately, especially when the residence period was prolonged. Table III summarizes the data given in Table II relative to the average residence period and current efficiency for each type of starting sheet.

In comparing the averages shown in Table III, residence time is more significant than current efficiency. Only in those cases in which the residence periods are equal can current efficiency be used as an index of reliability. It must also be borne in mind that different conditions existed in the separate tests; therefore, averages from one cannot be compared with those from another.

The position of the cathode in the cell was of little importance when highly purified solution was fed; but, as solution impurity increased, the cathode nearest the feed end of the cell suffered the earliest dam-

TABLE II. *Residence time and current efficiency obtained for various starting-sheet materials in the electrodeposition of zinc from solutions with a wide range of impurity content*

| No. | Cathode material | Soln. No. | Residence time | | Current efficiency | |
|---|---|---|---|---|---|---|
| | | | Days each | Days avg | Per cent each | Per cent avg |
| **Test No. 1** | | | | | | |
| A-1 | Aluminum | 1 | 2 | | 93.0 | |
| A-2 | do | 1 | 2 | | 91.7 | |
| A-3 | do | 1 | 5 | 3 | 88.9 | 90.6 |
| B-1 | Albany | 1 | 9 | 9 | 93.7 | 93.7 |
| C-1 | Aluminum* | 1 | 6 | | 92.1 | |
| C-2 | do | 1 | 3 | 4.5 | 91.9 | 92.0 |
| A-1 | do | 2 | 12 | 12 | 93.9 | 93.9 |
| B-1 | Albany | 2 | 12 | 12 | 91.3 | 91.3 |
| C-1 | Aluminum | 2 | 6.7 | | 89.4 | |
| C-2 | do | 2 | 5.3 | 6 | 90.0 | 89.7 |
| **Test No. 2** | | | | | | |
| A-1 | Horse Head | 3 | 2.75 | 2.75 | 92.2 | 92.2 |
| B-1 | Stripped | 3 | 2.75 | 2.75 | 91.3 | 91.3 |
| C-1 | Albany | 3 | 2.25 | 2.25 | 87.5 | 87.5* |
| C-2 | Aluminum | 3 | 0.50 | 0.50 | 89.9 | 89.9 |
| A-1 | Horse Head | 4 | 7.75 | 7.75 | 88.8 | 88.8 |
| B-1 | Stripped | 4 | 7.75 | 7.75 | 88.1 | 88.1 |
| C-1 | Albany | 4 | 7.75 | 7.75 | 87.6 | 87.6 |
| A-1 | do | 5 | 6.75 | 6.75 | 90.5 | 90.5 |
| B-1 | Stripped | 5 | 6.75 | 6.75 | 91.3 | 91.3 |
| C-1 | Horse Head | 5 | 6.75 | 6.75 | 91.5 | 91.5 |
| **Test No. 3** | | | | | | |
| A-1 | Albany | 6 | 3 | 3 | 88.3 | 88.3 |
| B-1 | Aluminum | 6 | 2 | | 93.5 | |
| B-2 | do | 6 | 1 | 1.5 | 90.8 | 92.6 |
| C-1 | Horse Head | 6 | 2 | 73.4 | | |
| C-2 | do | 6 | 1 | ‡ | 89.3 | 78.7 |
| A-1 | Albany | 7 | 10 | 10 | 84.8 | 84.8 |
| B-1 | Aluminum | 7 | 7 | | 85.2 | |
| B-2 | do | 7 | 3 | 5 | 93.4 | 87.7 |
| C-1** | Horse Head | 7 | 5 | | 87.9 | |
| C-2 | do | 7 | 5 | 5 | 94.0 | 90.9 |
| A-1 | Albany | 8 | 3 | 3 | 72.1 | 72.1 |
| B-1 | Aluminum | 8 | 3 | 3 | 58.7 | 58.7 |
| C-1 | Horse Head | 8 | 3 | 3 | 81.8 | 81.8 |
| A-1 | do | 9 | 2 | | 65.5 | |
| A-2 | do | 9 | 1.75 | 1.88 | 63.1 | 64.4 |
| B-1 | Aluminum | 9 | 0.66 | | 85.5 | |
| B-2 | do | 9 | 1.33 | | 81.8 | |
| B-3 | do | 9 | 0.75 | | 89.2 | |
| B-4 | do | 9 | 1 | 0.83 | 88.9 | 86.3 |
| C-1 | Albany | 9 | 2 | | 69.5 | |
| C-2 | do | 9 | 1.75 | 1.88 | 66.7 | 68.3 |
| A-1 | Horse Head | 10 | 6.25 | 6.25 | 85.0 | 85.0 |
| B-1 | Aluminum | 10 | 1 | | 92.5 | |
| B-2 | do | 10 | 3.25 | | 83.6 | |
| B-3 | do | 10 | 2 | 2.08 | 88.9 | 86.5 |

TABLE II—*Continued*

| No. | Cathode material | Soln. No. | Residence time | | Current efficiency | |
|---|---|---|---|---|---|---|
| | | | Days each | Days avg | Per cent each | Per cent avg |
| **Test No. 3—*Continued*** | | | | | | |
| C-1 | Albany | 10 | 6.25 | 6.25 | 88.6 | 88.6 |
| A-1 | Horse Head | 11 | 0.8 | | 84.4 | |
| A-2 | do | 11 | 1.66 | 1.25 | 66.0 | 71.9 |
| B-1 | Aluminum | 11 | 0.8 | | 88.3 | |
| B-2 | do | 11 | 1.33 | | 67.8 | |
| B-3 | do | 11 | 0.33 | 0.83 | 92.2 | 78.6 |
| C-1 | Albany | 11 | 0.8 | | 84.4 | |
| C-2 | do | 11 | 1.66 | 1.25 | 70.4 | 74.9 |

* This value is not reliable because a poor electrical contact developed at night.

‡ Continued in the next trial.

** This cathode is C-2 from the previous trial.

age. The deposition of impurities on the first cathode seemed to reduce the hazard to the others. The operating data given in Table II for test 3 show that Horse Head and Albany sheet were alternated in

TABLE III. *Average residence period and current efficiency*

| Material | Test No. | Residence, Average days | Current efficiency per cent |
|---|---|---|---|
| Aluminum | 1 | 4.2 | 90.0 |
| Albany | 1 | 10.5 | 93.6 |
| Aluminum* | 1 | 7.0 | 92.0 |
| Horse Head | 2 | 5.73 | 90.4 |
| Stripped | 2 | 5.73 | 89.8 |
| Albany | 2 | 5.58 | 88.8 |
| Horse Head | 3 | 3.16 | 82.4 |
| Aluminum | 3 | 1.89 | 80.8 |
| Albany | 3 | 3.56 | 82.9 |

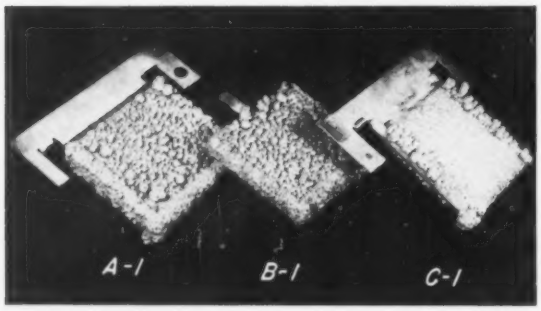


FIG. 2. Comparison of aluminum starting sheets without edge strips, Albany zinc, and aluminum with edge strips. Cathodes A-1, B-1, and C-1 deposited from solution 2.

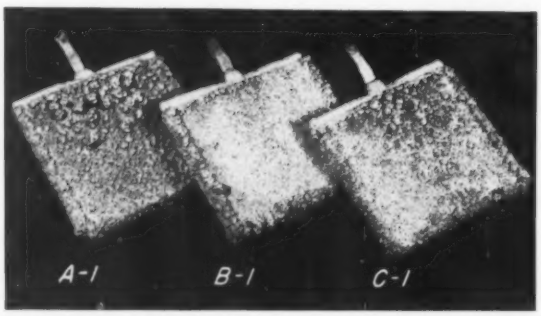


FIG. 3. 7.75-day deposits of zinc on Horse Head, stripped, and Albany zinc. Cathodes A-1, B-1, and C-1 deposited from solution 4.

positions "A" and "C" to compensate for the effect of position.

While edge strips are a necessity in commercial practice, test 1 shows that they are an important factor in limiting the residence periods of aluminum starting sheets. Impurity analysis of the stock solutions was not made for enough impurities to show all those that affect the deposition of zinc. Solution 1 was treated with permanganate to prepare solution 2. The difference in analysis was not significant, but longer residence periods were obtained with solution 2. The difference was attributed to the removal of undetected impurities. Fig. 2 shows cathodes from this test. The smoother appearance of C-1 is occasioned by its shorter residence.

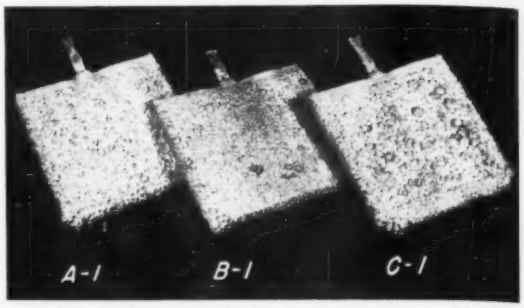


FIG. 4. 6.5-day deposits of zinc on Horse Head, stripped, and Albany zinc. Cathodes A-1, B-1, and C-1 deposited from solution 5.

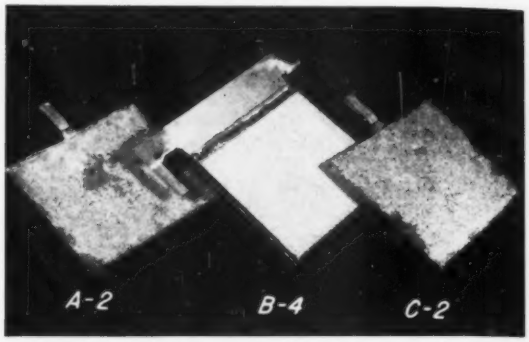


FIG. 5. Typical corrosion on cathodes operated in solution high in impurity. Cathodes A-2, B-4, and C-2 deposited from solution 9.

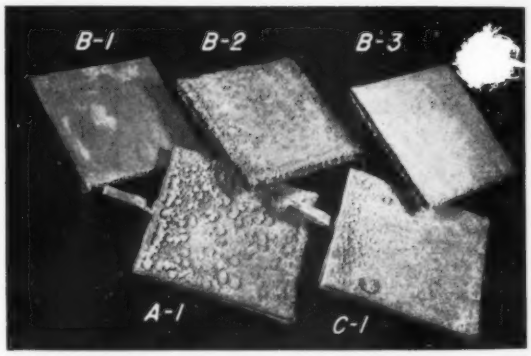


FIG. 6. Deposits from a 6.25-day trial that required three aluminum cathodes to equal the residence period of one each of Horse Head and Albany zinc. Cathodes A-1, B-1, B-2, B-3, and C-1 deposited from solution 10.

Test 2 compared the three types of zinc sheet. The apparent advantage of Horse Head over Albany zinc as shown by the table is reversed in test 3. Fig. 3 and 4 show deposits from test 2. Fig. 5 illustrates typical corrosion occurring in solutions with a high impurity content. The deposits pictured were made in solution 9 that contained manganese, cobalt, and iron in amounts exceeding the tolerance for residence periods longer than 1 day. The deposits shown in Fig. 6 are representative of the results to be expected from aluminum and zinc starting sheets. Recycling the electrolyte had no noticeable effect on deposition results. The deposits were not different from those obtained from stagnant electrolytes. The normal gassing at the electrodes provided sufficient agitation in the cells used without recirculation, probably because the anodes extended to the bottom of the cell.

## Conclusions

No significant differences in results were obtained from three different samples of four-nines grade zinc used as starting sheets for the deposition of zinc from acid solutions of zinc sulfate. All operated for longer residence periods than aluminum starting sheets. Aluminum starting sheets without edge strips were almost as long-lived as zinc. The edge strips, required on aluminum in commercial practice, induce early corrosion and result in a shorter residence period than would be possible without them.

Any discussion of this paper will appear in a Discussion Section, to be published in the June 1951 issue of the Journal.

## References

1. O. C. Ralston and W. J. Uren (To Phelps Dodge Corporation), U. S. Pat. 2,058,259, October 20, 1936.
2. G. C. Ware, H. E. Blake, Jr., and K. B. Higbie, *J. (and Trans.) Electrochem. Soc.*, **96**, 335 (1949).

# Detection of Soil Removal in Metal Cleaning by the Radioactive Tracer Technique[1]

J. C. Harris, R. E. Kamp, and W. H. Yanko

*Central Research Department, Monsanto Chemical Company, Dayton, Ohio*

ABSTRACT

The sensitivity of various methods for the determination of surface cleanliness is known in but few instances. The radioactive tracer technique as a quantitative method is used to define the apparent limits of sensitivity of the water break, fluorescent dye, and copper plate methods.

The methods in increasing order of sensitivity are: fluorescent dye, copper plate, water break, and radioactive tracer technique. Quantitative estimates of limits of sensitivity are given.

## Introduction

Because of its ease of application and apparent sensitiveness to soil retention, water break is a time-honored method for estimation of the extent of soil removal. Presence of water break in a film of water over a metal surface is generally indicative of the presence of some water-repellant material, generally of an oily or greasy nature. Unfortunately, there are no published data indicating the sensitivity of this method. One of its failings is that in practice it is possible to have a metal film evenly coated with a contaminating material which does not give water break, but which can cause processing defects. Some surface active agents can coat metals in this way, providing a film which does not repel water, and is of extremely minute thickness, but nevertheless soil, because it is "matter out of place."

Another recognized method for estimation of degree of cleanliness is either to weigh the metal piece being cleaned before and after the cleaning process, or to wash the cleaned piece with solvent, and weigh the extract. This method suffers from the gross nature of the pieces being cleaned, or if smaller test panels are used, the amount of soil remaining is less than the sensitivity of the balance in use. Again a metal piece is either clean or it is not, and the minute amount of materials causing water break are less than the sensitivity of the balance. With a good balance, and technique, a sensitivity of 0.00005 gram ($5 \times 10^{-5}$g) can be attained.

Zakarias (1) suggested that a satisfactory method for routine estimation of cleanliness was to rub the cleaned surface with white tissue paper and then observe for grease or soot. This test naturally is of a qualitative more than a quantitative nature.

Morgan and Lankler (2) developed a method for estimation of soil removal which involved the use of a fluorescent dye, which, if not completely removed, could be detected in ultraviolet light either visually or recorded by photographic means. The sensitivity of this method was said to be $4 \times 10^{-6}$ g/cm$^2$, as determined gravimetrically. Apparently these investigators washed soiled panels, degreased them to low ranges of fluorescence, then weighed the residue. If this was their procedure, then the $4 \times 10^{-6}$ g/cm$^2$ figure was calculated and not actual, but this is equally true for many methods of estimation. While considering methods of adding any tracer compounds to the soil used, the assumption and hope is that neither the soil nor the tracer material is removed preferentially during the course of the cleaning operation.

Edeler (3) suggested that small residues of oil to the extent of one part in 20,000 of solvent could be determined by dropping the volatile solvent solution from the cleaned panel onto photographic quality ground glass and observing for a ring appearance due to any nonvolatile oil present. This method could perhaps be extended by dilution technique to a quantitative method for estimation of oily soil on cleaned surfaces.

H ogaboom (4) recently suggested that a satisfactory method for determination of cleanliness of ferrous metals is to dip the cleaned part into a copper sulfate-sulfuric acid bath until a plate was formed, which then was examined for continuity and adherence. No estimate of sensitivity was made.

The most recent advance in the detection of soil retained by metal surfaces is use of the radioactive tracer technique (5) and is essentially the most sensitive of the quantitative methods now available. The radioactive tracer method for metal cleaning purposes is operated by combining with an oily soil a $C_{14}$ tagged organic compound dispersible in the oil, permitting a quantitative estimate of soil removal

[1] Manuscript received June 16, 1950. This paper prepared for delivery before the Buffalo Meeting, October 11 to 13, 1950.

or retention. The sensitivity of this method has been measured as $2 \times 10^{-7}$ g/cm².

A resume of the characteristics of the various test methods is given in Table I.

Tests such as water break, the fluorescent dye technique, and the radioactive tracer method do not alter the surface characteristics of the cleaned panel, permitting their estimation before subjecting the test piece to the plating method suggested by Hogaboom. Since the radioactive tracer method is quantitative and so sensitive, it was believed that it could be used successfully to outline the degrees of sensitivity of the other methods quantitatively.

TABLE I. *Tests for estimation of cleanliness*

| Test | Apparent sensitivity | Method of estimation | Investigator |
|---|---|---|---|
| Water break | Not known, but quite sensitive | — | — |
| Gravimetric | $5 \times 10^{-5}$ g | Very sensitive balance | — |
| Tissue paper | Not known | Visual | Zakarias (1) |
| Fluorescent dye | $4 \times 10^{-6}$ g/cm² | Gravimetric | Morgan and Lankler (2) |
| Spot | 1 part in 20,000 | Visual and actual trial | Edeler (3) |
| Copper plate | Not known | Visual | Hogaboom (4) |
| Radioactive tracer | $2 \times 10^{-7}$ g/cm² | Radioactive tracer | Harris, Kamp, Yanko (5) |

## Experimental

### *Soiling Composition*

The soiling composition was comprised of the following materials:

| | *By weight* |
|---|---|
| Lubricating oil (Sohio) SAE No. 60 | 97% |
| Fluorescent Green HW 175% (Wilmot and Cassidy, Inc.) | 2% |
| N,N,-di-n-butyl stearamide | 1% |

The fluorescent dye is oil soluble and is that recommended by Morgan and Lankler (2). The N,N,-di-n-butyl stearamide was oil dispersible, was preferentially chemisorbed, and was chosen with this factor in mind.

### *Soiling of Pans*

The pans were of surface-hardened No. 32 gauge sheet steel, the area on which the soil was distributed being 2.26 cm². Over this area was evenly spread 2.5 mg of the soiling mixture forming a very thin but essentially continuous layer.

### *Cleaning Technique*

The cleaning technique is that described previously (5). Essentially, it involved full immersion of the pans suspended from hooks in a boiling solution of the cleaning agent followed by rinsing by six dips each in two separate beakers of boiling distilled water. The time for immersion was varied to yield pans which had differing amounts of retained soil.

The cleaning solution was used at 5 per cent concentration in distilled water and was a mixture of 5 per cent of Santomerse No. 1 and 95 per cent sodium metasilicate.

### *Evaluation Scheme*

Since fluorescent dye was present in the soiling medium, and fluoresced strongly under a filtered ultraviolet light source, this was the first test to which the cleaned, rinsed, and dried pans were subjected.

The second test used was the determination of residual surface radioactivity, the pans having been evaluated for initial activity before washing. The technique and methods are those common to this procedure and described previously (5).

TABLE II. *Sensitivity of cleanliness tests*

| Sample No. | Counts/min* ± range | Maximum % soil remaining | Amount of soil remaining (g/cm²) | Reaction to test: Fluorescent dye | Water break | Copper plate |
|---|---|---|---|---|---|---|
| 1 | 261 ± 5 | 0.96 | 2.2 to 2.3 × $10^{-5}$ | + | + | + |
| 2 | 69 ± 4 | 0.26 | 5.7 to 6.4 × $10^{-6}$ | − | + | + |
| 3 | 25 ± 2 | 0.10 | 2.0 to 2.4 × $10^{-6}$ | − | + | − |
| 4 | 7 ± 2 | 0.03 | 4.4 to 7.9 × $10^{-7}$ | − | − | − |
| 5 | 0 ± 2 | 0.008 | 0 to 1.7 × $10^{-7}$ | − | − | − |

* Background count of 18 subtracted. Original count/minute 12,650 ± 15.

The third test was for water break after immersion in a stream of distilled water at room temperature.

The pans after the water-break test were immersed for three minutes in a solution comprised of:

| | g/l |
|---|---|
| Copper sulfate pentahydrate | 40 |
| Sulfuric acid | 17 |

At the end of a three minute plating period the pans were removed, examined for continuity of plate, and tested for tenacity of plate by vigorously rubbing the surface with several thicknesses of fine absorbent paper.

## Discussion of Results

The results obtained by these tests are shown in Table II.

It is at once apparent that the cleanliness tests

can readily be arranged in order from least to most sensitive: fluorescent dye, copper plate, water break, and radioactive tracer technique.

Since the radioactive tracer method is subject to a number of corrections, it is natural that statistical methods should be used in the treatment of such data. The accepted statistical method for ascertaining the range about a mean value is represented as follows:

$$\text{Probable error } (PE) = 0.67 \times \frac{\sqrt{\text{counts}}}{\text{minutes of count}} \quad (6)$$

Limits about mean

$$= \sqrt{PE^2 \text{ (observed count)} + PE^2 \text{ (background count)}}$$

The limits for the mean thus leads to the maximum and minimum values given in Table II. These limits are the square root of the sum of the squares of the probable errors for the initial count (or the final count) and that for the background count. Arranged to show increasing sensitivity, based on the fluorescent dye method as unity (and least sensitive), the following rating results:

| | *Comparative sensitivity* |
|---|---|
| Fluorescent dye | 1 |
| Copper plate | 4 |
| Water break | 11 |
| Radioactive tracer | 110 |

The method for calculating the amount of soil remaining follows:

$$\frac{\text{Final count}}{\text{Initial count}} \times \frac{\text{mg soil}}{\text{area pan}} = \text{soil remaining.}$$

Following is an example of the actual usage of this calculation:

$$\frac{256}{12665} \times \frac{2.5 \text{ mg}}{2.26 \text{ cm}^2} = 2.2 \times 10^{-5} \text{ g/cm}^2.$$

### *Surface Areas Involved*

Of interest is the consideration of the area it is estimated that would be covered by soil at some given value of cleanliness, or the molecular thickness of such soiling films. The main assumption to be made is the area of the molecule of N,N-di-n-butylstearamide. It very probably does not exceed the 52 $A^2$ area for hydrolecithin, and probably lies between that and oleic acid at 27 $A^2$. For our purposes an area equivalent to oleic acid was assumed. Other factors for the calculations are:

| | |
|---|---|
| Molecular weight | 398 |
| Average initial count (per minute) | 12,650 |
| Total area of pan | 2.26 cm² |
| Avogadro constant | $6.06 \times 10^{23}$ |
| Actual amount N,N-di-n-butyl stearamide used | $2.5 \times 10^{-5}$ g |

*1. Total possible area for radioactive stearamide:*

$$\frac{1}{398} \times 6.06 \times 10^{23} \times 2.5 \times 10^{-5} = 3.80 \times 10^{16}$$

molecules used.

$$3.80 \times 10^{16} \text{ molecules} \times 27 \times 10^{-16} \text{ cm}^2\text{/molecule} = 102.6 \text{ cm}^2.$$

*2. Area represented by the stearamide:*

$$\frac{102.6 \text{ cm}^2}{2.26 \text{ cm}^2} = 45 \text{ times pan area.}$$

*3. Coverage by radioactive stearamide at the limit of sensitivity:*

Limit of sensitivity is $2 \times 10^{-7}$ g/cm² of soil, but 1 per cent of this is radioactive or the limit of sensitivity for the radioactive compound is $2 \times 10^{-9}$ g/cm².

$$\frac{3.8 \times 10^{16} \text{ molecule} \times 2 \times 10^{-9} \text{ g/cm}^2}{2.5 \times 10^{-5} \text{ g}}$$

$$= 3 \times 10^{12} \text{ molecules/cm}^2 \text{ or } 6.7 \times 10^{12} \text{ molecules/pan}$$

$$6.7 \times 10^{12} \text{ molecules/pan} \times 27 \times 10^{-16} \text{ cm}^2\text{/molecules}$$

$$= 1.83 \times 10^{-2} \text{ cm}^2 \text{ covered, or } \frac{1.83 \times 10^{-2} \text{ cm}^2}{2.26 \text{ cm}^2} \times 100$$

$$= 0.81\% \text{ of total area at this sensitivity.}$$


## Summary

The comparative sensitivities of the methods for estimating cleanliness are, using the fluorescent dye method as unity (since it is least sensitive):

| | |
|---|---|
| Radioactive | 110 |
| Water break | 11 |
| Copper plate | 4 |
| Fluorescent dye | 1 |

At the point of the limit of sensitivity, assuming the same area per molecule as for oleic acid, the remaining radioactive stearamide covers approximately 0.81 per cent of the total area of the pan.

The various methods of determination of cleanliness cease to function for these systems between the following limits:

| | *In g of soil/cm²* |
|---|---|
| Fluorescent dye | $2.3 \times 10^{-5}$ to $5.7 \times 10^{-6}$ |
| Copper plate | $6.4 \times 10^{-6}$ to $2.0 \times 10^{-6}$ |
| Water break | $2.4 \times 10^{-6}$ to $4.4 \times 10^{-7}$ |
| Radioactive tracer | $1.7 \times 10^{-7}$ to 0 |


Any discussion of this paper will appear in a Discussion Section, to be published in the June 1951 issue of the JOURNAL.

## REFERENCES


1. L. ZAKARIAS, *Chimie & industrie*, **36**, 1095 (1936).
2. O. M. MORGAN AND J. G. LANKLER, *Ind. Eng. Chem. Anal. Ed.*, **14**, 725 (1942).
3. A. EDELER, *Ind. Eng. Chem. Anal. Ed.*, **15**, 282 (1943).
4. G. B. HOGABOOM, *Proc. Am. Electroplaters' Soc.*, **35**, 215 (1948).
5. J. C. HARRIS, R. E. KAMP, AND W. H. YANKO, *ASTM Bull.*, No. 158, 49 (1949).
6. D. WRIGHT WILSON, A. O. C. NIER, AND S. P. REIMANN, "Preparation and Measurement of Isotopic Tracers," pp. 83–108, J. W. Edwards, Ann Arbor, Michigan, (1947).

# Studies of Time-Potential Changes on an Electrode Surface during Current Interruption[1]

## I. Zinc-Steel Couple in Synthetic Sea Water

SIGMUND SCHULDINER AND ROGER E. WHITE

*Naval Research Laboratory, Washington, D. C.*

ABSTRACT

A d-c current interrupter method has been developed for oscilloscopic studies of time-potential changes at an electrode surface during short interruption intervals. A variable length square pulse with a very short rise time and with a duty factor of approximately one per cent was used to interrupt the current flow in a cell. Studies were conducted using interruption times from one microsecond to 120 microseconds.

This interrupter technique permitted correction for the resistance error in closed circuit potential measurements. Polarization decay and build-up could be followed as the current was cut off and turned on, and the potential changes and double layer capacity effects occurring at an electrode surface during interruption could be measured. These phenomena have been discussed in terms of an equivalent electrical circuit. An initial study of polarization phenomena on the zinc anode-steel cathode system in a synthetic sea water electrolyte was carried out using this interrupter method.

### INTRODUCTION

The study of polarization phenomena at an electrode surface requires the separation and determination of the various factors involved. When the closed circuit potential of a working electrode is measured, there is included in this measurement: (*a*) the *IR* drop due to resistance between the reference electrode and the double layer at the electrode surface; (*b*) the voltage drop due to the polarization voltage across the adsorbed double layer on the surface of the electrode; and (*c*) the voltage drop due to the polarization voltage across the diffuse double layer at the electrode surface. Other factors may also affect the potential measured, but it is believed that the above three are the primary ones.

In order to measure these polarization factors, an electronic d-c current interrupter was devised. Corrosion cells consisting of pure zinc anodes and mild steel cathodes with a synthetic sea water (1) electrolyte under constant current conditions were studied in this investigation.

Many studies have been made of the polarization factors outlined above, and several techniques have been used for these investigations. This study involves the use of d-c transients. These d-c transients are produced by interrupting the flow of current in a cell and studying the potential decay at the electrode surface. When the flow of current is again resumed, the build-up of potential can also be studied.

Two general methods used for the interruption of current flow are the commutator and the electronic interrupter methods. The commutator method has been extensively investigated by Newberry (2, 3, 4) and Ferguson (5, 6). An electronic interrupter method was devised by Hickling (7), which allowed him to study potential decay during interruption of current from a minimum period of $10^{-5}$ second to a maximum period of $20 \times 10^{-5}$ second. Hickling and Salt (8) later extended this range to a period of $10^{-1}$ second. The resistance error due to an *IR* drop between the reference electrode and the electrode surface was eliminated by measuring the potential at a sequence of increasing interruption intervals and then extrapolating back to zero time.

Frumkin (9) criticized this extrapolation method for eliminating resistance error claiming that polarization decay in the order of 0.1 to 0.2 volt during the first $5 \times 10^{-5}$ second was possible. In order to satisfy this criticism, Salt (10) decreased the interruption time to the order of $2 \times 10^{-6}$ second.

In conjuction with a cathode-ray oscilloscope, d-c transients can be used for the determination of the resistance error and study of the capacity effects at the electrode-solution interface. Bowden and Rideal (11) used an oscillographic method to determine electrode capacities of metallic surfaces and, by comparing with that of mercury, claimed that they were able to determine the ratio: true area/apparent area. Newberry (4) used an oscilloscope in con-

[1] Manuscript received May 23, 1950. This paper prepared for delivery before the Buffalo Meeting, October 11 to 13, 1950.

junction with his studies of hydrogen overvoltage decay during interruption of current.

The structure of the double layer at the surface of an electrode has been extensively investigated. A recent review of the studies on this subject has been made by Grahame (12).

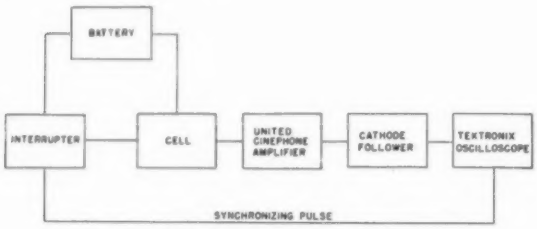


FIG. 1. Block diagram of test circuit

other control allows the length of pulse applied to the diode to be varied. Pulse amplitudes up to 5 volts and pulse lengths from one to 120 microseconds are available. In order that the duty cycle of the interruption applied to the current passing through the cell will not be varied, the repetition rate of the pulse is varied by the same control as the pulse length in such fashion as to maintain the duty cycle constant at approximately one per cent. The voltage pulse has a rise time from 0 to 90 per cent of maximum amplitude of 0.08 microsecond and a fall time to 10 per cent of maximum amplitude of 0.10 microsecond. No detectable overshoots are present and the pulse top is maintained flat over the entire range of variation of pulse lengths. A separate

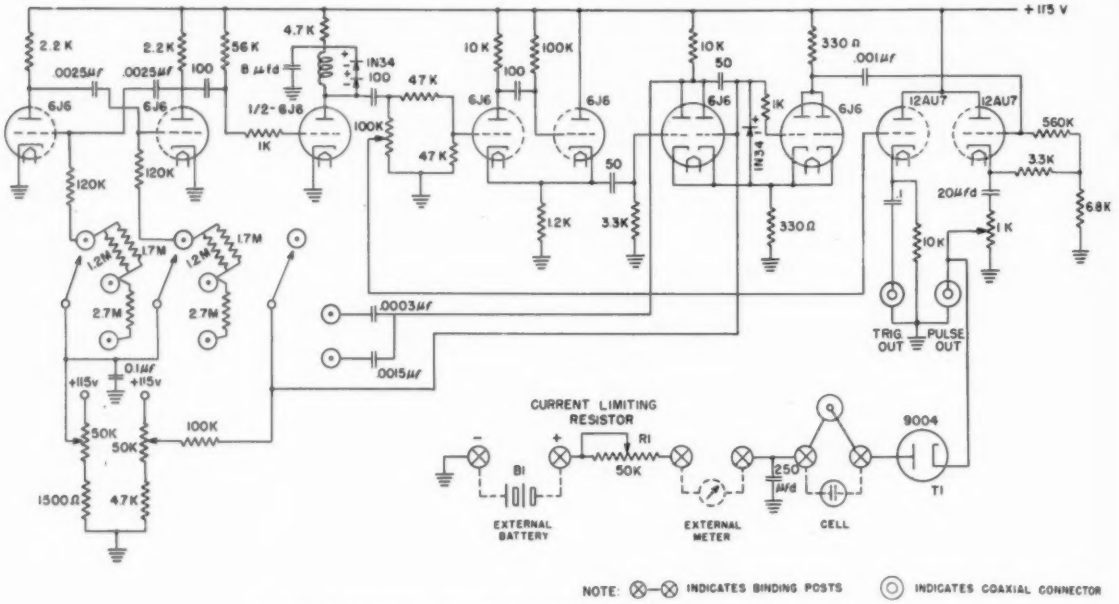


FIG. 2. Interrupter circuit. Capacities in μμf unless noted otherwise

## EXPERIMENTAL METHOD

### *Instrumentation*

The test equipment (Fig. 1) consists of an interrupter circuit and a viewing circuit. The interrupter (Fig. 2) produces a voltage pulse of variable amplitude and duration which is applied to the diode, T1, in such a fashion as to interrupt the current flowing in the circuit furnished by the battery, B1. The cell is connected in series with the battery, B1, a current limiting resistor, R1, a current measuring meter, and the interrupter circuit. Two controls are furnished on the interrupter circuit. One control allows variable amplitudes of pulse to be applied to the diode so that a pulse amplitude just sufficient to interrupt the current may be chosen, and the trigger pulse is also furnished by this circuit which serves to synchronize the external viewing scope.

The impedance offered by the cell to the flow of electric current is in order of 25 ohms, and with a current of less than one milliampere this produces a voltage drop of a few millivolts. To display the voltage pulse developed across the cell on an oscilloscope, an overall amplification as high as 10,000 is sometimes required. Also, to pass the frequency components contained in the rise of this pulse, uniform gain response must be maintained up to four megacycles or better. In the test set-up employed here, this gain was provided by two video amplifiers in tandem. The first of these amplifiers is a high-gain amplifier built for the Naval Research

Laboratory by the United Cinephone Company. This amplifier has a nominal response of 4 megacycles, but at higher gain levels this response slopes off considerably at the high frequency end. The input impedance of this amplifier is 2.2 megohms shunted by 40 micromicrofarads which is sufficient'y high to place a negligible load on the cell under measurement. The second amplifier is internal to the Tektronix oscilloscope, Type 511 AD, and has a nominal bandwidth of approximately 8 megacycles. The lack of required bandwidth on the United Cinephone amplifier shows up in two ways: (1) as a deterioration of the rise and fall times of the pulse, and (2) as an oscillation on the leading edge of the pulse. This effect becomes evident only when the waveform developed across the cell has a very sharp rise time (Fig. 12, 1 microsecond interruption at 2 hours) and thus is usually encountered when measuring the potential with respect to the cathode where the capacity effects are less pronounced.

The input impedance of the Tektronix oscilloscope is shunted by 40 micromicrofarads. If this capacitance were shunted across the high impedance output of the Cinephone amplifier a serious limitation of overall bandwidth would occur. To avoid this, a cathode-follower impedance transformer was inserted between the output of the Cinephone amplifier and the input of the Tektronix oscilloscope.

The interrupter described here was designed for a specific set of tests and does not indicate the range of pulse lengths and amplitudes possible. Should a requirement arise, pulses either much shorter or longer or of much greater amplitude could be obtained. It must be kept in mind, however, that reductions in pulse lengths with corresponding improvements in rise and fall times place severe requirements upon the bandwidths required in the accompanying amplifiers. Constructural techniques consistent with the frequency components involved here must be maintained throughout the entire test set-up as well as the interrupter circuit.

### *Analysis of the Time-Potential Trace*

In the study of the cathode-ray oscilloscope traces obtained during current interruption, it was helpful to consider the time-potential changes at an electrode surface in terms of an analogous electrical circuit. This circuit (Fig. 3) consisted of a capacitor in parallel with a resistance and both of these in series with another resistance.

If the square pulse used to interrupt the current flow is considered as the switch, $S$, which cuts off the current, then, when $S$ is opened the capacitor, $C$, will discharge through the parallel resistor, $R_p$. The equation for the change in voltage, $E_C$, across the capacitor during discharge when $R_pC$ is much greater than the rise time of the square pulse is

$$E_C = Ee^{-t/R_pC}$$

where $t$ is time and $E$ is the voltage across the capacitor at $t$ equal to zero.

When the interruption of current is ended, $S$ is closed and current starts to flow. The electrical condition at the electrode surface is more complex than during discharge. Here the series resistance, $R_s$, comes into the circuit and the change in voltage across the capacitor during charging will take place as shown by the following equation

$$E_C = E\left(\frac{R_p}{R_s + R_p}\right)(1 - e^{-t/C(1/R_s+1/R_p)}).$$

When the circuit (Fig. 3) consists only of a resistance, the left hand side of the cathode-ray trace (Fig. 7) shows the drop in voltage across the resistance as the current is switched off, and the right hand side of the trace shows the increase in voltage as the current is turned on. The time constant of a pure resistance is of a much lower order than the time required for the switching off or on of the current. Therefore, the time required for voltage change across a pure resistance will only depend on the rise and fall time of the voltage pulse. With the pulse employed here, the times required to interrupt and restore the current were approximately 0.1 microsecond each. As shown in Fig. 7, this rise time is deteriorated to 0.15 microsecond by the amplifier response.

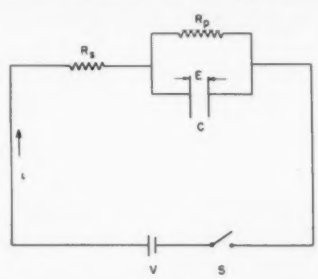


FIG. 3. Electrical analogy of a time-potential trace

The potential change across a circuit (Fig. 3), in which $C$ was a 0.102 microfarad condenser, $R_p$ a 20.8 ohm carbon resistor, $R_s$ an 11.1 ohm carbon resistor, and the current flow, $i$, was 2.93 milliamperes, was observed on the oscilloscope during current interruptions of one microsecond and 50 microseconds. A study of the traces obtained (Fig. 4 and 5) shows that the total time required for essentially complete discharge of the capacitor was about 6 microseconds. Therefore, the one-microsecond interruption (Fig. 4) does not allow full discharge of the capacitor. However, since time intervals in the order of 0.02 microsecond can be

determined, this short interruption time permits an accurate and easy determination of the voltage drop due to the series resistance.

At the instant the interruption is applied, both the series resistance and the discharge of the capacitor will contribute to the potential change observed in the trace. However, since the time constant for the series resistance is of a much shorter order than the time constant of the condenser discharging through the parallel resistor, the voltage change

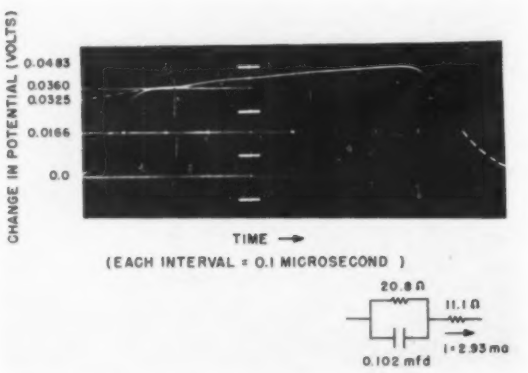


FIG. 4. Voltage change across circuit illustrated during a one-microsecond interruption.

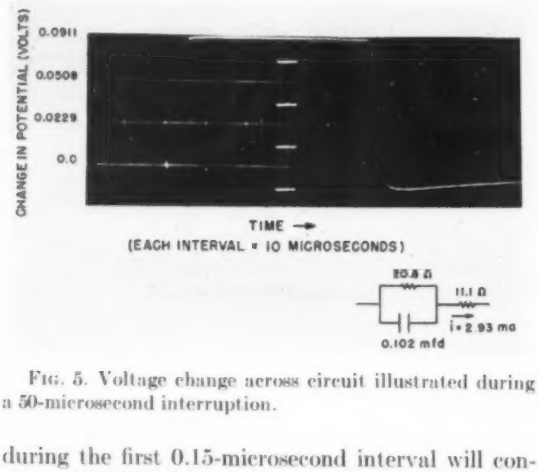


FIG. 5. Voltage change across circuit illustrated during a 50-microsecond interruption.

during the first 0.15-microsecond interval will consist primarily of the change across the series resistance. The amount of capacitor voltage change during this first 0.15-microsecond interval can be closely approximated by extrapolation back on the capacitor decay curve to the zero time axis. This voltage can be subtracted from the total change at 0.15 microsecond to give the voltage drop across the series resistance during current flow. The series resistance is determined by dividing the voltage drop by the current, $i$.

The time-potential trace (Fig. 5) is used to determine the parallel resistance and the capacity values. The steady state voltage drop across the parallel resistor, $iR_p = E$ is determined by subtracting from the maximum voltage drop during the 50-microsecond interruption the voltage drop across the series resistor. The capacity is determined by finding the voltage $E_c$ across the capacitor when $t = R_pC$. When this condition is satisfied, $E_c$ will be equal to 0.368 times the voltage across the capacitor at zero time. The time when this value of voltage is reached is found from the time-potential trace and the capacity is determined by dividing this time by $R_p$.

In the experiment the values for the series resistance, parallel resistance, and capacity were determined from the traces (Fig. 4 and 5) using the above method. The value of the series resistance

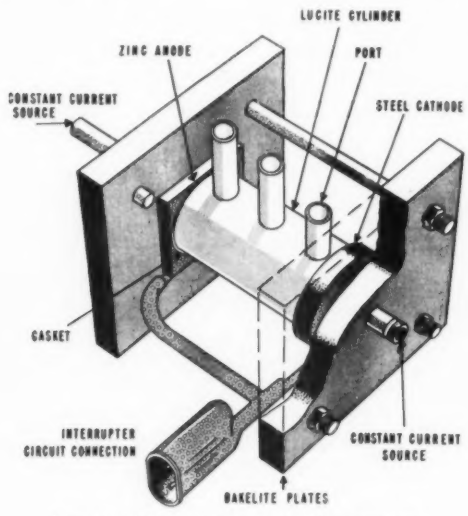


FIG. 6. Cell used in polarization studies

was found to be 11.1 ohms as compared with the actual value of 11.1 ohms. The value of the parallel resistor was 20.0 ohms as compared to its true value of 20.8 ohms. Finally, the value determined for the capacitor was 0.108 microfarads as compared to its true value of 0.102 microfarads. This correlation of computed values to the true values indicates the magnitude of the errors to be expected.

### *Zinc-Steel Couple in Synthetic Sea Water*

A study of polarization phenomena at pure zinc anodes and mild steel cathodes was undertaken using the interrupter technique developed. The corrosion cells (Fig. 6) used in these experiments consisted of Lucite cylinders 10 centimeters in length. The ends of the cylinders were carefully machined to give smooth parallel surfaces. Ports were placed in three positions so that a reference electrode could

be placed in any position and also the solution resistance could be determined by measuring the potential drop across a known length of the cell. These ports were also used to allow a slow flow of synthetic sea water through the cell.

This type of cell was used because it was compact and permitted connection to the interrupter circuit with the shortest possible leads. Consideration of compactness is very important in this work, since otherwise undesirable capacity and inductance effects may be introduced. The cylindrical type of cell also gives the most uniform current distribution on both the electrodes and in the electrolyte, and permits a determination of solution resistance. Examination of the electrodes after a run readily revealed that edge effects were essentially eliminated by this cell.

The choice of reference electrode used in measuring the potential change during interruption was found to be critical. It was essential in the study of d-c transients at the electrode surfaces that the reference electrode remain constant during the interruption period and that it also have a very rapid response to voltage change. A saturated calomel reference electrode was first tried and was found to show a capacity effect. The reason for this is not fully understood and this phenomenon is to be studied further. However, it was found that a pure zinc, magnesium, or platinum rod reference electrode was suitable for this work.

In order to test the suitability of pure zinc as reference electrodes, two zinc rods were inserted at the end port openings of a corrosion cell in the interrupter circuit. This was done so that each zinc rod would be at opposite ends of the potential field across the solution. These zinc rods were connected across the amplifier-oscilloscope circuit where the time-potential traces, which were due to the *IR* drop in the solution between the two rods, were investigated. Traces for one- and 50-microsecond interruptions (Fig. 7 and 8) show that the potential change during interruption was due purely to solution resistance and that the zinc rods themselves showed no discernible capacity effect or time lag in potential response.

Two cells were used in this study: one had an internal diameter of 3.18 centimeters, and the other had an internal diameter of 6.35 centimeters. Both the zinc and steel electrodes were machined to a smooth surface and polished down to 3/0 metallographic emery paper. After cleaning the electrodes with water and ethyl alcohol, a gasket of polyethylene, one mil in thickness, was placed on the edges of the Lucite cylinder and the electrodes were bolted into position (Fig. 6).

In the small cell an apparent area of 7.94 cm² of each electrode was exposed; for the large cell this area was 31.67 cm². A slow continuous flow of synthetic sea water which was saturated with air was passed through each cell during the run. In the small cell the rate of flow was 5–10 ml/min, and in the large cell this rate was from 10–15 ml/min. It was believed that these rates of flow were sufficient to keep a continuous supply of fresh solution in contact with the electrode surface.

During each run, closed circuit potentials against a saturated calomel reference electrode were continuously measured on a recording potentiometer. A continuous constant current, maintained by using a high voltage battery source across a voltage regulator vacuum tube, was passed through each cell.

Runs were made by starting with the circuit open for a period of about two hours. At this time the open circuit potentials of the zinc and steel were stable and close to −1.09 volts for the zinc and −0.75 volt for the steel electrodes. A predetermined constant d-c current was then applied to the cell.

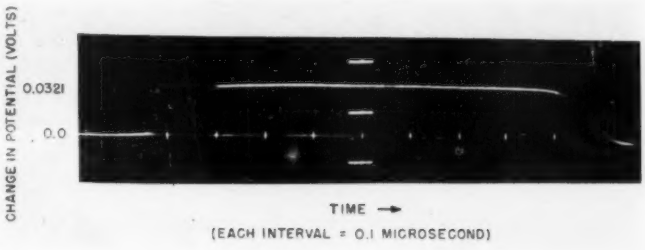


FIG. 7. Time-potential trace of voltage drop across cell due to solution resistance. One-microsecond interruption. Zinc reference electrodes.

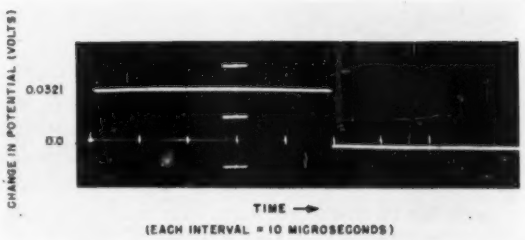


FIG. 8. Time-potential trace of voltage drop across cell due to solution resistance. 50-microsecond interruption. Zinc reference electrodes.

When the polarization factors were to be measured, the flow of sea water was stopped in the cell and it was disconnected from its current source. It was immediately connected to the interrupter circuit. The current flow through the interrupter circuit was maintained at the same value as the constant current source. Closed circuit potentials of each electrode using a saturated calomel electrode were then taken at each port opening. A pure zinc reference electrode consisting of a zinc rod long enough to extend almost to the bottom of the cell was then placed in either the center port opening or the opening farthest from the electrode being investigated. This was done so that the polarization measurements would average out over the entire zinc or steel surface. Time-potential traces were then photographed for each electrode surface for both a one-microsecond interruption and a 50- (or more) microsecond interruption depending on the time required for the polarization to decay to a steady value. The electrical connections

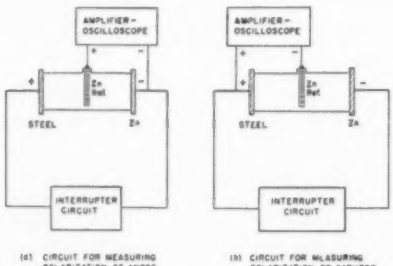


FIG. 9. Circuit arrangements used to obtain time-potential traces during interruption of current.

which were used to obtain the time-potential curves are shown in Fig. 9.

After the time-potential traces were photographed for each electrode surface, the closed circuit potentials at each port opening were then retaken with a saturated calomel electrode. The cell was then disconnected from the interrupter circuit and connected to its source of steady current. The oscilloscope was then calibrated for each amplifier setting used in the previous measurements by taking the potential drop across a known carbon resistor in the interrupter circuit at known current values.

The duration of each run was from one to two weeks. Interrupter measurements were made at regular intervals during the run. There was no temperature control of the synthetic sea water electrolyte and it ranged from 24° to 33°C. The apparent current densities used were 0.1, 0.2, and 0.5 ma/cm$^2$ for the small electrodes and 0.01, 0.05, and 0.1 ma/cm$^2$ for the large electrodes.

At the end of each run the electrodes were examined. The steel cathodes, in all cases, had a uniform calcareous coating over the entire surface. A small amount of zinc metal precipitated at the bottom of the steel surface and was most noticeable for the higher current densities. There was no rust evident on the steel surfaces and after cleaning off the coating the steel was in practically the same condition as when new. The zinc electrodes were well pitted and the formation of a white coating was observed on all specimens. The zinc electrodes that were in the cells with the higher current densities were fairly evenly corroded; however, the anodes which were run at the lowest current densities showed large areas with no evident corrosion. There were relatively deep pits on these electrodes.

## Data and Experimental Results

### *Analysis of Time-Potential Traces*

Time-potential traces showing potential change on the surface of an electrode during interruption were analyzed in the same way as for the circuit (Fig. 3) previously described. This electrical analogy was assumed to hold for the potential changes taking place at the electrode surfaces during interruption. The series resistance was assumed to be the total resistance from the reference electrode to the double layer. This would include solution resistance plus resistance effects near the electrode surface due to concentration and other factors. The capacity effect was assumed to be due to one part of the double layer and the parallel resistance due to the resistance across that part of the double layer.

In order to show how the equations previously given for change in voltage across a capacity during discharge and charge fit the traces photographed, several typical ones are analyzed. The values determined for capacity, series, and parallel resistance were substituted in the equations. The voltage across the capacity, $E_c$, was then determined from these equations for various intervals of time. Fig. 10 and 11 show two typical time-potential traces, one of a zinc anode and one of a steel cathode, with the points calculated from the discharge and charge equations shown as dots superimposed on the trace.

### *Electrode Potentials and Polarization of Zinc Anodes*

The data obtained for the zinc anodes are shown in Table I. The values for series resistance are primarily due to solution resistance. The reference electrode was not always the same distance from the zinc electrode, since in certain cases it was desirable to change this. Solution resistance was also determined by taking the potential change at various port openings in the cell. There was a definite indication that the series resistance was, in general, greater than could be accounted for by solution resistance measurements. This was probably due

largely to the decrease in effective solution area at the double layer.

As can be seen in Table I, the parallel resistance for each particular run generally increased with time. This is believed to be due to the decrease in area of the adsorbed double layer because of film build-up at the electrode surface.

The time constant, $t = R_p C$, generally decreased with time and as the apparent current density increased. Also the time constant for the large electrodes was of a higher order, even for the same apparent current density.

The capacity polarization for each run markedly increased with time due to the increase in parallel resistance. Increased current density also usually increased the capacity polarization.

The closed circuit potentials shown in Table I are the measured values against a saturated calomel electrode corrected for the $IR$ drop due to series resistance. They, therefore, represent the polarization due to the adsorbed double layer plus the diffuse double layer plus any other possible polarization effects. The polarization due to what is believed to be the adsorbed double layer is the value $E_c$ which is called the capacity polarization. The other polarization effects have been lumped together and called the residual polarization. This is obtained by taking the open circuit steady value of potential for zinc, which is $-1.09$ volts in synthetic sea water, and subtracting the closed circuit potential value plus the capacity polarization value. It is probable that this residual polarization is primarily due to concentration polarization effects. As can be seen from the table, this residual polarization for each run increases rapidly at first and after a few days levels off to a fairly constant value.

Time-potential traces (Fig. 12) of a zinc anode for a typical run were photographed for five periods during the run. The one-microsecond traces were used to determine the series resistance values. As indicated on the traces, the capacity decay during the one-microsecond interruption was negligible for the first day or two, after which it became significant. The longer 50- or 70-microsecond interruptions shown on the traces indicate a marked change in the capacity and the parallel resistance effects with time. These longer traces, of course, were used to determine the capacity and the parallel resistance.

The accuracy of the determination of polarization factors varied widely depending on the particular trace. For traces with a relatively long time constant and high capacity polarization, the accuracy of the capacity determination was in the order of 10 per cent. For traces with very short time constants and small capacity polarization, the accuracy was undoubtedly much less. The accuracy for determination of the voltage drop due to series and parallel resistance was estimated to be in the order of one millivolt for most cases.

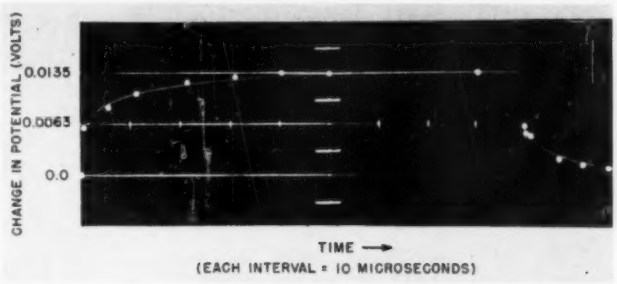


FIG. 10. Time-potential trace for zinc anode during current interruption. Large cell, apparent current density of 0.05 ma/cm² after 169 hours. Circles indicate calculated values.

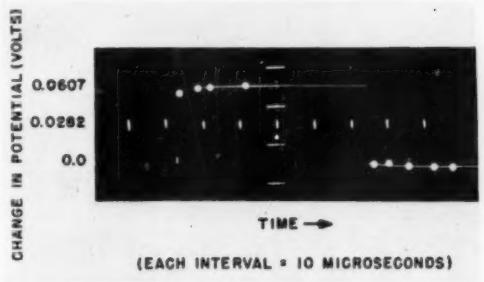


FIG. 11. Time-potential trace for steel cathode during current interruption. Small cell, apparent current density of 0.5 ma/cm² after 237 hours. Circles indicate calculated values.

### *Electrode Potentials and Polarization of Steel Cathodes*

The time-potential traces for the steel cathodes were handled in the same manner as those for the zinc anodes. The capacity effects for steel cathodes under the experimental conditions used were not as marked as they were in the case of the zinc anodes and, in many cases, the capacity could not be determined with any degree of accuracy. The series resistance, however, could be determined in all cases and the closed circuit potential determination corrected for it. The parallel resistance was determined for all runs when it had a measurable effect during the maximum interruption time available.

TABLE I. *Electrode potentials and polarization of zinc anodes*

| Apparent area of electrode ($cm^2$) | Apparent current density ($ma/cm^2$) | Duration of run (hr) | Series resistance $R_s$ (ohms) | Solution resistance (ohms) | Parallel resistance $R_p$ (ohms) | Time constant ($t = R_pC$) ($10^{-6}$ sec) | Capacity polarization $E_C$ (v) | Capacity C ($\mu f$) | Closed circuit potential (no series resistance) (v) | Residual polarization (v) |
|---|---|---|---|---|---|---|---|---|---|---|
| 31.67 | 0.01 | 3 | 3.15 | — | — | — | — | — | −1.090 | 0 |
| | | 27 | 5.05 | — | 1.26 | 3.64 | 0.0004 | 2.9 | −1.040 | 0.050 |
| | | 51 | 5.05 | — | 1.58 | 7.7 | 0.0005 | 4.8 | −1.028 | 0.061 |
| | | 71 | 5.05 | — | 1.89 | — | 0.0006 | — | −1.015 | 0.074 |
| | | 146 | 5.36 | — | 2.20 | 20 | 0.0007 | 9.1 | −1.004 | 0.085 |
| | | 170 | 4.42 | — | 3.79 | — | 0.0012 | — | −0.999 | 0.090 |
| | | 191 | 8.20 | — | 6.31 | — | 0.0020 | — | −0.994 | 0.094 |
| | | 214 | 4.73 | — | 6.00 | 14 | 0.0019 | 2.3 | −0.993 | 0.095 |
| | | 240 | 4.73 | — | 5.36 | 14 | 0.0017 | 2.6 | −0.993 | 0.095 |
| 31.67 | 0.05 | 3 | 2.28 | 2.85 | — | — | — | — | −1.062 | — |
| | | 23 | 3.04 | 2.65 | 1.08 | 7.7 | 0.0017 | 7.1 | −1.017 | 0.071 |
| | | 47 | 3.42 | 2.28 | 2.34 | 22.3 | 0.0037 | 9.5 | −0.999 | 0.086 |
| | | 70 | 3.35 | 2.59 | 3.35 | 15.0 | 0.0053 | 4.5 | −0.995 | 0.090 |
| | | 95 | 3.04 | 2.72 | 3.80 | 12.3 | 0.0060 | 3.2 | −0.993 | 0.091 |
| | | 169 | 3.10 | 2.85 | 5.44 | 10.0 | 0.0086 | 1.8 | −0.993 | 0.088 |
| | | 192 | 3.04 | 2.53 | 5.63 | 9.6 | 0.0089 | 1.7 | −0.992 | 0.089 |
| | | 239 | 4.62 | 2.85 | 8.30 | 8.0 | 0.0131 | 1.0 | −0.999 | 0.077 |
| 31.67 | 0.05 | 4 | 4.24 | 4.45 | 0.25 | 0.5 | 0.0004 | 1.9 | −1.075 | 0.015 |
| | | 25 | 4.30 | 4.24 | 2.60 | 11.8 | 0.0041 | 4.6 | −1.003 | 0.083 |
| | | 49 | 4.81 | 4.37 | 2.98 | 11.8 | 0.0047 | 4.0 | −1.001 | 0.084 |
| | | 71 | 5.31 | 4.30 | 3.42 | 10.5 | 0.0054 | 3.1 | −1.002 | 0.083 |
| | | 100 | 4.94 | 4.24 | 4.05 | 10 | 0.0064 | 2.5 | −1.001 | 0.083 |
| 31.67 | 0.10 | 2 | 2.65 | 2.49 | — | — | — | — | −1.064 | — |
| | | 23 | 2.52 | 2.46 | 0.73 | 3.4 | 0.0023 | 4.7 | −1.017 | 0.071 |
| | | 46 | 2.68 | 2.24 | 1.92 | 11.35 | 0.0061 | 5.9 | −1.000 | 0.084 |
| | | 70 | 3.12 | 2.24 | 2.59 | 10.0 | 0.0082 | 3.9 | −0.992 | 0.090 |
| | | 95 | 3.00 | 2.43 | 3.98 | 6.6 | 0.0126 | 1.7 | −0.987 | 0.090 |
| | | 168 | 2.93 | 2.37 | 3.38 | 7.3 | 0.0107 | 2.2 | −0.980 | 0.099 |
| | | 191 | 3.28 | 2.46 | 3.06 | 10.5 | 0.0096 | 3.4 | −0.976 | 0.104 |
| | | 217 | 2.97 | 2.21 | 6.97 | 6.6 | 0.0221 | 0.95 | −0.968 | 0.100 |
| | | 238 | 3.06 | 2.56 | 9.03 | 6.4 | 0.0286 | 0.71 | −0.961 | 0.100 |
| | | 262 | 3.25 | 2.33 | 11.00 | 7.0 | 0.0350 | 0.64 | −0.955 | 0.100 |
| 7.94 | 0.10 | 3 | 11.5 | 11.2 | — | — | — | — | −1.064 | — |
| | | 26 | 11.8 | 10.3 | 1.8 | 3.9 | 0.0014 | 2.2 | −1.032 | 0.057 |
| | | 50 | 11.2 | 11.1 | 7.2 | 3.6 | 0.0057 | 0.50 | −1.008 | 0.076 |
| | | 71 | 11.2 | 11.0 | 8.4 | 4.0 | 0.0067 | 0.48 | −1.003 | 0.080 |
| | | 146 | 10.5 | 9.3 | 12.6 | 3.4 | 0.0100 | 0.27 | −1.012 | 0.068 |
| | | 170 | 11.1 | 9.7 | 13.2 | 3.9 | 0.0105 | 0.29 | −1.009 | 0.070 |
| | | 190 | 11.5 | 11.0 | 19.4 | 3.2 | 0.0154 | 0.16 | −1.010 | 0.065 |
| | | 214 | 11.3 | 10.7 | 25.6 | 3.6 | 0.0201 | 0.14 | −1.006 | 0.064 |
| | | 239 | 12.4 | 10.8 | 29.2 | 3.6 | 0.0232 | 0.12 | −1.001 | 0.066 |
| 7.94 | 0.20 | 2 | 10.6 | 10.8 | 3.02 | 4.1 | 0.0048 | 1.3 | −1.018 | 0.067 |
| | | 22 | 11.6 | 11.6 | 6.41 | 4.0 | 0.0102 | 0.63 | −1.014 | 0.066 |
| | | 46 | 11.6 | 11.8 | 7.67 | 2.6 | 0.0122 | 0.34 | −1.006 | 0.072 |
| | | 69 | 11.3 | 11.8 | 6.79 | 2.9 | 0.0108 | 0.43 | −1.001 | 0.078 |
| | | 94 | 10.3 | 10.6 | 5.91 | 2.3 | 0.0094 | 0.39 | −1.005 | 0.076 |
| | | 167 | 12.4 | 11.4 | 7.23 | 2.7 | 0.0115 | 0.38 | −0.995 | 0.083 |
| | | 191 | 11.9 | 11.1 | 8.68 | 2.7 | 0.0138 | 0.32 | −0.996 | 0.080 |
| | | 237 | 13.4 | 12.2 | 9.31 | 3.0 | 0.0148 | 0.32 | −0.994 | 0.081 |
| 7.94 | 0.20 | 4 | 9.94 | 9.7 | 0.63 | 0.7 | 0.0010 | 1.1 | −1.057 | 0.032 |
| | | 24 | 10.0 | 10.1 | 3.52 | 1.1 | 0.0056 | 0.32 | −1.011 | 0.073 |
| | | 49 | 10.8 | 10.8 | 7.61 | 2.0 | 0.0121 | 0.27 | −0.995 | 0.083 |
| | | 72 | 10.8 | 10.8 | 9.37 | 1.8 | 0.0149 | 0.19 | −1.006 | 0.069 |
| | | 100 | 11.1 | 10.8 | 13.2 | 2.3 | 0.0209 | 0.17 | −0.998 | 0.071 |

TABLE I. *Electrode potentials and polarization of zinc anodes* (Continued)

| Apparent area of electrode ($cm^2$) | Apparent current Density ($ma/cm^2$) | Duration of run (hr) | Series resistance $R_s$ (ohms) | Solution resistance (ohms) | Parallel resistance $R_p$ (ohms) | Time constant ($t = R_pC$) ($10^{-6}$ sec) | Capacity polarization $E_C$ (v) | Capacity $C$ ($\mu f$) | Closed circuit potential (no series resistance) (v) | Residual polarization (v) |
|---|---|---|---|---|---|---|---|---|---|---|
| 7.94 | 0.50 | 2 | 10.0 | 10.0 | 0.43 | 6.4 | 0.0017 | 14.8 | −1.043 | 0.045 |
| | | 23 | 10.7 | 9.7 | 1.54 | 1.8 | 0.0061 | 1.2 | −1.024 | 0.060 |
| | | 45 | 10.7 | 9.7 | 2.47 | 2.1 | 0.0038 | 0.83 | −0.997 | 0.083 |
| | | 70 | 10.9 | 9.7 | 5.06 | 2.0 | 0.0201 | 0.40 | −0.991 | 0.079 |
| | | 94 | 10.9 | 9.9 | 7.28 | 1.4 | 0.0289 | 0.19 | −0.994 | 0.067 |
| | | 168 | 10.5 | 9.3 | 5.49 | 1.4 | 0.0218 | 0.25 | −0.995 | 0.073 |
| | | 190 | 10.8 | 9.6 | 5.72 | 1.4 | 0.0227 | 0.24 | −1.005 | 0.062 |
| | | 237 | 10.8 | 9.7 | 5.04 | 0.9 | 0.0200 | 0.18 | −1.003 | 0.067 |
| | | 262 | 11.4 | 9.9 | 5.79 | 1.1 | 0.0230 | 0.20 | −1.000 | 0.067 |

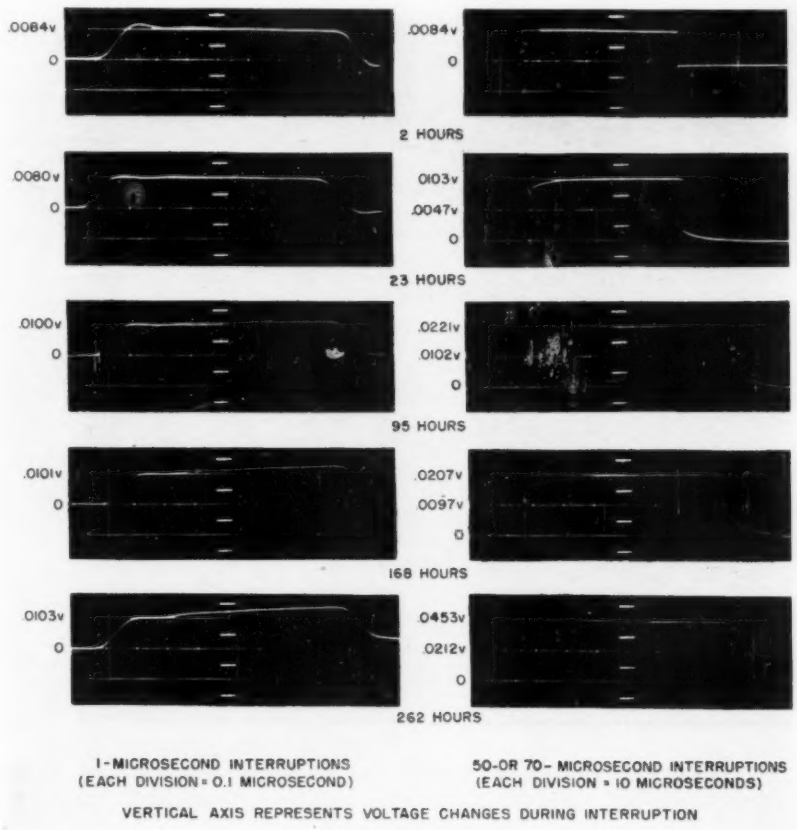


FIG. 12. Time-potential traces of interruptions for 31.67-$cm^2$ zinc anode at apparent current density of 0.1 $ma/cm^2$

Table II summarizes the measurements made for the steel cathodes. Here the series resistance, as in the case of the zinc anodes, is also primarily due to solution resistance. There was, in several cases, a marked increase in series resistance with time which was attributed primarily to a decrease in the effective area on the cathode surface because of film formation.

The parallel resistance and capacity polarization values were both of a lower order than for the zinc anodes and did not seem to vary as greatly with time.

The closed circuit potentials here are also corrected for series resistance and they represent the potential at the double layer. The residual polarization effects have been obtained by taking the open circuit steady value of potential for steel in synthetic sea water of −0.75 volt and subtracting the closed circuit potential value minus the capacity polarization value. As can be seen from Table II, the residual polarization effects for the steel cathodes have been much higher and apparently more sensitive to current density than for the zinc anodes.

TABLE II. *Electrode potentials and polarization of steel cathodes*

| Apparent area of electrode ($cm^2$) | Apparent current density ($ma/cm^2$) | Duration of run (hr) | Series resistance $R_s$ (ohms) | Solution resistance (ohms) | Parallel resistance $R_p$ (ohms) | Time constant ($t = R_pC$) ($10^{-6}$ sec) | Capacity polarization $E_C$ (v) | Capacity $C$ ($\mu f$) | Closed circuit potential (no series resistance) (v) | Residual polarization (v) |
|---|---|---|---|---|---|---|---|---|---|---|
| 31.67 | 0.01 | 3 | 5.05 | — | — | — | — | — | −0.805 | — |
| | | 27 | 5.68 | — | — | — | — | — | −0.841 | — |
| | | 51 | 5.36 | — | — | — | — | — | −0.970 | — |
| | | 71 | 5.05 | — | — | — | — | — | −0.996 | — |
| | | 146 | 4.73 | — | — | — | — | — | −1.028 | — |
| | | 171 | 4.42 | — | — | — | — | — | −1.062 | — |
| | | 191 | 8.20 | — | — | — | — | — | −1.099 | — |
| | | 214 | 4.73 | — | — | — | — | — | −1.115 | — |
| | | 240 | 5.99 | — | — | — | — | — | −1.117 | — |
| 31.67 | 0.05 | 3 | 5.00 | 5.06 | — | — | — | — | −1.019 | — |
| | | 23 | 4.81 | 4.81 | — | — | — | — | −1.039 | — |
| | | 47 | 5.25 | 4.12 | — | — | — | — | −1.063 | — |
| | | 70 | 4.62 | 4.67 | 0.51 | 1 | 0.0008 | 2 | −1.087 | 0.335 |
| | | 95 | 4.94 | 4.87 | — | — | — | — | −1.098 | — |
| | | 169 | 5.19 | 5.06 | 0.95 | 1.8 | 0.0015 | 1.9 | −1.151 | 0.399 |
| | | 192 | 5.06 | 4.55 | 1.27 | 1 | 0.0020 | 0.8 | −1.144 | 0.392 |
| | | 239 | 5.44 | 5.06 | 1.39 | 1 | 0.0022 | 0.7 | −1.158 | 0.406 |
| 31.67 | 0.05 | 4 | 3.98 | 4.43 | — | — | — | — | −1.038 | — |
| | | 25 | 4.18 | 4.24 | 1.0 | 0.7 | 0.0016 | 0.7 | −1.093 | 0.341 |
| | | 49 | 5.00 | 4.37 | 0.70 | 1.4 | 0.0011 | 2.0 | −1.128 | 0.377 |
| | | 71 | 5.00 | 4.30 | 1.1 | 1.1 | 0.0017 | 1.1 | −1.143 | 0.391 |
| | | 100 | 4.94 | 4.24 | 1.1 | 0.9 | 0.0017 | 0.8 | −1.146 | 0.394 |
| 31.67 | 0.10 | 2 | 2.59 | 2.49 | — | — | — | — | −1.105 | — |
| | | 23 | 4.92 | 4.42 | — | — | — | — | −1.165 | — |
| | | 46 | 4.73 | 4.07 | — | — | — | — | −1.191 | — |
| | | 70 | 4.79 | 4.04 | 0.32 | 0.7 | 0.0010 | 2 | −1.213 | 0.462 |
| | | 95 | 4.76 | 4.32 | 0.32 | 0.7 | 0.0010 | 2 | −1.236 | 0.485 |
| | | 168 | 4.64 | 4.26 | 0.25 | 0.5 | 0.0008 | 2 | −1.244 | 0.493 |
| | | 191 | 3.06 | 4.42 | 0.16 | 0.5 | 0.0005 | 3 | −1.253 | 0.502 |
| | | 218 | 4.23 | 4.01 | 0.66 | 0.9 | 0.0021 | 1.4 | −1.252 | 0.500 |
| | | 238 | 5.05 | 4.57 | 0.25 | 0.9 | 0.0008 | 3.6 | −1.272 | 0.521 |
| | | 262 | 5.05 | 4.19 | 0.25 | 0.9 | 0.0008 | 3.6 | −1.273 | 0.522 |
| 7.94 | 0.10 | 3 | 21.6 | 21.6 | — | — | — | — | −1.032 | — |
| | | 26 | 21.8 | 20.0 | — | — | — | — | −1.075 | — |
| | | 50 | 20.9 | 20.7 | — | — | — | — | −1.101 | — |
| | | 71 | 22.3 | 21.2 | 2.0 | — | 0.0016 | — | −1.112 | 0.360 |
| | | 146 | 19.0 | 18.5 | 3.3 | — | 0.0026 | — | −1.135 | 0.382 |
| | | 170 | 19.1 | 18.8 | 1.8 | — | 0.0014 | — | −1.132 | 0.381 |
| | | 190 | 21.1 | 21.2 | 1.6 | — | 0.0013 | — | −1.149 | 0.398 |
| | | 214 | 25.2 | 20.7 | 0.5 | — | 0.0004 | — | −1.150 | 0.400 |
| | | 239 | 32.2 | 21.0 | — | — | — | — | −1.151 | — |
| 7.94 | 0.20 | 2 | 11.6 | 10.8 | — | — | — | — | −1.126 | — |
| | | 22 | 11.9 | 11.9 | — | — | — | — | −1.168 | — |
| | | 46 | 12.5 | 11.9 | — | — | — | — | −1.184 | — |
| | | 69 | 12.0 | 11.9 | 0.8 | 10 | 0.0013 | 12 | −1.190 | 0.439 |
| | | 94 | 10.9 | 10.8 | 1.0 | 9 | 0.0016 | 9 | −1.183 | 0.431 |
| | | 167 | 11.8 | 11.6 | 1.0 | 9 | 0.0016 | 9 | −1.206 | 0.454 |
| | | 191 | 11.6 | 11.3 | 0.75 | 4.5 | 0.0012 | 6 | −1.190 | 0.439 |
| | | 237 | 12.5 | 12.4 | 0.4 | 5 | 0.0006 | 13 | −1.191 | 0.440 |
| 7.94 | 0.20 | 4 | 17.0 | 18.9 | — | — | — | — | −1.089 | — |
| | | 24 | 18.1 | 19.6 | 1.5 | — | 0.0024 | — | −1.166 | 0.337 |
| | | 49 | 20.5 | 20.7 | 1.7 | — | 0.0027 | — | −1.208 | 0.455 |
| | | 70 | 21.6 | 21.0 | 1.3 | — | 0.0021 | — | −1.210 | 0.458 |
| | | 100 | 21.8 | 21.0 | 2.4 | — | 0.0038 | — | −1.214 | 0.460 |

TABLE II. *Electrode potentials and polarization of steel cathodes* (Continued)

| Apparent area of electrode ($cm^2$) | Apparent current density ($ma/cm^2$) | Duration of run (hr) | Series resistance $R_s$ (ohms) | Solution resistance (ohms) | Parallel resistance $R_p$ (ohms) | Time constant ($t = R_pC$) ($10^{-6}$ sec) | Capacity polarization $E_C$ (v) | Capacity C ($\mu f$) | Closed circuit potential (no series resistance) (v) | Residual polarization (v) |
|---|---|---|---|---|---|---|---|---|---|---|
| 7.94 | 0.50 | 2 | 10.7 | 10.2 | — | — | — | — | −1.125 | — |
| | | 23 | 10.7 | 9.9 | 1.4 | 2.7 | 0.0057 | 1.9 | −1.204 | 0.448 |
| | | 45 | 11.4 | 9.8 | 1.1 | 4.8 | 0.0042 | 4.5 | −1.240 | 0.486 |
| | | 70 | 12.0 | 9.8 | 0.5 | 3.2 | 0.0021 | 6.0 | −1.273 | 0.521 |
| | | 94 | 11.7 | 10.1 | 0.9 | 0.5 | 0.0037 | 0.5 | −1.276 | 0.522 |
| | | 168 | 11.8 | 9.5 | 1.1 | 8.6 | 0.0043 | 8.0 | −1.316 | 0.562 |
| | | 190 | 12.1 | 9.8 | 1.6 | 3.6 | 0.0065 | 2.2 | −1.330 | 0.573 |
| | | 237 | 13.5 | 9.9 | 1.8 | 3.6 | 0.0072 | 2.0 | −1.380 | 0.623 |
| | | 262 | 13.4 | 10.1 | 1.8 | 2.7 | 0.0071 | 1.5 | −1.457 | 0.700 |

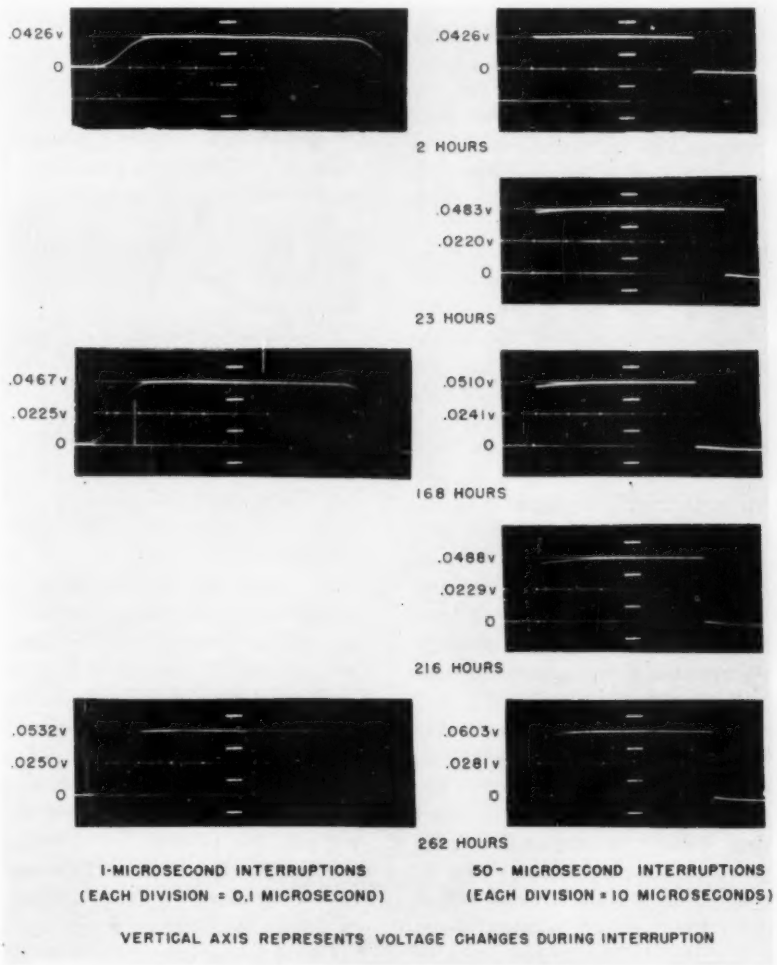


FIG. 13. Time-potential traces of interruptions for 7.94-$cm^2$ steel cathode at apparent current density of 0.5 $ma/cm^2$ taken at intervals indicated.

Time-potential traces of steel cathodes for a single run were made (Fig. 13). The one-microsecond traces for the entire run indicated that there was an inappreciable amount of polarization decay during this interval and that this potential change was due to series resistance. The fifty-microsecond interruptions after the first day showed capacity effects which could be measured.

Since the changes occurring during interruption at the cathode surfaces were less pronounced than

for the anode surfaces the accuracy, in most cases, of the measurements is less satisfactory.

## Discussion

### *General Theory*

When the current flowing through a cell is cut off, a series of phenomena takes place which tends to make the measured potential more electronegative at the anode and more electropositive at the cathode surfaces. Each of these events will add to the total change at each electrode at the instant the current is decreased. However, the amount of potential change contributed by each of these at any particular time will depend on its individual rate of change. The total change in voltage, therefore, at any time will be the sum of the potential changes for each event at that time.

At current cut-off there are believed to be three factors of major importance in causing potential change occurring at the electrode surface (Fig. 14). Each of these can be considered a capacity in parallel with a resistance. Hence, an appropriate "time constant" can be attached to every one of these factors. This time constant is the product of the resistance and the capacity values.

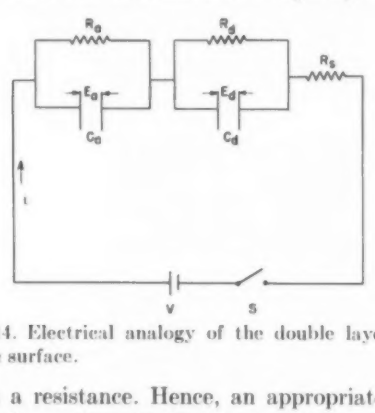


Fig. 14. Electrical analogy of the double layer at an electrode surface.

The first of these factors is the $IR$ drop due to the series resistance, $R_s$, between the reference electrode and the double layer at the electrode surface. The time constant for this event will be very short since the capacity attached to this resistance will be very small. As shown earlier in this paper the decay in potential due to this resistance will take place within the time required for current cut-off, which, for the experimental conditions used, was in the order of $0.15 \times 10^{-6}$ seconds.

The second factor, the voltage discharge, $E_a$, of the capacity due to the adsorbed double layer through its parallel resistance, $R_a$, will have a larger time constant than the series resistance; however, there may be some discharge during the cut-off time. This polarization effect for all the cases encountered could easily be separated from the $IR$ drop, due to series resistance, because the time constants of the former were appreciably greater in all runs than the cut-off time.

The third factor encountered in polarization measurements is the voltage drop, $E_d$, across the diffuse double layer. This is considered primarily a concentration effect, and it is evident that its time constant will also be larger than that of the series resistance.

There may be considerable overlapping between the three factors. This may consist of a diffuse double layer discharge with a time constant of the same order as the cut-off time and the adsorbed layer discharge. Or it may consist of an adsorbed double layer discharge which overlaps the diffuse double layer discharge time, both being considerably larger than the cut-off time. In interrupter studies of polarization phenomena, it is important, if possible, to arrange the experimental conditions so that the time constants of each of these three factors may be as widely separated as possible.

Stern (13) proposed the structure of the double layer outlined above. He combined the Helmholtz (14) simple fixed adsorbed layer with the Gouy (15) diffuse layer.

Gatty and Spooner (16) from a study of the electrocapillary curve stated that close to the potential of the electrocapillary maximum the double layer is largely of the diffuse type. However, farther away from the potential of the electrocapillary maximum the capacity seemed constant over a considerable range of potential suggesting to them that the double layer is predominantly of the Helmholtz or adsorbed layer type.

Grahame (12, 17) assumes that the adsorbed double layer only contains such ions as may be specifically adsorbed on the metal surface. Since, at the cathode, specific cation adsorption can be considered negligible, each ion in the double layer will confer its own characteristic value of capacity on the adsorbed layer, the actual value being an average depending on the relative amounts of the several ions in the neighborhood of the adsorbed layer. Further, except near the electrocapillary maximum for very dilute solutions, the capacity of the adsorbed layer will be much smaller than the capacity of the diffuse layer.

Changes in concentration at the electrode surface result in concentration polarization phenomena. These concentration changes cause such occurrences as film formation, hydrogen liberation at the cathode, and liberation of oxygen at the anode. In addition to the diffuse layer formed by concentration changes, the formation of dielectric films may result in an effective decrease in the area of the bare metal. Capacity effects, due to this dielectric film being inter-

posed between the surface and the double layer, will be present. Actually the capacity and resistance effects on the electrode surface must be looked upon as a complex network of parallel and series combinations. The dielectric constants and their thicknesses at different areas of the surface may vary greatly. Also the current density at various areas will probably vary from essentially zero to a relatively high value depending on the shunting resistances. The potential and capacity measurements made by the interrupter technique developed here represent an overall average effect. In addition to the above complications, capacity and resistance values are not necessarily constant during interruption as is assumed in the analysis of the time-potential traces. However, there is an indication that, for the short period of time required for these measurements, the change in these values is not appreciable.

### *Zinc Anodes*

The experimental results obtained for the zinc anodes indicated that for these runs the time constant for the capacity potential discharge was appreciably greater than the cut-off time. This permitted a good separation from potential drop due to series resistance. Since the total voltage drop due to polarization was not accounted for by the voltage drops across the capacity decay for the maximum interruption time available, it was evident that this polarization decay did not represent the total discharge of the double layer. Instead, it is believed that the adsorbed and the diffuse double layers had widely different time constants. The capacity discharge observed was for the section of the double layer having a time constant which allowed complete discharge during the interruption time used. The time constant of the remaining part of the double layer was of a much higher order and its discharge during this time was negligible.

It appears that the polarization decay observed at the zinc anodes is due to the discharge of the adsorbed double layer rather than that of the diffuse double layer. The capacity effect at the adsorbed double layer is due to a layer of adsorbed anions plus the concentration effects of neighboring ions in the diffuse layer. The adsorbed anions would react with the zinc ions going into solution, thus not allowing the capacity effect due to this specific adsorption of anions to build up to a high value. The formation of films due to the precipitation of the reaction products of zinc and the anions in the sea water would also tend to reduce the value of the adsorbed layer capacity because of the effective increase in dielectric thickness. The diffuse layer, however, will consist of a high concentration of positive zinc and other ions which should result in a high capacity value for this layer.

In the electrical analogy for the anode surface (Fig. 14) the value of $C_aR_a$ is considered to be appreciably less than $C_dR_d$. There is virtually complete discharge of the adsorbed layer within the maximum interruption time available with the several possible exceptions which are shown in Table I. For apparent current density values of 0.10 ma/cm² and below, there was no measurable potential change in practically all runs until after the first day. The runs at high current densities all showed relatively high capacities after the first several hours which dropped considerably the next day. The diffuse double layer discharge, however, apparently had a much larger time constant and its contribution to the potential change during interruption was negligible.

It was hoped that the capacity values found by this method could be used to determine the relative true current densities. The data, however, showed that there was no simple direct linear relationship between true area and capacity. The reason for this is believed to be mainly due to the fact that the capacitors formed by the adsorbed layer on the electrode surface are not flat plate condensors, because the contour of the surface is very irregular. The relative contour of the surface is also apparently not the same at different current densities or at different times during a run. There was, however, a fair relationship between area and capacity found for the large electrodes which were run at the lower current densities and the small electrodes run at the higher current densities, each taken as an individual group (Fig. 15). The relative current density was calculated by assuming a direct linear relationship between area and capacity. The capacity value used as a base was the initial value found for the run at the highest apparent current density of 0.5 ma/cm². This was 14.8 microfarads and this value was divided by the apparent area of the electrode to give the relative area.

### *Steel Cathodes*

The separation of the $IR$ drop due to series resistance from the capacity voltage drop for the steel cathodes was easily accomplished since there were essentially no capacity voltage changes during the one-microsecond interruptions. The voltage change due to the capacity discharge was generally much smaller than for the zinc anodes and, in many cases, no potential change could be detected even at the maximum interruption time.

Table II shows that the measured capacity polarization was usually much less than one per cent of the total polarization. Hence, the major polarization change did not take place since it apparently had

a considerably higher time constant than 100 microseconds. It was not apparent in the case of steel cathodes whether the capacity effect observed consisted of the adsorbed or diffuse layer discharge.

Potential changes representing capacity discharge at the early part of the runs, especially at the lowest current densities, were negligible in most cases. This was apparently due to the large surface of steel exposed which resulted in high capacities and low shunting resistances for both parts of the double layer. As the calcareous coating was formed a large part of the original area of the electrode surface was effectively reduced. This resulted in a reduction of the capacity of the part of the double layer discharged plus an increase in the parallel resistance across it. The increase in the parallel resistance would give a larger *IR* drop across this part of the double layer which, together with a possible decrease in the time constant, would result in a measurable decay within the interruption time used.

The use of capacity measurements for the determination of relative true area was not satisfactory. In addition to the reasons given for zinc anodes, there was also the fact that the accuracy in determining these values was not very high. This was because of the very low potential changes and difficulty in accurately determining the time constants.

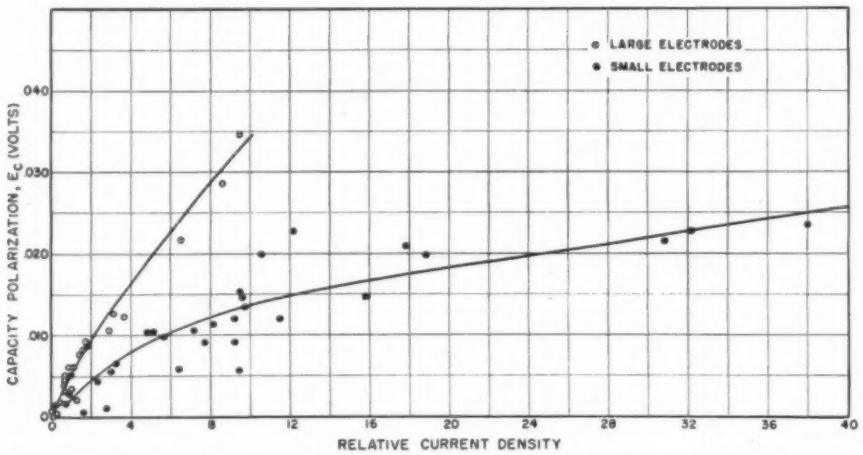


FIG. 15. Relationship between relative current density and capacity polarization of zinc anodes.

## SUMMARY

An electronic d-c current interrupter method has been developed which should be helpful in fundamental studies of electrode phenomena. The useful range of this interrupter can be extended and varied for the investigation of particular problems.

This electronic interrupter technique has been used to carry out a fundamental study of the zinc-steel couple in a synthetic sea water electrolyte. Series resistance effects in the measurement of closed circuit potentials can be determined and corrected for. This method also permitted the placing of the reference electrode at a distance from the electrode being observed, thus eliminating local area effects and measuring the average potential on the electrode surface. This further resulted in more stable and, therefore, more accurate potential measurements.

The measurement of capacity effects, due to the double layer and the polarization phenomena associated with these effects, were carried out for the zinc and steel electrodes. This information should help to lead to a basic understanding of the electrochemical properties of these metals.

These investigations are preliminary; further studies of this type are necessary to give a more complete understanding of electrode processes.

The zinc-steel couple in a synthetic sea water electrolyte is a very complex system. Investigations of this couple in sea water are to be supplemented by studies of more elementary systems. For example, the study of mercury as an electrode in simple electrolytes should be helpful in associating the measurements obtained by the interrupter method with the basic electrocapillary and double layer theories.

## ACKNOWLEDGMENTS

The assistance of a number of the personnel of the Naval Research Laboratory was instrumental in carrying out this study. Thanks are due to Emmanuel Goldstein for his suggestions on the use of pulses for current interruption, and to Neil Davis and Emerson Zettel for their assistance and advice in the necessary electronic instrumentation.

Any discussion of this paper will appear in a Discussion Section, to be published in the June 1951 issue of the JOURNAL.

## REFERENCES


1. T. P. MAY, G. S. GORDON, AND S. SCHULDINER, "Anodic Behavior of Zinc and Aluminum-Zinc Alloys in Sea Water," "Cathodic Protection—A Symposium," p. 158, The Electrochemical Society and National Association of Corrosion Engineers, Houston, Texas (1949).
2. E. NEWBERRY, *J. Chem. Soc.*, **125,** 511 (1924).
3. E. NEWBERRY, *Trans. Electrochem. Soc.*, **58,** 187 (1930).
4. E. NEWBERRY, *Trans. Faraday Soc.*, **43,** 127 (1947).
5. A. L. FERGUSON, *Trans. Electrochem. Soc.*, **76,** 113 (1939).
6. A. L. FERGUSON, *Disc. Faraday Soc.*, **1,** 50 (1947).
7. A. HICKLING, *Trans. Faraday Soc.*, **33,** 1540 (1937).
8. A. HICKLING AND F. W. SALT, *Trans. Faraday Soc.*, **37,** 450 (1941).
9. A. FRUMKIN, *Acta Physicochim.* U.R.S.S., **18,** 23 (1943).
10. F. W. SALT, *Disc. Faraday Soc.*, **1,** 169 (1947).
11. F. P. BOWDEN AND E. K. RIDEAL, *Proc. Roy. Soc. London*, **120A,** 59, 80 (1928).
12. D. C. GRAHAME, *Chem. Revs.*, **41,** 441 (1947).
13. I. STERN, *Z. Elektrochem.*, **30,** 508 (1924).
14. H. VON HELMHOLTZ, *Wiss. Abhandl. physik.-tech. Reichsanstalt*, **1,** 925 (1879).
15. G. GOUY, *J. phys.* **9,** 457 (1910).
16. O. GATTY AND E. C. R. SPOONER, "The Electrode Behavior of Corroding Metals in Aqueous Solutions," p. 481, Clarendon Press, Oxford (1938).
17. D. C. GRAHAME, *J. Am. Chem. Soc.*, **68,** 301 (1946).

# Effect of Magnetic Transformation at the Curie Temperatures on Oxidation Rates of Chromium-Iron Alloys[1]

HERBERT H. UHLIG AND ANTON DE S. BRASUNAS
*Corrosion Laboratory, Massachusetts Institute of Technology, Cambridge, Massachusetts*

ABSTRACT

Oxidation rates of chromium-iron alloys containing 9.2 to 24 per cent chromium have been carried out in oxygen at temperatures above and below the Curie temperatures. Plots of the logarithms of the oxidation rates with the reciprocal absolute temperatures show discontinuities at the Curie temperatures. In general, activation energies calculated from the oxidation rate data are higher above the Curie temperatures than below.

The data lend support to the view that rate of formation of thin films is controlled by reaction phenomena at the metal-oxide interface. Rideal and Jones showed earlier that the rate-controlling step may involve transfer of electrons from the metal; therefore, a higher work function for the metal above than below the Curie temperatures may be associated with the observed trend of activation energy.

Since the Curie temperature is an electronic transition, the data also support the view that electronic changes in the chromium-iron alloys can affect the initial reaction rates.

The current theory regarding oxidation of metals emphasizes the part played by an oxide or other compound as a diffusion barrier (1). The classic work of Wagner (2) made clear the complex nature of the barrier, and proved that oxidation rates, in many instances, are controlled by diffusion of metal ions, not atoms, outward through the barrier (or lattice vacancies inward) and also by the electrical resistance of the barrier to accompanying electrons also moving outward (or positive holes moving inward). Using only independent physicochemical data, Wagner calculated the rate of tarnish of silver and oxidation of copper in close agreement with the observed rates. This electrochemical theory of oxidation was applied specifically to situations where the square of the film thickness on a metal is proportional to the time of reaction, or the so-called quadratic reaction rate equation is obeyed. For these cases, the specific structure of the metal is not important. Instead, only the relative ease with which diffusion can occur in the semi-conductor barrier needs to be considered.

A review of data on oxidation and tarnish, however, reveals the fact that the base metal cannot always be ignored. For example, when thin oxide films are formed, orientation of the metal grains has a pronounced effect on oxidation rate (3), as is well known to metallographers who sometimes use heat tinting to differentiate one grain from another. Also, Tammann showed experimentally many years ago that the iron-nickel alloys undergo a discontinuous change in the oxidation rate above and below the alpha-gamma allotropic transformation temperatures (4). Later Portevin, Prétet, and Jolivet (5), investigating the oxidation of iron, showed a similar change in rate at the critical temperature. This was followed by an investigation of Fischbeck and Salzer (6) showing the same trend at the critical temperature of iron oxidized in carbon dioxide, oxygen, and other gases. Tammann and Siebel's work went further in demonstrating that discontinuities in the oxidation rate also occur at the temperature of transformation from ferromagnetism to paramagnetism, or at the Curie temperatures of their alloys. Their paper, however, was largely forgotten, perhaps because of doubt that their measurements of film thickness by interference colors were sufficiently precise.

The possible effect of Curie temperature on oxidation rate, however, is basic to our understanding of oxidation mechanism. Further experiments seemed worthwhile, therefore, if for no other reason than to prove or disprove the conclusions reached by Tammann from data on iron-nickel alloys.

We considered the chromium-iron alloys well suited to the further exploration of this study. Iron, for example, oxidizes so rapidly at the critical temperature of 910°C, or at the Curie temperature of 769°C, that control of the variables is not easily attained. The thick oxide, formed in relatively short time, spalls in unpredictable fashion during oxidation and afterward. The chromium-iron alloys, on the other hand, oxidize more slowly, and, in addition, the Curie temperatures, by and large, are below that of iron.

## EXPERIMENTAL PROCEDURE

The alloys studied were laboratory induction melts prepared from low metalloid iron and ferrochrome. The ingots were homogenized, hot swaged, then

[1] Manuscript received May 16, 1950. This paper prepared for delivery before the Buffalo Meeting, October 11 to 13, 1950.

hot rolled to sheets 0.1 in. (0.25 cm) thick. The analyses are given in Table I.

Specimens measured $1\frac{1}{4}$ in. by 3 in., or 6 in. (3.2 cm by 7.6 cm, or 15 cm) and were abraded first on moving belts, then by hand to successively finer grades of emery paper, finishing with 00 paper. Since surface contamination of any kind, such as by fingerprints, changed the oxidization rate, it was necessary to work with gloves, both in handling the specimens during the fine abrading and also during and after the cleaning operation in boiling redistilled benzene. If a single specimen was used again for a subsequent test, it was found necessary to remove not only the oxide in accord with the above procedure, but also a definite amount of metal sufficient to eliminate that portion of the surface depleted in chromium by the oxidation reaction. Otherwise, the oxidation rates were higher than the rates obtained with specimens not used previously. The serious and persistent effect of minor contamination was also found by Vernon (7) and his co-workers in their careful work on the oxidation rates of zinc. They found that grease, once thoroughly in contact with a zinc surface, could not be removed by ordinary methods of degreasing nor even by abrading with emery paper, the oxidation rates thereafter being considerably higher than normal. Leontis and Rhines (8) also reported an erratic effect in their study on the oxidation of magnesium at elevated temperatures, which may have had its source in a similar cause. We had ample evidence of this factor in our work with the chromium-iron alloys.

For all alloys, total thickness of films, assuming a density of oxide equal to 5.2, ranged from 300 Å to 5800 Å, except for the 10.6 per cent Cr alloy above the alpha-gamma transition temperature, where the films were thicker. Visible spalling with such thin films was not observed, and, hence, no precautions were considered necessary regarding oxide loss during heating and cooling.

Oxidation tests were carried out in an oxygen atmosphere with gas flowing through the furnace at a rate of 600 ml per minute. Temperature of the furnace was controlled automatically by a photoelectric controller and the absolute temperature was established by reference to a platinum-platinum rhodium thermocouple.

## Results

The logarithms of the oxidation rates calculated as milligrams per square decimeter weight-gain per total exposure time are plotted with the reciprocal of the absolute temperature in Fig. 1 to 5. In accord with the Arrhenius reaction rate equation,

$$k = Ae^{-\Delta E/RT} \qquad \text{(I)}$$

(where $k$ is the reaction rate, $A$ is a constant, $\Delta E$ is the activation energy, $R$ is the gas constant, and $T$ is the absolute temperature) data so plotted are straight lines. Significantly, a discontinuity in slope occurs at the specific Curie temperature for each alloy considered, where Curie temperatures are taken from data assembled by Hansen (9). In addition, because data for the 10.6 per cent chromium alloy were carried to temperatures above the alpha-gamma transformation temperatures, a second discontinuity exists at the change of lattice structure from body-centered cubic to face-centered cubic. Weight gains for the 24.1 per cent Cr alloy (Fig. 5) are given only above the Curie temperature (615°C) because the weight changes below were too small for adequate determination of the slope. Scattering of the data for some alloys owed to the fact that data were obtained by more than one investigator, accounting possibly for slightly differing surface preparation, despite tedious precautions.

The data are sufficiently concordant, nevertheless, to establish that the oxidation rates are altered by electronic changes in the alloys occurring at the Curie temperatures. Less weight should be placed on the actual slopes of log rate vs. $1/T$ because of the inherent difficulty of reproducing such slopes from one run to another, or from one investigator to another, in the same sense that previous investigators found difficulty. The empirical slopes plotted with composition of the alloys in the form of $\Delta E$, or the activation energy[2], plotted with per cent chromium, are shown in Fig. 6 and appear reasonably consistent. Activation energies obtained from available data of other investigators are also included. The activation energies were calculated assuming that the weight gain $W$ per specified time is proportional to the logarithm of the time of exposure as was indicated to be the case by Tammann and co-workers for thin films on iron, nickel, zinc, and other metals (4, 10, 11) and by Vernon *et al.* (7) for iron and zinc. We have, therefore,

$$W = k \log (t + 1) \qquad \text{(II)}$$

where $k$ is a constant and $t$ is the time of exposure. Also

$$\log W = \log k + \log \log (t + 1). \qquad \text{(III)}$$

TABLE I. *Analyses of alloys*

| % Cr | % C | % Si | % Mn |
|---|---|---|---|
| 9.22 | 0.09 | 0.18 | 0.34 |
| 10.59 | 0.06 | 0.17 | 0.34 |
| 12.22 | 0.07 | 0.19 | 0.30 |
| 13.84 | 0.05$_5$ | 0.25 | 0.34 |
| 19.12 | 0.07 | 0.32 | 0.36 |
| 24.08 | 0.08 | 0.32 | 0.40 |

[2] The activation energies discussed here and further on should be considered apparent values without any necessary operational interpretation.

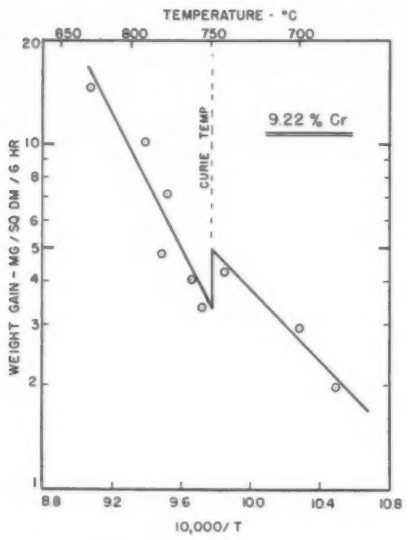


FIG. 1. Oxidation of 9.22% Cr-Fe alloy in oxygen for 6-hour exposure as a function of temperature.

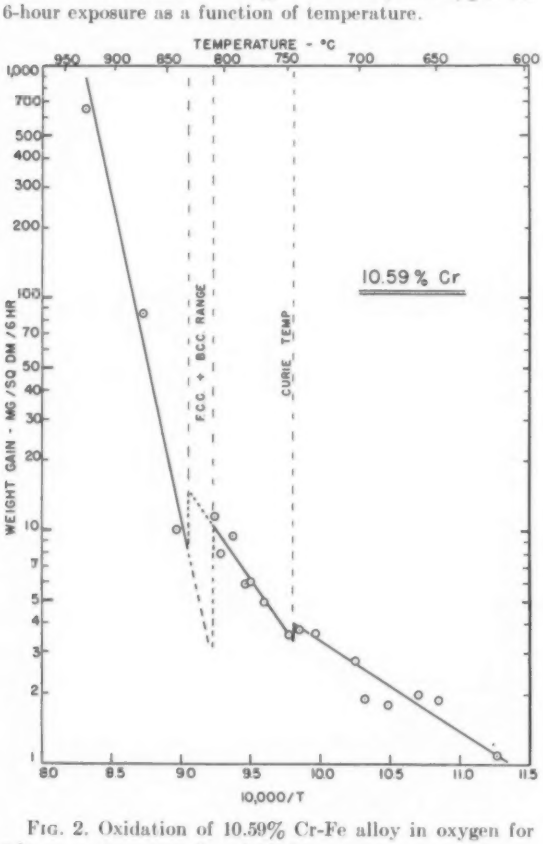


FIG. 2. Oxidation of 10.59% Cr-Fe alloy in oxygen for 6-hour exposure as a function of temperature.

Hence, plotting log $W$ vs. $1/T$ for an established value of $t$ is essentially the same as plotting log $k$ vs. $1/T$, the slope of which in both cases is $\Delta E/2.303\ R$ [refer to equation (I)].

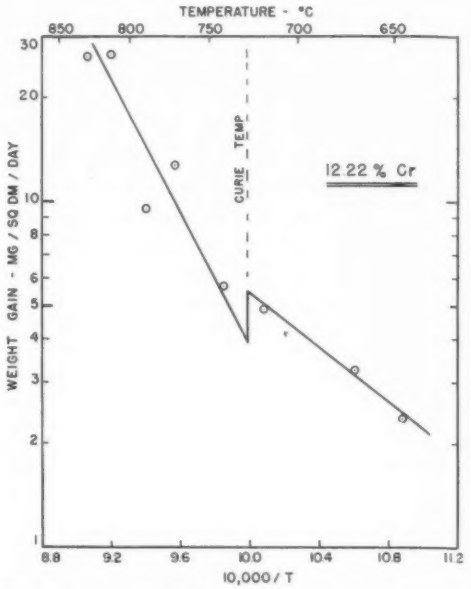


FIG. 3. Oxidation of 12.22% Cr-Fe alloy in oxygen for 24-hour exposure as a function of temperature.

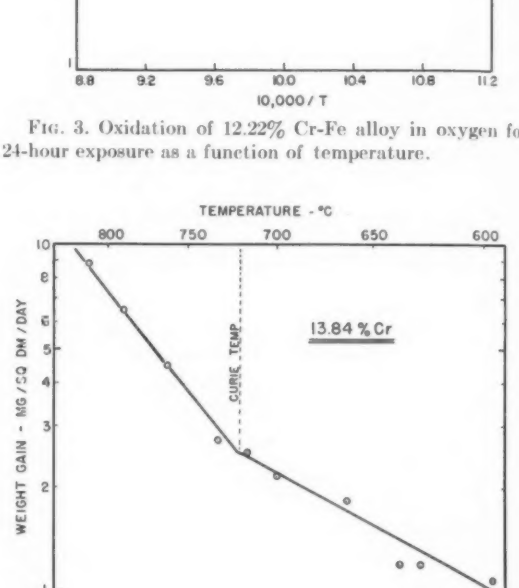


FIG. 4. Oxidation of 13.84% Cr-Fe alloy in oxygen for 24-hour exposure as a function of temperature.

The immediate conclusion from Fig. 6 is that the activation energies for oxidation above the Curie temperatures lie higher than values below. The limited data of McAdam and Geil (12) lead to the same conclusion, although these investigators did not analyze their data in this way. Their values of rates plotted in a manner similar to Fig. 1 to 5 also show a change in slope at the Curie temperatures for the 13.6 per cent and 24.4 per cent compositions, the two alloys for which they obtained data above and below the Curie temperatures. Activation energies above the Curie temperatures are in fair agreement

with our values, but activation energies below are consistently lower. This is most likely caused by differences of incidental impurities in their alloys compared with ours, although other factors may also enter.

Activation energies for iron, where thin films are formed, calculated from data of Tammann and Köster (11), and also of Vernon, Ackeroyd, and Stroud (7), as well as of McAdam and Geil (12), are all within the range of 4,000 to 9,000 calories per mole. This establishes a relatively low value of $\Delta E$ for iron, definitely less than the approximate 20,000 calories per mole value for the 9 to 12 per cent Cr compositions below the Curie temperatures. It seems likely, therefore, that a maximum in the curve is reached at a chromium composition below 9 per cent.

## Discussion

Rideal and Jones (13) showed from their study of the oxidation of platinum at elevated temperatures, and from their analysis of data on rate of oxidation of tungsten and carbon, that the following equation holds:

$$\Delta E = \phi - K$$

where $K$ is a constant equal to 3.6 electron volts and $\phi$ is the work function of the metal or carbon. The work function, it will be remembered, is the energy in electron-volts necessary to remove an electron from a metal or other conductor. This relation holds very well for the substances named, as data of Table II indicate.

Accordingly, the higher the work function, the higher is the activation energy for reaction. It also follows that for metals with work functions equal to or below 3.6 electron volts, such as sodium (2.37 ev) and magnesium (3.60 ev) the activation energy is essentially zero, and these metals react immediately, therefore, upon exposure to oxygen. By the same token, when the work function is higher and an activation energy exists, reaction is not immediate but is preceded by adsorption of gas on the metal surface. The relative life of the adsorbed gas-atoms before becoming part of a true surface oxide lattice depends both on the temperature and the magnitude of the activation energy. This view accords reasonably well with the facts, and also with the property of passivity in metals like chromium and the stainless steels, where adsorbed films are thought, according to one viewpoint, to accompany this property (14).

If, in general, a higher value of work function leads to a higher activation energy for oxidation, the present data indicate that the work function of the chromium-iron alloys above the Curie temperatures should be higher than below the Curie temperatures, since the activation energies of Fig. 6 are in this order. Data on the work functions of the chromium-iron alloys are not available, but parallel data have been obtained for nickel. Here it was shown, indeed, that the work function for nickel is higher above the Curie temperature than below, the values for outgassed nickel (15) being 5.05 ev below and 5.20 ev above. The difference of 0.15 ev is equivalent to

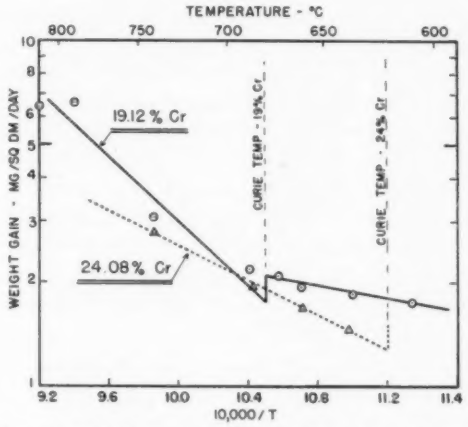


FIG. 5. Oxidation of 19.12% Cr-Fe alloy, and 24.08% Cr-Fe alloy in oxygen for 24-hour exposure as a function of temperature (24.08% alloy above Curie temperature only).

TABLE II. *Relation of activation energy of oxidation to work function (Rideal and Jones)*

Electron volts

| Substance | $\Delta E$ | $\phi$ | $\phi - E$ |
|---|---|---|---|
| Pt | 2.74 | 6.35 | 3.61 |
| W | 0.87 | 4.48 | 3.61 |
| C | 0.52 | 4.31 | 3.79 |

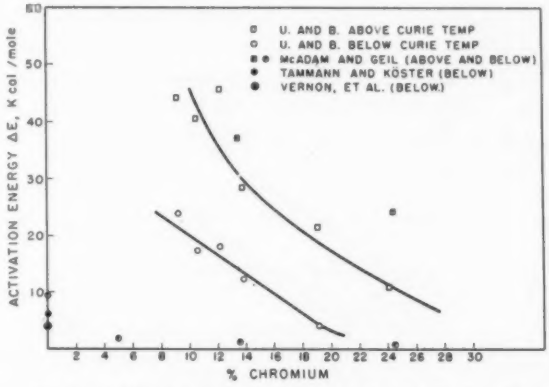
U. AND B. ABOVE CURIE TEMP
U. AND B. BELOW CURIE TEMP
McADAM AND GEIL (ABOVE AND BELOW)
TAMMANN AND KÖSTER (BELOW)
VERNON, ET AL. (BELOW)
ACTIVATION ENERGY ΔE, K cal /mole
% CHROMIUM

FIG. 6. Activation energies for oxidation of Cr-Fe alloys above and below the Curie temperatures.

3,460 calories per mole. This value is less than the difference shown in Fig. 6 where the activation energies above and below the Curie temperatures differ by about 20,000 calories per mole or about 0.9 ev. Presumably, therefore, the work functions for the chromium-iron alloys above and below Curie temperatures differ by more than the corresponding values for nickel.

It is pertinent that a partial dependence of oxidation on work function of the metal is implied by the theory of Mott (16) for growth of thin films. As must surely be the case, factors in addition to work function also enter the general rate equation, as Mott suggested. More than casual comparison of his theory with experiment has not yet been carried out, but the point of view to which it leads, namely that the reaction rate involving thin films is controlled at the metal-oxide interface, rather than within the oxide, is in accord with the present data.

From the Rideal-Jones relation it appears plausible that some metal-oxide reactions involving thin films are controlled only by rate of transfer of electrons from metal to oxide, measured by the work function of the metal. This point of view is consistent with differing oxidation rates of metal crystal faces, since the work function also differs with orientation (3). The relation can also account in part for differing activation energies for reaction above and below phase transformations, as well as above and below magnetic transformations, since the work function of the metal changes with lattice structure (17, 18).

Finally, since the Curie temperature transformation is essentially an electronic change in the metal, the fact that the activation energy for oxidation also changes at this temperature may be taken as evidence that electronic changes affect the initial reaction rates of the chromium-iron alloys and the iron-nickel alloys, data for the latter coming from Tammann and Siebel.

### Acknowledgment

The authors express their appreciation to Milton Stern for able assistance in weighings and specimen preparation. The investigation was made possible by a grant from the Office of Naval Research on Contract No. N5ori-78, T. O. 15.

Any discussion of this paper will appear in a Discussion Section, to be published in the June 1951 issue of the JOURNAL.

### REFERENCES

1. U. R. EVANS, "Metallic Corrosion Passivity and Protection," pp. 134–149, Edward Arnold and Co., London (1946).
2. C. WAGNER, "Handbuch Der Metall-Physik," Edited by G. Masing, **1,** No. 2, pp. 124–165, Leipzig (1940), reprinted by Edwards Brothers, Ann Arbor, Michigan.
3. A. T. GWATHMEY, "Corrosion Handbook," Edited by H. H. Uhlig, pp. 33–5, John Wiley & Sons, Inc., New York (1948).
4. G. TAMMANN AND G. SIEBEL, *Z. anorg. Chem.*, **148,** 297 (1925).
5. A. PORTEVIN, E. PRÉTET, AND H. JOLIVET, *Rev. mét.*, **31,** 221 (1934).
6. K. FISCHBECK AND F. SALZER, *Metallwirtschaft*, **14,** 753 (1935).
7. W. H. J. VERNON, E. ACKEROYD, AND E. STROUD, *J. Inst. Metals*, **65,** 301 (1939).
8. T. E. LEONTIS AND F. N. RHINES, *Trans. Am. Inst. Mining Met. Engrs.*, **166,** 265 (1946).
9. M. HANSEN, "Zweistofflegierungen," p. 525, Berlin (1936), reprinted by Edwards Brothers, Ann Arbor, Michigan.
10. E. SCHRÖDER AND G. TAMMANN, *Z. anorg. Chem.*, **128,** 179 (1923).
11. G. TAMMANN AND W. KÖSTER, *Z. anorg. Chem.*, **123,** 196 (1922).
12. D. J. MCADAM, JR., AND G. W. GEIL, *J. Research Nat. Bur. Standards*, **23,** 63 (1939).
13. E. K. RIDEAL AND O. H. WANSBROUGH-JONES, *Proc. Roy. Soc. London*, **123A,** 202 (1929).
14. H. H. Uhlig and R. B. Mears, "Corrosion Handbook," Edited by H. H. Uhlig, pp. 22–33, John Wiley & Sons, Inc., New York (1948).
15. A. B. CARDWELL, *Phys. Rev.*, **76,** 125 (1949).
16. N. F. Mott, *Trans. Faraday Soc.*, **43,** 429 (1947).
17. A. GOETZ, *Phys. Rev.*, **33,** 373 (1929).
18. A. B. CARDWELL, *Phys. Rev.*, **38,** 2033 (1931).

# Studies on Galvanic Couples

## III. Polarization and Cathodic Protection[1]

H. D. Holler

*National Bureau of Standards, Washington, D. C.*

ABSTRACT

The mechanism of polarization of a galvanic couple is developed. By means of separate elements in an electric network, the roles of electrode potentials and of resistive-potential differences are demonstrated in polarization and cathodic protection. Several methods of showing the relation between polarizing current and galvanic-couple potential are discussed. The electrical conditions which determine the distribution of current flowing to a galvanic couple are defined. The use of the term "current density" in cathodic protection should be carefully qualified; otherwise, it may be meaningless.

### I. Introduction

In any electrochemical process, a counter electromotive force usually results from the flow of current. This phenomenon, known as polarization, is an important retarding factor in the galvanic corrosion of metals. The usual method of studying the polarization of a galvanic cell consists of first measuring its emf with no external current flowing and then determining the potential-current relations for different currents, the latter being measured in the external circuit.

However, the electrode surfaces themselves behave like short-circuited galvanic cells with internal currents not subject to direct measurement, and the polarization thereon affects the electrode potentials. Although polarization opposes these currents, they cannot be extinguished entirely by self-polarization, because the latter requires some current to maintain it. They may, however, be reduced to zero by increasing the polarization through the application of external current. This is the mechanism of stopping galvanic corrosion by cathodic protection.

It is the purpose of this paper to relate the behavior of a galvanic couple toward external current to the problem of ascertaining when cathodic protection is accomplished.

### II. Behavior of a Galvanic Couple toward Applied Current

Let a galvanic couple $G$, consisting of an anode $A$ and cathode $C$, be joined electrically to an auxiliary electrode $X$ in the same electrolyte. When $X$ is cathodic to $G$, external current $I$ will flow in the direction indicated in Fig. 1. The total current from the anodic area $A$ will then be $I + i$, where $i$ is the internal current within the galvanic couple. Any increase in polarization at the anode, caused by the higher current density resulting from $I$, reduces the magnitude of $i$. Such a reduction in $i$, caused by increased polarization, has been called the "difference effect" (1).

In accordance with Faraday's law,

$$W = (I + i)kt \qquad \text{(I)}$$

where $W$ = weight of metal dissolved, $k$ = electrochemical equivalent, and $t$ = time.

Since $i$ is not included in the meter reading, which indicates $I$ only, the total anodic weight-loss represented by equation (I) may be greater than that equivalent to the observed current. The *apparent* current efficiency is then over 100 per cent. If, through the "difference effect," $i$ becomes zero, the measured current $I$ will represent the true rate of metal dissolution.

When $X$ is anodic to $G$ the current pattern will be that shown in Fig. 2, where the total current flowing to cathode $C$ is $I + i$. Any increased polarization, at the cathode, resulting from the larger cathodic current, opposes the internal current $i$. Any reduction in $i$, resulting from this increased cathodic polarization, is called "cathodic protection." If this effect is great enough to reduce $i$ to zero, the loss of metal on the anodic area due to galvanic corrosion is completely stopped.

Now let an external emf $E_t$ be introduced (Fig. 3). If $E_t$ is adjusted until $I = 0$, then $E_t = (E_G - e_x)$. If $E_t$ is increased, then

$$E_t = (E_G - e_x) + IR_t \qquad \text{(II)}$$

where $E_G$ = the potential of the galvanic couple, $e_x$ = the potential of the auxiliary electrode, and $R_t$ = the total resistance in the circuit.

If we vary the magnitude and direction of $E_t$, and simultaneously measure $I_a$, $I_c$, and $I$ we obtain the three polarization curves shown in Fig. 4, one for anode $A$, one for cathode $C$, and one for couple $G$, respectively. These relations are fundamental in the

[1] Manuscript received May 1, 1950. This paper prepared for delivery before the Buffalo Meeting, October 11 to 13, 1950.

FIG. 1. Path of current $I$ when $X$ is cathodic to couple $G$ in same electrolyte.




FIG. 2. Path of current $I$ when $X$ is anodic to couple $G$ in same electrolyte.




FIG. 3. Path of current $I$ depends on relation, $E_t \gtreqless E_G - e_x$.

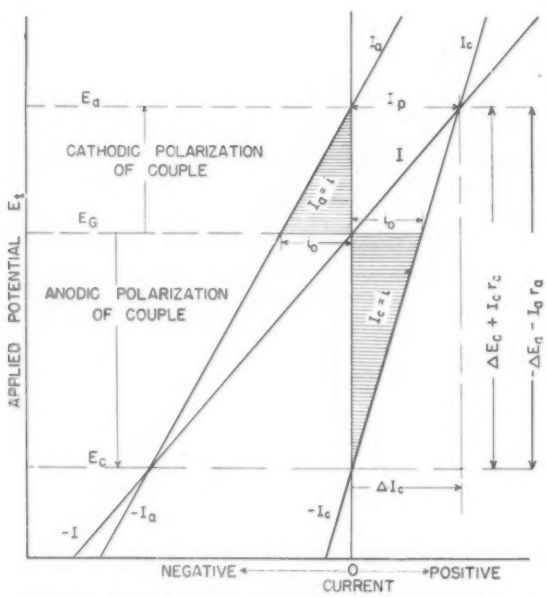


FIG. 4. Three polarization curves showing relation of $I_a$, $I_c$, and $I$ to $E_t$.

study of cathodic protection. For example, complete cathodic protection is achieved when anodic current $I_a = 0$. The applied current required to do this is $I_p$ and the total polarization (emf + $ir$) of the cathode is

$$\Delta E_c + I_p \cdot r_c$$

where $r_c$ = the resistance of the cathodic path of current $I_p$ and $\Delta E_c$ = emf of polarization. The condition for cathodic protection as defined by Mears and Brown (2) is then

$$E_c + \Delta E_c + I_p \cdot r_c = E_a \qquad \text{(III)}$$

which means that the polarized potential of the cathodic area is equal to the open-circuit potential of the anodic area. The value of $E_a$ here depends upon the environment created by the flow of current until a steady state exists.

## III. Determination of "Protective Current" and "Protective Potential"

The logical approach to this problem is the correlation of the causative factor $E_t$ with any measurable effects which are related to the reduction of $i$ to zero. Among these are changes in $ikt$, $E_G$, and $I$. The determination of the rate, or extent of corrosion, by weight-loss ($ikt$) is seldom practicable except on small test-specimens. The measurement of $E_G$ may serve as a criterion for cathodic protection if its relation to $E_a$ is already known for the given environment. Any change in the relation of $E_G$ or $E_t$ to $I$, occurring at $I_p$, may also be used as criteria of complete cathodic protection.

In equation (II) it may be seen that any change in $E_G$ will be reflected in $E_t$. Therefore, if attainment of $I_p$ is accompanied by an increment in $E_G$, a corresponding inflection in the $E_t/I$ curve, as well as the $E_G/I$ curve, will indicate cathodic protection. If conditions are favorable, we then have the possibility of at least four electrical criteria of cathodic protection: first, the relation of $E_G$ to $E_a$, if the latter is known; second, an inflection in the $E_G/I$ curve; third, a corresponding inflection in the $E_t/I$ curve; fourth, any relation of $E_G$ to $I$, at $I_p$, indicating hydrogen overvoltage.

The measurement of $E_G$ has been described in Part I (3). When the reference electrode $E_s$ is introduced in Fig. 5, the resistive components, $Ir_s$ and $IR_G$, are deducted by balancing the Wheatstone bridge. Then the emf $(E_G - E_s)$ is observed as $2V_g$, where

$$E_G = e_a - i_o r_a \qquad \text{(IV}a\text{)}$$

$$= e_c + i_o r_c \qquad \text{(IV}b\text{)}$$

and

$$i_o = \frac{e_a - e_c}{r_a + r_c} \qquad \text{(V)}$$

## IV. Elementary Relations in Application of Cathodic Protection

For the purpose of illustration, the electrode potentials of several metals in wet clay are given in Table I, as measured with a high-resistance poten-

tiometer using the carbon-manganese dioxide electrode as reference. Although no external current was flowing to or from these metals during measurement, the observed potentials must not be considered values of $E_a$. Due to local galvanic currents on their surfaces, the potentials observed were really some mean value of the galvanic couple potentials $E_G$, being somewhere between the polarized potentials of the local anodes and cathodes. The tabulated values must, therefore, not be considered accurately reproducible, since they depend upon the particular status of the galvanic couples at the moment of measurement. The open-circuit potential $E_a$ might have been observed for each metal if it had been cathodically polarized just the right amount, that is, until the condition in equation (III) is met. The problem of determining this "right amount" is the basic problem of cathodic protection.

If we assemble a galvanic couple of iron and copper, using meters to measure the currents as indicated in Fig. 3, we find that in order to prevent galvanic current flowing between the two metals, they must be brought to the same potential. This may be accomplished by polarizing one of the metals, as for example, by passing current to the copper from some auxiliary anode as carbon, until the polarized potential of copper becomes $-1.26$ volts, which is that of iron under the given environment. This is the result of electrochemical action at the phase boundary of copper caused by cathodic current $\times$ time, or coulombs.

It should be fully realized that the polarized potential is the result of a change in environment produced by the current, the metal itself remaining unchanged.

It is informative to consider the difference in the magnitude of $E_t$ required to drive current from carbon to copper before, and after, it is joined to iron. The emf of the carbon/copper cell is

$$e_x - (-0.56) = e_x + 0.56.$$

Before joining, current will begin to flow to copper when

$$E_t > e_x + 0.56.$$

After joining, current will begin to flow to the copper when

$$E_t > e_x - E_G$$

where $E_G$ is somewhere between $-0.56$ and $-1.26$; and as $E_t$ is gradually increased, current flows to copper because its potential is exceeded first. On further increasing $E_t$, the increased current to the copper polarizes the copper until its potential $e_c + I_c \cdot r_c$ becomes equal to that of the iron. Then current flows to the iron also; that is, when

$$E_t > e_x + 1.26$$

where $e_x + 1.26$ is the emf of the carbon/iron cell.

One might imagine $E_G$ as a potential "barrier" or "hurdle," which must be exceeded by $E_t$ before the current "spills over" to the copper, the barrier being there by virtue of its contact with iron. If current flows to the iron for a period of time, its potential shifts to higher values as a result of higher alkalinity. When the pH reaches a value of about 9.5 the emf of the iron-hydrogen cell becomes zero and the galvanic corrosion of iron is stopped. The open-circuit potential of iron is then $E_a$.

In studying polarization effects, we have a choice between controlling current and observing variations in potential or controlling potential and observing variations in current, known as the "constant current" or "constant potential" methods, respectively. Since current-density $\times$ time is the immediate cause of polarization, it should be the controlled variable if known. This, however, is rarely the case and in cathodic protection is almost meaningless because of unknown current distribution. For example, the current density at edges or nearby areas may be an order of magnitude greater than on more remote areas. If current is kept constant by the usual practice of maintaining a high resistance and a high applied-voltage in the circuit to reduce the effect of any variations in emf, the purpose of the experiment is largely defeated, because it is the relation between current and any variation in counter emf which we wish to determine.

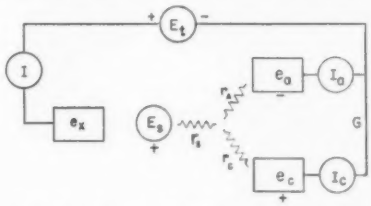


FIG. 5. Introduction of reference electrode $S$ for measuring $E_G$.

TABLE I. *Observed potentials of several metals in wet clay referred to the carbon-manganese dioxide electrode*

| Metal | Volts |
|---|---|
| Magnesium | −2.08 |
| Zinc | −1.57 |
| Aluminum | −1.27 |
| Iron | −1.26 |
| Lead | −1.02 |
| Nickel | −0.63 |
| Copper | −0.56 |
| Carbon-manganese dioxide | 0.00 |

Consequently, if we reduce the resistance in the circuit to a minimum and keep the applied potential constant, any change in current resulting from counter emf may be significant. For this reason, the "constant potential," or polarographic method, is preferred. The relation between $E_t$ and $I$ may be as informative as the relation between $E_G$ and $I$. The technique is, therefore, one of maintaining potential, and allowing current to adjust itself in accordance with the counter emf and with Ohm's law.

In Fig. 4 it is shown that the directions of the currents through a galvanic couple are determined by the magnitude and direction of the applied emf $E_t$. The importance of $E_t$ becomes apparent if we refer to Fig. 5 again and write the equations for the two-mesh network.

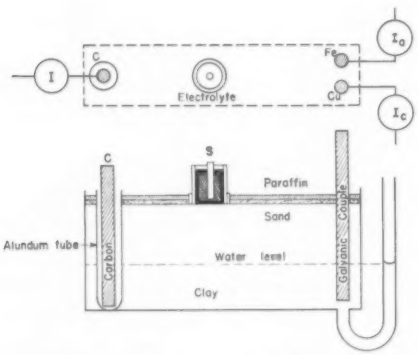


FIG. 6. Laboratory cell for making measurements on a galvanic couple.

Proceeding clockwise, we have

$$E_t - (e_a - e_z) - Ir_z - I_a r_a = 0 \qquad \text{(VI)}$$

and

$$(e_a - e_c) - I_c r_c + I_a r_a = 0. \qquad \text{(VII)}$$

Rearranging for the use of determinants,

$$-I_a r_a = -E_t - (e_a - e_z) - Ir_z \qquad \text{(VIII)}$$

and

$$I_a r_a - I_c r_c = -(e_a - e_c). \qquad \text{(IX)}$$

Expansion of determinants and simplification then gives

$$\frac{I_a}{I_c} = \frac{E_t - Ir_z - (e_a - e_z)}{r_a} \cdot \frac{r_c}{E_t - Ir_z - (e_c - e_z)} \qquad \text{(X)}$$

If we let $E$ = the potential applied across the couple, then

$$E = E_t - Ir_z + e_z$$

and

$$\frac{I_a}{I_c} = \frac{(E - e_a)}{r_a} \cdot \frac{r_c}{(E - e_c)} \qquad \text{(XI)}$$

This relation defines the magnitude and direction of $I_a$ and $I_c$. For example, if $E < e_a$, $I_a$ is negative, which means that current is flowing from the anode to the electrolyte. If $E = e_a$, $I_a = 0$, which means that cathodic protection is achieved. If $E > e_a$, $I_a$ is positive and current is flowing to the area, initially anodic.

This equation of current partition may be used as an electrode potential criterion for cathodic protection, which is achieved when $E = e_a$. This equality should be written $E = E_a$, since the requirement of Mears and Brown still holds. Then since $E$ also equals $E_G + IR_G$, $E_a = E_G + IR_G$ for cathodic protection.

## V. Partition of Current in Galvanic Couples

In order to demonstrate some of these relations for iron-hydrogen couples, a simple cell was set up (Fig. 6) in a Lucite box containing clay which was kept wet by maintaining a water-level as indicated. The couple elements of equal apparent areas were $\frac{5}{16}$-inch (0.79 cm) rods, about 1 inch (2.5 cm) apart, extending $4\frac{3}{4}$ (11 cm) inches into the clay. The auxiliary electrode was a graphite rod dipping in the water in an alundum tube about 11 inches (28 cm) from the rods. The reference electrode was a manganese-dioxide-carbon element of a specially prepared dry cell, containing zinc chloride and calcium chloride solution. This element was sealed into a Lucite tube, having a cotton canvas diaphragm-bottom, moistened with calcium chloride to make electrolytic contact with the clay. Comparison of this element with a second one standing by indicated it to be sufficiently near constancy for the purpose. It had been made for field use and was used here because of convenience. The surface of the clay was covered with a $\frac{1}{4}$-inch (0.64 cm) layer of sand and the sand was covered with about the same depth of paraffin to minimize evaporation. The galvanic cell was, therefore, exposed to very moist and poorly aerated conditions.

The wet clay practically eliminated convection in the electrolyte and was, therefore, conducive to reproducibility of results. The maintenance of the phase boundary was the result of the effects of current density and of diffusion processes, including that of air downward and moisture upward, providing conditions for a differential aeration cell. To some extent, therefore, the rate of corrosion may be said to have been largely "diffusion controlled."

In order to obtain values for $r_z$, $r_a$, and $r_c$ (Fig. 5) the composite resistances $X_1$, $X_2$, and $X_3$ were measured according to the method in Part I (3) where

$$X_1 = r_s + r_a$$
$$X_2 = r_s + r_c$$
$$X_3 = r_s + R_G$$

and

$$R_G = \frac{r_a r_c}{r_a + r_c}.$$

By the use of quadratic formulas, the separate path resistances were calculated.

Polarization curves for iron and copper separately, and for the Fe/Cu couple, are given (Fig. 7). The effect of time on the potential of the copper cathode, which is actually a hydrogen electrode, is shown by the three curves, the dotted one being arbitrarily selected to represent the values of $e_c + I_c r_c$ during polarization of the couple. At a current of 860 $\mu$a the polarized potential of copper (hydrogen electrode) is equal to that of iron. The potential $E_G$ is so near that of iron, since the cathodic polarization of copper is much greater than the anodic polarization of iron.

In accordance with the relations expressed in equation (XI) and using increments,

$$\frac{\Delta E - \Delta e_A}{r_a} = \Delta I_a \quad \text{and} \quad \frac{\Delta E - \Delta e_c}{r_c} = \Delta I_c \qquad \text{(XII)}$$

where the emf-difference ratio,

$$\frac{\Delta E - \Delta e_a}{\Delta E - \Delta e_c}, \quad \text{not} \quad \frac{r_c}{r_a} \quad \text{alone},$$

is an important relation in determining the current ratio.

Since

$$\frac{E - E_G}{R_G} = I \qquad \text{(XIII)}$$

$\Delta E = \Delta E_G + R_G \Delta I$, and so $\Delta E$ may be computed from the experimental data. Then $\Delta e_a$ and $\Delta e_c$ may be obtained from equation (XII). Numerically of course, the above emf-difference ratio is also equal to the ratio of the respective resistive components, $\frac{\Delta I_a r_a}{\Delta I_c r_c}$.

If the increments in counter emfs, $\Delta e_a$ and $\Delta e_c$, should become equal, then the emf-difference ratio will become unity and, at this moment, the current ratio $\Delta I_a/\Delta I_c$ is equal to the resistance ratio $r_c/r_a$.

Similar curves were obtained for an iron-magnetite couple arranged in the same manner (Fig. 3) as for the iron-copper couple. The magnetite element was prepared by heating a $\frac{5}{16}$-inch (0.76 cm) iron rod at 1020°F (550°C) 2 hours to give an adherent oxide coating. The readings on the Fe/$Fe_3O_4$ couple are given in Table II as obtained in accordance with the relations in Fig. 4.

The values of $r_a$ and $r_c$ included meter resistances of 18.6 ohms. The direction of $I_a$ reversed when the external current was 353 $\mu$a and $E_G - E_s$ was 1216 mv. This was the result of the iron and magnetite reaching the same potential. Above this potential, current flowed to both iron and magnetite. The

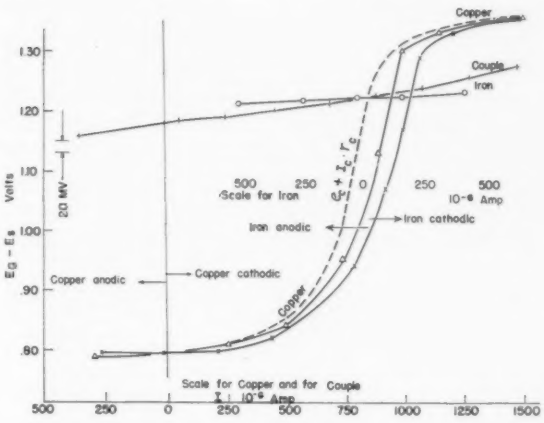


FIG. 7. Polarization curves for copper, iron, and an iron-copper couple.

TABLE II. *Readings on an iron-magnetite couple in wet clay. Auxiliary electrode, graphite*

| $E_t$ | $I$ | $I_a$ | $I_C$ | $E_G - E_s$ 1200 + mv |
|---|---|---|---|---|
| *volts* | $\mu$a | $\mu$a | $\mu$a | mv |
| 0 | −404 | −715 | +311 | 0 |
| 0.25 | −217 | −535 | 318 | 4 |
| 0.50 | −45 | −375 | 330 | 7 |
| 0.75 | +125 | −215 | 340 | 10 |
| 1.00 | 262 | −80 | 342 | 14 |
| 1.14 | 353 | 0 | 353 | 16 |
| 1.25 | 430 | +70 | 360 | 19 |
| 1.50 | 568 | 195 | 373 | 25 |
| 1.75 | 675 | 290 | 385 | 32 |
| 2.00 | 765 | 370 | 395 | 39 |
| 2.25 | 867 | 450 | 417 | 47 |
| 2.50 | 940 | 505 | 435 | 55 |

TABLE III. *Measured resistances*

| Resistance | Ohms |
|---|---|
| $r_s$ | 16 |
| $r_a$ | 24.6 (including meter) |
| $r_c$ | 40.0 ( " " ) |
| meter | 18.6 in each path |
| $R_G$ | 15.2 |

increments in potentials and currents are given in Tables IV and V for different potential levels represented by $E_t$, after $I_a$ became positive.

If the partition of current between the paths were governed by resistance alone, then $\Delta I_a/\Delta I_c$ should equal $r_c/r_a$ or 1.6. However, as is apparent in column

5, Table IV, $\Delta I_a/\Delta I_c$ varies from 10 to 3.1. Hence some other factor must be dominant.

The emf-difference ratio, given in column 7, Table V when multiplied by the resistance ratio, 1.6, gives the actual partition ratio, column 5, Table IV. The smaller increment in current through the cathodic path is, therefore, not due to its higher resistance $r_c$ alone, but mainly to the higher counter emf $e_C$ in that path.

The relation expressed in equation (XI) has wide application in cells where current is flowing to cathodic areas in parallel. In electroplating, it is concerned with determining the "throwing power" of the electrolyte, whereby current is diverted from the nearer areas of high current density to the farther

TABLE IV. *Increments in readings for iron-magnetite couple after $I_a$ reverses*

| 1 | 2 | 3 | 4 | 5 | 6 | 7 |
|---|---|---|---|---|---|---|
| $E_t$ | $\Delta I$ | $\Delta I_a$ | $\Delta I_c$ | $\Delta I_a/\Delta I_c$ | $\Delta E_G$ | $R_G \Delta I$ |
| volts | μa | μa | μa | | mv | mv |
| 1.25 | 77 | 70 | 7 | 10 | 3 | 1.17 |
| 1.50 | 138 | 125 | 13 | 9.6 | 6 | 2.10 |
| 1.75 | 107 | 95 | 12 | 7.9 | 7 | 1.60 |
| 2.00 | 90 | 80 | 10 | 8.0 | 7 | 1.37 |
| 2.25 | 102 | 80 | 22 | 3.6 | 8 | 1.55 |
| 2.50 | 73 | 55 | 18 | 3.1 | 8 | 1.11 |

TABLE V. *Increments in computed values of iron-magnetite couple after $I_a$ reverses*

| 1 | 2 | 3 | 4 | 5 | 6 | 7 |
|---|---|---|---|---|---|---|
| $E_t$ | $\Delta E$ | $\Delta I_a r_a$ | $\Delta I_c r_c$ | $\Delta e_a$ | $\Delta e_c$ | $\frac{\Delta E - \Delta e_a}{\Delta E - \Delta e_c}$ |
| volts | mv | mv | mv | mv | mv | |
| 1.25 | 4.2 | 1.7 | 0.3 | 2.5 | 3.9 | 5.7 |
| 1.50 | 8.1 | 3.1 | 0.5 | 5.0 | 7.6 | 6.2 |
| 1.75 | 8.6 | 2.3 | 0.5 | 6.3 | 8.1 | 4.6 |
| 2.00 | 8.4 | 2.0 | 0.4 | 6.4 | 8.0 | 5.0 |
| 2.25 | 9.6 | 2.0 | 0.9 | 7.6 | 8.7 | 2.2 |
| 2.50 | 9.1 | 1.4 | 0.7 | 7.7 | 8.4 | 2.0 |

areas of lower current density. Likewise in cathodic protection, the current tends to spread out from areas of greater polarization to the surrounding areas. Thus, polarization favors the required distribution of the protective current. Since partition of current is governed by the relation in equation (XI) the term current density, as applied to the whole couple, has an indefinite meaning. For example, while $E_t$ was being increased from 1.25 to 2.50 volts, the total current $I$ increased from 353 to 940 μa. Of this increase of 587 μa, current on the magnetite increased 82 while that on the iron increased 505 μa. Current to the area initially anodic is unnecessary, since it is the current density $I_c/_d$ on the cathode which is providing the protection, where $d$ = the usually unknown area of the cathode.

The relations in equation (XI) may also be expressed in such a way as to make resistance and polarization additive. For example, since

$$\Delta I_a = \frac{\Delta E - \Delta e_a}{r_a} \quad \text{and} \quad \Delta I_c = \frac{\Delta E - \Delta e_c}{r_c}$$

then

$$\Delta E = I_a r_a + \Delta e_a \quad \text{or} \quad \frac{\Delta E}{\Delta I_a} = r_a + \frac{\Delta e_a}{\Delta I_a}$$

and

$$\Delta E = \Delta I_c r_c + \Delta e_c \quad \text{or} \quad \frac{\Delta E}{\Delta I_c} = r_c + \frac{\Delta e_c}{\Delta I_c}.$$

By elimination of $\Delta E$ we have

$$\frac{\Delta I_a}{\Delta I_c} = \frac{r_c + \Delta e_c/\Delta I_c}{r_a + \Delta e_a/\Delta I_a} \qquad \text{(XIV)}$$

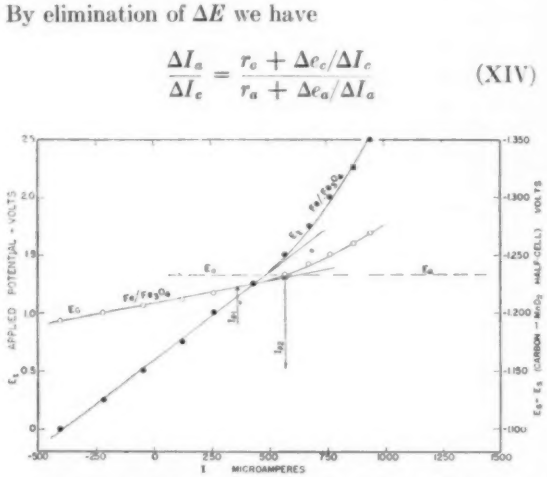


FIG. 8. Relation of protective currents to polarization curves for iron-magnetite couple.

where $\frac{\Delta e_c}{\Delta I_c}$ and $\frac{\Delta e_a}{\Delta I_c}$ represent the rates of change of the emf of polarization with current. This expression, however, does not show the relation of the important term $E$ to current partition.

## VI. Possible Relations of $E_G$ and $E_t$ to $I_p$

In Fig. 8, both the values of $E_G$ and of $E_t$ are plotted against the external current $I$ for the $Fe/Fe_3O_4$ couple. It is apparent that the value of $I_{p1}$ is reached at a potential slightly below $E_a$, the open-circuit potential of iron. The reason for this apparent discrepancy is probably as follows: When the potential of magnetite becomes equal to that of the iron, the value of $I_a$ becomes zero. However, the iron itself behaves like a galvanic couple, so that a still larger current $I_{p2}$ is necessary to polarize the cathodic areas of the iron, as well as the magnetite to the open-circuit potential $E_a$ of iron. In this respect, the use of separate galvanic elements, to include meters,

has its limitation in studying cathodic protection, unless the anodic element has a very small area. Another reason for $E_G$ being below $E_a$ at $I_{p1}$ is that $E_G < E_a$ by the amount $I_p \cdot R_G$ when cathodic protection is complete.

When the anodic area is large, as in Fig. 9, where an iron plate, 2 x 6 inches (5.1 x 15 cm), is joined to the same copper rod used above, we have $I_{p1}$ required to polarize the copper to the potential of the iron plate, and then $I_{p2}$ required to polarize both iron plate and copper to the open-circuit potential of iron. It is apparent that the use of the term "current density" for cathodic protection must be qualified. For example, the value of $I_p/30$ cm² for copper is about 3.3 ma/dm²; and $I_p/155$ for iron is about 0.45 ma/dm, assuming uniform current distribution.

As indicated in Fig. 8, the change in relation of $E_t$ to $E_a$ is distinct. The accelerated rise in $E_G$, which occurs probably because of the beginning of liberation of hydrogen on the formerly anodic area, is reflected in $E_t$. Any error of measurement, due to $IR$ potential drops, is avoided here, since the increment in $E_G$ manifests itself directly. If a nonpolarizable auxiliary anode is on hand, or if the polarization of the anode is linear, this is an accurate method of observing any change in $E_G$.

The conditions for cathodic protection are graphically summarized in Fig. 11 where (A) shows the relations for $I$ below cathodic protection; (B) for $I$ at cathodic protection; and (C) for $I$ above cathodic protection.

## VII. Methods of Interpretation of Relation of $E_G$ to $I$

Assuming the validity of the usual overvoltage relation

$$E_G = a + b \log I \qquad \text{(XV)}$$

where '$a$' and '$b$' are constants, $E_G$ may be plotted against log $I$ as in Fig. 10, and the values of $I_p$ are indicated, for the iron-copper and iron-magnetite couples. Obviously, there are no inflections in these logarithmic curves corresponding to $I_p$. Such curves are, therefore, of limited use in determining $I_p$, unless excessive currents are used for the customary testing and extrapolation of the straight-line portions of the curves to their intersections if there are any such linear portions. Another disturbing feature of the $E_G$/log $I$ curve is its similarity in some cases to a log $IR$ curve. For example, in Fig. 10, $IR$ is plotted against log $I$ for a resistance of 50 ohms giving a curve which is almost coincident with the $E_G$/log $I$ curve for the iron-magnetite couple. It seems evident, therefore, that the shape alone is not sufficient proof that we are dealing with a hydrogen overvoltage curve.

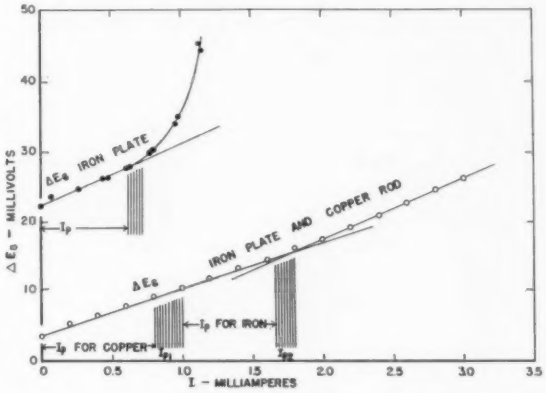


Fig. 9. Relation of protective currents to polarization curves for iron plate.

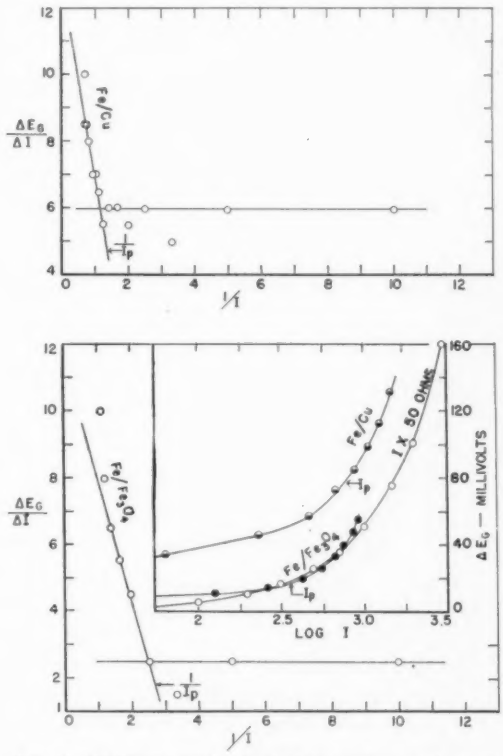


Fig. 10. Different methods of plotting some polarization curves.

If, however, we differentiate equation (XV), we obtain,

$$\frac{dE_G}{dI} = b/I \qquad \text{(XVI)}$$

which is also plotted in Fig. 10 for both couples. If the potential-current relation were that of a re-

sistance, then the plotting of $\frac{dE_G}{dI}$ against the reciprocal of $I$ would give a horizontal line. The two intersecting lines leave no doubt that the relation is other than an $IR$ drop, and the intersection corresponds closely to the values of $1/I_p$ for both couples. The curves shown in Fig. 10 for the polarization of galvanic couples suggest that the usual hydrogen overvoltage relations for different metals really represent the same phenomenon, that is, the polarization of galvanic cells on their surfaces. For example, the value of $I_p$ corresponds to the minimum current required to liberate hydrogen, the potential for currents above $I_p$ being the overvoltage.

under conditions of very limited aeration, it is fortunate that, under these same conditions, polarization curves may better serve as criteria for determining the cathodic protection. Correlation of results of measurements in the field with corrosion rates is necessary to determine whether such polarization curves can be so interpreted. Even in a deaerated environment the success of cathodic protection may depend very largely upon the emf of polarization, as reflected in the measured values of $E_G$.

## Conclusions

Under laboratory conditions of restricted aeration in wet clay, polarization of an iron-hydrogen couple

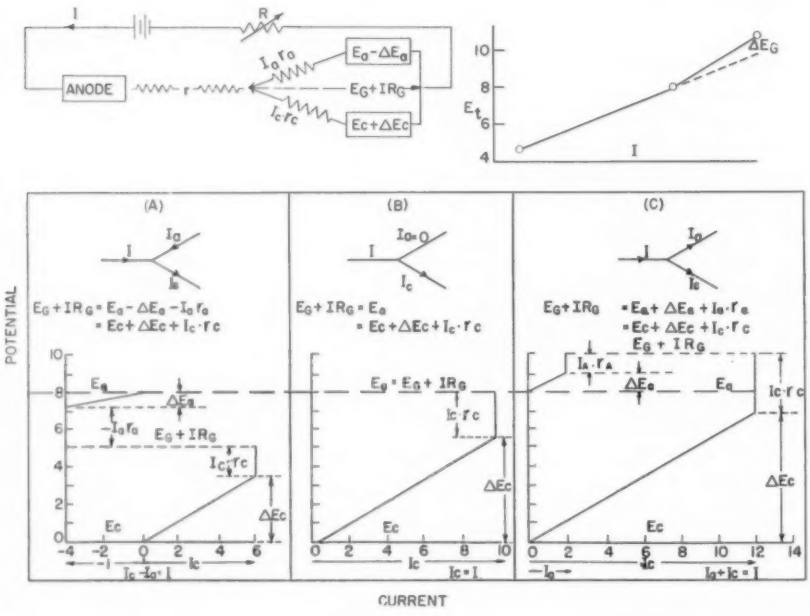
I
R
ANODE
r
$I_a r_a$
$I_c r_c$
$E_a - \Delta E_a$
$E_G + IR_G$
$E_c + \Delta E_c$
$E_t$
$\Delta E_G$
(A)
(B)
(C)
$E_G + IR_G = E_a - \Delta E_a - I_a r_a = E_c + \Delta E_c + I_c \cdot r_c$
$E_G + IR_G = E_a = E_c + \Delta E_c + I_c \cdot r_c$
$E_G + IR_G = E_a + \Delta E_a + I_a \cdot r_a = E_c + \Delta E_c + I_c \cdot r_c$
POTENTIAL
CURRENT

Fig. 11. Conditions preceding (A) and after (C) cathodic protection obtained in (B).

## VIII. Effect of Aeration

The couples used in these experiments were poorly aerated and this was an important factor in the results obtained. Since the polarization, and more especially its acceleration soon after the applied current reached $I_p$, was evidence of incipient hydrogen, any increased aeration should have an adverse effect, and this was found to be the case.

Excessive aeration of the iron completely removed such evidence of cathodic protection from the polarization curves. In this case, cathodic protection depends less upon the emf of polarization and to a larger extent on the resistive component of polarization. As a result, a very high value of $I_p$ may be required. If the emf component of polarization is too low, cathodic protection may not be practicable.

Since underground corrosion is usually most severe by an applied current may be used to evaluate the internal current and, therefore, also the applied potential and current required for the cathodic protection of iron. The importance of phase-boundary resistances in polarization measurements is demonstrated. Methods of interpreting polarization curves and their relation to cathodic protection are described.

The application of these principles to cathodic protection when the ratio of cathodic area to anodic area is very large and the full importance of the principle of current partition to current distribution should be studied for long distances underground. The criterion of cathodic protection based on applied potential may be useful, particularly where the open-circuit anode potential may vary with conditions and with time. Application of the required constant

potential, the applied current adapting itself to that necessary to maintain the constant potential, should result in economy of power.

An explanation of hydrogen overvoltage on the basis of polarization of galvanic couples in the phase-boundary is suggested. A practical criterion for de-determining the current, or potential, required for cathodic protection, in the poorly aerated conditions underground, may require detection of the usual hydrogen overvoltage relation, such as that in equation (XVI) and Fig. 10.

Any discussion of this paper will appear in a Discussion Section, to be published in the June 1951 issue of the JOURNAL.

## REFERENCES

1. M. A. STREICHER, *J.* (*and Trans.*) *Electrochem. Soc.*, **93,** 285 (1948); Pittsburgh International Conference on Surface Reactions," p. 35, Corrosion Publishing Co., Pittsburgh (1948).
2. R. B. MEARS AND R. H. BROWN, *Trans. Electrochem. Soc.*, **74,** 519 (1938); *J.* (*and Trans.*) *Electrochem. Soc.*, **95,** 1 (1949).
3. H. D. HOLLER, *J.* (*and Trans.*) *Electrochem. Soc.*, 97, 271 (1950).

# Discussion Section

## EFFECT OF ADSORBED POLAR ORGANIC COMPOUNDS ON ACTIVITY OF STEEL IN ACID SOLUTION

**Norman Hackerman and E. L. Cook** (pp. 1–9)

H. H. Uhlig[1]: It is hardly necessary to point out that basic information of the kind presented by Messrs. Hackerman and Cook is vitally important to an understanding of the mechanism whereby corrosion inhibitors operate. We need more fundamental information of this kind.

I should like to ask the authors whether there was any evidence from their data of activated adsorption. In other words, was there evidence that a measurable time factor was involved in the adsorption of substances on the surface of metal powders?

Norman Hackerman and E. L. Cook: There was a definite time factor in the adsorption of these compounds on metal powder, something of the order of days. This can be attributed largely to diffusion control since the way in which the experiments were carried out caused this type of control to obscure any other factors which might have been involved. We made an attempt to determine the temperature coefficient by carrying out the experiments at several elevated temperatures. With the systems we used, complications arose due to the fact that reaction occurred between the metal and the sorbing species.

## RECENT DEVELOPMENTS IN TITANIUM

**E. A. Gee, W. H. Van Derhoef, and C. H. Winter, Jr.** (pp. 49–53)

W. J. Kroll[2]: Any publication concerning the production and fabrication of titanium or zirconium without contamination by air constituents will be read by metallurgists, concerned with rare metals, with great curiosity. The paper presented by Gee, *et al.*, is not to be excepted, despite the fact that its interest resides in the size of the equipment used, and not in the novelty of the procedures. It is questionable, however, whether a large, quartz-tube, high-frequency furnace could seriously be contemplated for the melting of 100-pound titanium ingots on a commercial scale.

The article generally does not give satisfaction to the originators of important developments and credit is frequently given to those to whom it does not belong. Since some day the history of the development of the titanium and zirconium metallurgy will be written, it is worth while correcting erroneous references concerning decisive steps, which lead to the techniques employed now by Gee, *et al.*, so that these errors will not be carried over in textbooks.

The second commercial method for the production of ductile titanium, besides the iodide process, mentioned by the authors, is not "the reduction of titanium halides with active metals such as sodium, calcium, or magnesium," but it is: the reduction of titanium chloride with fused magnesium under helium, which is used by the Du Pont Company, shortly to be called the "Kroll" process (Ref. 9). Neither calcium nor sodium reduction plays today any role for the production of cold malleable titanium from halogenides. The "Kroll" process is patented in the United States under number 2,205,854 (1940), but the rights have been seized by the Alien Property Custodian. This action is subject to litigation in court.

Gee, *et al.*, are giving the U. S. Bureau of Mines undue credit for the aqueous extraction process for chloride and excess magnesium from the reacted mixture, which procedure is well described in Reference 9, and in U. S. Patent, 2,205,854. On the other hand, the fact that the Albany, Oregon, station of the U. S. Bureau of Mines originated and put to practice the vacuum separation at elevated temperature, which yields sponge of the type produced by the Du Pont Company, is entirely ignored. This method was made known for the first time in the Transactions of The Electrochemical Society[3], and was recommended for titanium as well as for zirconium.

The same reference reports the important discovery that zirconium and titanium can be melted with negligible contamination on a graphite layer. This is the subject of a pending patent application. Melting in graphite enabled the Mallory and Du Pont companies to produce titanium and titanium alloy ingots.

The history of the arc melting methods for producing titanium ingots is also given incorrectly. It was not Battelle Memorial Institute which first arc-melted titanium. This method, used before for tantalum melting, is fully described in Reference 9. The first samples of arc-fused titanium were shown by the author of this discussion in this country in 1938. A considerable improvement over the existing techniques was introduced by Parke and Ham[4], who melted molybdenum in vacuo in a water-cooled sleeve, thus producing an ingot instead of a flat cake of metal. The same principle of arc melting in a sleeve appears in Battelle's arc furnace, which operates under argon of atmospheric pressure and is, therefore, of simpler design.

It may also be mentioned that the idea of compacting metal powders at elevated temperature in a metal sheath was initiated by G. Wassermann[5].

This Discussion Section includes discussion of papers appearing in the Journal of The Electrochemical Society, **97**, No. 1–6 (January–June 1950).

[1] Department of Metallurgy, Massachusetts Institute of Technology, Cambridge, Massachusetts.

[2] Consulting Metallurgist, Albany, Oregon.

[3] W. J. Kroll, et al., *Trans. Electrochem. Soc.*, **92**, 99 (1947).

[4] *Trans. Am. Inst. Mining Met. Engrs., Inst. Metals Div.*, **171**, 416 (1947).

[5] *Z. Metallkunde*, **2** [5], 129 (1947).

Its application by Long to compacting titanium powder is correctly reported.

Considering the many rectifications given above as to the true origin of the various steps made in the development of the metallurgy of titanium, it is left to the reader to judge the novelty of the procedures described by Gee, *et al.*

## ELECTRODEPOSITION OF CHROMIUM-TUNGSTEN ALLOY PLATES

**Donald G. Rogers and Arthur A. Burr** (pp. 67–69)

A. D. Muir[6]: If sodium ions are undesirable in the electrolyte, what is the influence of other metallic ions, such as those introduced by the cathode itself?

Since the Cr:W ratio is shown to be relatively constant irrespective of major alterations in the concentrations of other variables, is some definite structural aggregate being built up?

Donald G. Rogers: Either nickel or steel anodes were attacked slightly by the solution, and at times some copper ions from the cathode undoubtedly entered the solution. As far as could be determined, in the small amounts present, none of these ions had any effect on the deposition of the alloy. Spectrographic analysis failed to show more than perhaps a trace of any of them in the plate.

At present it is not possible to offer an explanation for the fact that the Cr:W ratio in the plates is relatively independent of solution composition and plating conditions. The chromium-tungsten phase diagram is reported to consist solely of a continuous solid solution, and if this is true it is very unlikely that any definite structural aggregate is being formed. An attempt was made to study the crystal structure of the plate by x-ray diffraction techniques, but due to the extremely fine-grained nature of the deposit, no patterns were ever obtained which permitted determination of the structure.

H. J. Wiesner[7]: Did you make any relative scratch hardness or abrasion resistance measurements of the alloy and, say, chromium plate?

Donald G. Rogers: In attempting to determine the hardness of extremely thin deposits, the hardness reading obtained will depend largely on the hardness of the base metal on which the plate is deposited. No quantitative hardness data were, therefore, taken on these plates. Most of the deposits were made on copper cathodes, and if these were scratched with any reasonably sharp steel object, the underlying copper base metal was exposed. This was the only observation made on plate durability.

## ON THE DETERMINATION OF THE ROUGHNESS OF METALLIC SURFACES

**Carl Wagner** (pp. 71–82)

H. H. Uhlig[8]: The subject of true surface of metals is one of great importance to many measurements. It is an important factor in interpreting experiments on catalysis, heterogenous reaction rates, electron emission, and on polarization and overvoltage. Theory in many of these fields has been delayed because of the fact that surface area, which enters directly into such measurements, has been unknown. Although the method of Brunauer, Emmett, and Teller (gas adsorption), or that of Bowden and Rideal (electrode-electrolyte capacity), is now available, each is fairly complex and not easily accomplished experimentally. The first method, because of the out-gassing technique required, may actually alter the surface area from the standpoint of some types of measurements. The method which Dr. Wagner presents, therefore, is of a special interest, because it uses a small specimen, requires no out-gassing at elevated temperatures, and is relatively simple. It is hoped that the method will be as generally applicable as the preliminary experiments of Dr. Wagner indicate it to be.

J. J. Bikerman[9]: The assumption of a close correlation between the polarization capacity of an electrode and its roughness may be substantiated, it seems, by yet another method. Gouy's "equivalent thickness" $\tau$ of diffuse double-layer increases when the concentration of the solution decreases. When $\tau$ is considerably greater than the height of an average asperity on the solid surface, the increase in charge of the liquid (and consequently of the solid) per cm$^2$ of the apparent surface on a definite increase in the voltage becomes independent of the degree of roughness. Hence, the ratio of the polarization capacities of a rough to an ideally smooth surface should decrease with increasing dilution and should tend to unity; and it should reach a value near unity at a dilution which decreases as the surface becomes smoother.

Carl Wagner: It is true that the surface area derived from measurements of the polarization capacity will be too small if there are hills and valleys having a breadth comparable to Gouy's equivalent thickness of the diffuse electrical double layer. In a one-molar solution as used in the measurements reported, the equivalent thickness of the electrical double layer amounts to $3 \cdot 10^{-8}$ cm, i. e., the order of the diameter of ions and atoms. Thus the error due to the finite thickness of the electrical double layer will be of the same order of magnitude as the error due to the finite size of atoms or molecules of an adsorbed substance if the surface area is determined with the aid of adsorption measurements of a monoatomic or diatomic gas such as argon or nitrogen.

In most cases this error seems insignificant, since imperfections of a surface will disappear very rapidly by dissolution and redeposition or by two-dimensional diffusion inasmuch as the change in free energy for rearrangement of a single atom is of the order of the thermal energy per atom or higher. Thus it seems likely that hills and valleys on a metallic surface in contact with an aqueous solution have in general a breadth greater than $3 \cdot 10^{-8}$ cm.

In a 0.01$N$ solution, however, the equivalent thickness of the diffuse electrical double layer equals $3 \cdot 10^{-7}$ cm. Measurements of the polarization capacity in such dilute solutions may, therefore, yield too small surface areas, as in the case with adsorption measurements involving large organic molecules.

[6] Ontario Research Foundation, Toronto Canada.

[7] Bendix Products Division, South Bend, Indiana.

[8] Department of Metallurgy, Massachusetts Institute of Technology, Cambridge, Massachusetts.

[9] 45-35 46th Street, Woodside, Long Island, New York.

UMI

## A UNIFIED MECHANISM OF PASSIVITY AND INHIBITION, PART II

**R. B. Mears and R. H. Brown** (pp. 75–82)

MORTIMER C. BLOOM[10]: Do single crystals of metals show deviations experimentally from the thermodynamically calculated electrode potentials?

R. B. MEARS: Yes, single crystals of metals also show marked deviations experimentally from the thermodynamically calculated electrode potentials. See, for example, the paper by C. J. Walton[11].

H. H. UHLIG[12]: The authors apparently prefer to look upon all corrosion reactions from the standpoint of electrochemical polarization, neglecting what actually happens at the electrode surfaces to bring about such electrochemical change. Although this viewpoint is adequate for obtaining the correct answer, it seems to me that a still more basic approach includes the nature of electrode surfaces and electrode reactions that account for such electrochemical polarization as Messrs. Mears and Brown report. Besides providing increased interest in the study of corrosion reactions, a study of surface equilibria and kinetics provides new and useful information not obtained otherwise.

I should like to ask Dr. Mears whether any experiment has been performed showing that steels containing a variety of cathodic impurities show a variety of potentials when immersed in chromate solutions. Were this proved, it would constitute proof that chromate polarizes steels anodically. Were all potentials the same, however, one would assume that chromates adsorb generally without regard to anodes or cathodes.

R. B. MEARS: It seems to us that Dr. Uhlig is proposing that we run before we can walk. We have no objection to a fundamental approach which would result in separating and measuring the individual factors that together make up polarization. In fact, we would like to give encouragement to any such approach. At the present time it is relatively easy to measure $E_a$ or $E_c$, the overall polarization at the anode or cathode, respectively. As we pointed out in the first paper of this series, these bulk polarizations are made up of at least two components. It would be very desirable to measure these components separately. We would be glad to see someone make such measurements.

Our fundamental point is, if corrosion is indeed electrochemical, as seems probable, let us express all effects in electrochemical terms. It is not sufficient from an electrochemical standpoint to say that a film prevents or reduces corrosion since we wish to know how the film behaves electrochemically. Does it introduce a high resistance in the circuit, is it similar to a condenser, or just what is its electrochemical action?

Dr. Uhlig inquires if experiments have been performed showing that steels containing a variety of cathodic impurities show a variety of potentials when immersed in chromate solutions. Our work with chromates was confined to aluminum. We have no direct evidence that chromates anodically polarize steel, although it seems probable that they do. We have noted that when steel is coupled to copper and immersed in a chloride solution the potential of the couple is nearly the same as that of steel indicating that steel does not polarize appreciably anodically in chloride solutions. However, if chromates are added to the solution, the potential of the iron-copper couple shifts in a cathodic direction and is about half way between the open circuit potential of the iron and that of the copper. This indicates that chromates do polarize the steel anodically, although this may not be the sole effect of the chromates in inhibiting corrosion of steel.

The observed values were as follows:

| The solution contained 0.01% NaCl and 1.0% $Na_2CrO_4 \cdot 4H_2O$ | |
|---|---|
| Open circuit potential of copper | 0.09 volt |
| Open circuit potential of steel | 0.39 volt |
| Potential of couple (copper and steel) | 0.16 volt |

In sodium chloride solution *not* containing chromates, the potential of the couple is nearly the same as that of steel alone.

M. J. PRYOR[13]: The recent paper by the authors, while being an interesting contribution to the understanding of inhibition and passivity, does not, however, get to the roots of the problem. In fact, the conclusion that the inhibiting action of sodium chromate is "mainly the result of polarization of local anodes," is little more than a restatement of the usual definition of an anodic inhibitor. In the opinion of the writer, a mechanism of inhibition should explain, not only the steps leading to this polarization, but also give some account of the kinetics of the overall reaction; in the latter case, a study of chemical thermodynamics can give no useful information.

In a recent paper[14] the inhibiting action of chromate on the corrosion of iron was attributed to a heterogeneous reaction between adsorbed chromate ions and the iron surface, with the result that the iron ions were oxidized, without first passing into solution, to $\gamma$-$Fe_2O_3$ which formed a thin, continuous surface film. This was concluded from the failure to detect any constituent other than $\gamma$-$Fe_2O_3$ during an electron diffraction examination of films formed by the action of 0.01*M* potassium chromate solution on originally film-free iron. More recent work[15] has shown that this same reaction takes place in de-aerated solutions. It would be interesting to know whether the authors have any information concerning the nature of the film formed by the action of sodium chromate on aluminium.

The authors' conclusions concerning the depolarization of the cathodic reaction by chromate ions are at variance with those of other investigators. Hoar[16] has pointed out that the reduction of the chromate ion in neutral solutions is very sluggish and experiments by the writer have indicated that the cathodic reduction of chromate ions, in chromate/chloride mixtures, is not appreciable at pH values above 3.0. Similar results have also been obtained

[10] Naval Research Laboratory, Washington, D. C.

[11] *Trans. Electrochem. Soc.*, **85,** 239 (1944).

[12] Department of Metallurgy, Massachusetts Institute of Technology, Cambridge, Massachusetts.

[13] National Research Council, Ottawa, Canada.

[14] J. E. O. MAYNE AND M. J. PRYOR, *J. Chem. Soc.*, **1949,** 1831.

[15] J. E. O. MAYNE AND M. J. PRYOR, Unpublished Work.

[16] *Trans. Electrochem. Soc.*, **76,** 157 (1939).

with neutral solutions of nitrites[17]. It may be, therefore, that the decrease in cathodic polarization with increasing chromate ion concentration (Fig. 1) is due merely to a progressive decrease in size of the anodic areas and corresponding enlargement of the cathodic areas; this will lead to a decrease in the cathodic current density and hence to a reduction of the cathodic polarization.

R. B. MEARS: The authors were interested in Dr. Pryor's discussion. They believe, however, that Dr. Pryor does not understand the real significance of their study of the mechanism of inhibition by sodium chromate. It is true, as Dr. Pryor indicates, that other workers have suspected that sodium chromate was an anodic inhibitor. As far as the authors are aware, however, no one previously has isolated electrically the local anodes and cathodes and proved by direct measurement that the addition of chromate to the solution increases the anodic polarization. It can be argued that the electrochemical behavior of an inhibitor is of more importance than is the determination of the physical or chemical state of the reaction product. Corrosion is an electrochemical phenomenon. The most significant information to learn is how the inhibitor affects the electrode reactions. A film of reaction product may or may not appreciably influence the electrode reactions, depending on the character of this film. Just to say that a film of $\gamma$-$Fe_2O_3$ is formed *does not* explain why corrosion is reduced. It is necessary to go further and determine how this film affects the electrode reactions.

It is not believed that the cathodic areas altered appreciably as chromates were added for two reasons:

1. The anode area was a single pit that was started by immersing the aluminum sample in uninhibited sodium chloride solution. This same pit remained the anode as chromate was added to the solution.

2. The area of the cathode, even in the uninhibited solutions, was over one hundred times the area of the anode. Thus, it would be impossible for the cathode area to increase by more than 1 per cent.

M. G. FONTANA[18]: Dr. Mears has presented his usual high quality paper and has done a fine job of covering some of the fundamentals of electrochemical corrosion. With regard to passivity, however, I do not agree that an explanation of the anode-cathode relationships is necessary in all cases. For example, if one postulates that stainless steel is passive because of an oxide layer, an hydrous oxide film, a chemisorbed film, and/or a physically adsorbed gas thus setting up a barrier between the base metal and the corrosive environment, what further explanation is required? Lead supposedly becomes passive in sulfuric acid because of the formation of a lead sulfate coating. To draw an almost direct analogy we could ask the question—why does a paint coating often protect steel from corrosion? In addition, all corrosion is not necessarily electrochemical in nature. Unfortunately, the determination of anode and cathode potentials is a difficult, if not almost impossible, procedure.

If we assume that passivity involves practically no corrosion then cathodic and/or anodic polarization must be almost complete. In other words, the polarization lines must be almost vertical or coincide with the vertical axis of the figures Dr. Mears has drawn. Interpretation of the word passivity is also involved. If the corrosion rate on a metal is reduced from 200 to 100 mils per year, I would not interpret this as a result of passivity. The information presented by Dr. Mears is particularly valuable in the study of inhibitors.

We are in complete agreement with Dr. Mears' statement that the single electrode potential is not a measure of passivity. Our work on passivation of stainless steels has shown a wide variety of single electrode potentials (both plus and minus) for steels treated.

R. B. MEARS: The authors wish to thank Dr. Fontana for his discussion. It can be readily recognized that the formation of a film is not sufficient to account for passivity. The properties of the film are also important. The properties of the film which are of most importance are its electrical or electrochemical properties. For example, it must be agreed by all that carbon steel in many environments forms a film of corrosion products (rust). Unfortunately, this film frequently causes little reduction in corrosion rate. The reason is that the film does not retard the electrode reactions. It can be asked why a lead sulfate film reduces corrosion of lead in sulfuric acid. The fact that a film is formed is not sufficient to explain the reduction of corrosion. The film must interfere with electrode processes or corrosion is not retarded. The most accurate way of studying this effect is to determine the influence of the film on the anode and cathode processes separately.

While it is true, as Dr. Fontana implies, that the flow of electric current has not been demonstrated for all types of corrosion reaction, still there is now sufficient quantitative and qualitative evidence to make it seem probable that corrosion of metals, in aqueous solutions at least, is electrochemical in nature.

It is our belief that the mechanisms of passivity and inhibition are identical. Therefore, if the theory presented is applicable to inhibitors—it is also applicable to passivity.

HERBERT CHARLES COCKS[19]: I feel that a great service has been performed by Messrs. Mears and Brown in elucidating the part played by oxygen in determining the values of the potentials of metals in salt solutions.

I am of the opinion that this point should be clearly stated in textbooks on electrochemistry and that many investigators in the field of electrochemistry, especially workers on corrosion, omit consideration of this fact.

My own view is that the static potentials of nearly all, if not all, metals in most solutions are determined not only by the metal/metal ion equilibria but, to some extent, by the metals behaving as gas electrodes in a similar manner to the hydrogen electrode. By static potentials I mean, of course, those measured when there is no flow of current from another electrode. The gas electrode equilibria would usually be that of the oxygen electrode, but sometimes that of the hydrogen electrode. In broad terms, the static potentials of metals in solutions as ordinarily measured are to varying degrees partly determined by adsorbed or absorbed oxygen or hydrogen on their surfaces as well as by the metal/metal ion equilibria. This factor affecting

[17] M. COHEN, Private Communication.

[18] Ohio State University, Columbus, Ohio.

[19] Royal Aircraft Establishment, Farnborough, Hampshire, England.

the potential would be quite apart from the well-known influence of the presence of local anodes and cathodes due to heterogeneity of the metal surface.

Experimental support for these observations was given many years ago by Kahlenburg and French[20] and I found some evidence in the case of zinc in zinc sulfate solutions[21]. That the potential of magnesium in acid and alkaline solutions is largely determined by its hydrogen overvoltage rather than by the metal/metal ion equilibrium is strongly indicated by the work of G. E. Coates[22].

R. H. Brown: We were very pleased to have Dr. Cocks' views on the nature of electrode equilibria and, in general, it is believed that he is in essential agreement with our discussion. There are some minor differences if our understanding of Dr. Cocks' discussion is correct. It is our feeling that it is of minor consequence whether the oxidation and reduction reactions occur at separate discreet areas or whether the areas are indistinguishable. If the areas are discreet it may be necessary to keep in mind that the conditions of dynamic equilibria at each area may differ. It is not clear if we are in agreement with Dr. Cocks' discussion regarding the potential of magnesium in acid and alkaline solutions being largely determined by its hydrogen overvoltage rather than by the metal to metal ion equilibrium.

If the magnesium to magnesium ion reaction is not polarized to as great an extent as the hydrogen to hydrogen ion reaction then we would prefer to say that the potential is controlled by the hydrogen to hydrogen ion reaction. If on the other hand, the polarization of the magnesium to magnesium ion reaction is appreciable relative to that of the hydrogen to hydrogen ion reaction, both reactions would help determine the measured potential of the electrode. Stated in another way, it is our belief that the potential of a single electrode in the solution is determined by all possible reactions that could occur and those which polarize to the greatest extent control the potential of the electrode. Furthermore, it is felt that the oxidation and reduction reactions cannot be considered as occurring independently. It is believed that these two reactions are interdependent.

## STUDIES ON THE STRUCTURE OF HARD CHROMIUM PLATE

**Cloyd A. Snavely and Charles L. Faust** (pp. 99–108)

P. H. Brace[23]: From the authors' remarks I have gained the impression that when deposition commences relatively large elongated crystals grow outward from the surface of the basis metal. Now, with reference to the striations shown by the photomicrographs, I suggest the possibility that during electrolysis there is an accumulation within the interstices between the initial crystals of secondary products of electrolysis and that in time these products reach concentrations sufficient to cause them to act as do addition agents and give rise to a finely crystalline deposit and a smooth surface from which a second cycle of growth of elongated crystals begins, and so on repeatedly, thus giving rise to the striated deposit.

Cloyd A. Snavely and Charles L. Faust: Mr. Brace's suggestion relating to the accumulation of secondary products of electrolysis to affect crystal growth is very interesting to the authors. We are unable to offer evidence for or against the hypothesis, though our own outlook has been somewhat different. It should be noted that a considerable change in the character of the plate surface during plating is accompanied by equivalent changes in the actual current density. Possibly, lowering the current density is enough to cause discontinuance of deposition on the larger crystals.

A. D. Muir[24]: Would the authors venture to comment upon the nature and origin of the striations found on the cross-sectional photomicrographs?

Cloyd A. Snavely and Charles L. Faust: In answer to Mr. Muir's question, we have nothing to offer beyond the foregoing comments and the discussion in the paper.

M. M. Sternfels[25]: Have you observed any signs of superficial cracking of the deposit arising from heat treating? Hidnert's work[26] on the coefficient of expansion of chromium shows initial contraction on heating, and the question refers to the possibility that this contraction results in cracking.

Cloyd A. Snavely and Charles L. Faust: Our interpretation of the physical causes and significance of the contractile phenomena reported by Hidnert has been detailed in an earlier paper[27].

H. J. Wiesner[28]: What sort of variation in hardness in the chromium plated samples existed before the various heat treatments?

Cloyd A. Snavely and Charles L. Faust: Careful checks were not made on the hardness of the plate specimens before annealing treatments. The hardness of other plates made under identical conditions varied between Knoop numbers of 900 and 1050 when measured on the cross-section surface.

J. J. Dale[29]: I do not agree with the contention of the authors (p. 104) that the exceptional hardness of bright chromium electrodeposits is more reasonably explained on the basis of fine grain size and internal stress than it is by the dispersed oxide theory. Actually, all of these mechanisms should be considered as complimentary, rather than conflicting, each one contributing its part. The following evidence, apparently not considered by the authors, leads me to believe that finely dispersed oxide or hydroxide particles confer the greater part of its hardness upon electrolytic chromium.

1. There is much more oxygen present in deposits than that which occurs as oxide in the visible inclusions. Brenner, *et al.*[30], obtained oxygen contents of the order of 0.5 per

[20] *Trans. Electrochem. Soc.*, **54,** 163 (1928).
[21] *Trans. Faraday Soc.*, **26,** 525 (1930).
[22] *J. Chem. Soc.*, **1949,** 483.
[23] Research Laboratories, Westinghouse Electric Corporation, East Pittsburgh, Pennsylvania.
[24] Ontario Research Foundation, Toronto Canada.
[25] Chromium Corporation of America, Waterbury, Connecticut.
[26] *Phys. Rev.*, **39,** 186 (1932).
[27] *Trans. Electrochem. Soc.*, **92,** 537 (1947).
[28] Bendix Products Division, South Bend, Indiana.
[29] Defense Research Laboratories, Maribyrnong, Victoria, Australia.
[30] *J. Research Nat. Bur. Standards*, **40,** 31 (1948).

cent by vacuum fusion of chromium deposits, while Cohen[31] has separated and weighed the visible inclusions and found them to be 0.05 per cent of the whole. This latter figure has been confirmed by the writer[32]. Some of the extra oxygen may be present in water of hydration, but I doubt if all of it exists in that form. Accurate oxygen determinations after heating samples at various temperatures will help to answer this question.

2. In the microexamination of heated chromium deposits it has been observed that, after heating in the range 700°–1100° C, fine spots appeared in the chromium between the major inclusions (Fig. 1)[32]. This is just what might be expected to occur if a very finely dispersed phase were present before heating. A possible reason why these spots were not observed in the present work is that a hydrochloric acid etch was used. In the writer's experiments referred to above, the etch used was that recommended by Cymboliste, namely, anodic etching in hot chromic acid.

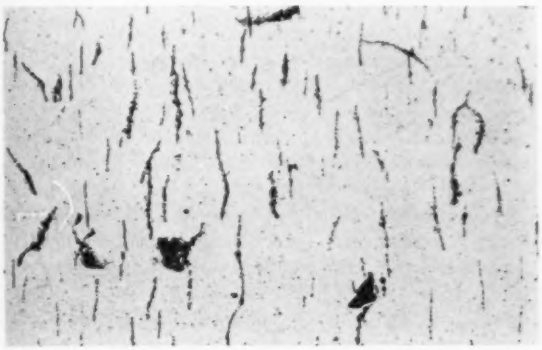

FIG. 1. Sample of Cr heated at 1100°C, etched anodically in hot chromic acid. 200×.

CLOYD A. SNAVELY AND CHARLES L. FAUST: After careful examination of the excellent photomicrographs published by Mr. Dale, it does appear that there are oxide or other particles in annealed chromium plates which are not in line with crack-filling inclusions. This is not a certainty, however, as any photomicrograph shows only one plane through the plate, and many or all of the seemingly isolated particles might be in line with inclusions on other planes. Such apparently isolated particles can also be seen in the photomicrographs presented by the authors, though less clearly.

It should be kept in mind that as-plated chromium has a finer grain size than is possible of achievement in most other metals by any known means. Therefore, an extrapolation of information gained with other metals is necessary if comparisons are to be made. The theory supported by the authors is admittedly an extrapolation, backed up by experimental evidence of recrystallization during softening. The dispersed-oxide theory is another extrapolation, based on appearance of particles of oxide at temperatures somewhat above the softening range. More experimental results to support one or the other of these theories (or both, as Mr. Dale suggests) will be most welcome.

ABNER BRENNER[33]: In their discussion of the causes of the hardness of electrodeposited chromium, the authors took the position that the hardness is mainly the result of the fine-grained structure of the deposit. They considered that their work has disproved our hypothesis that a dispersion of fine oxide particles plays a part. However, they have not quite correctly interpreted our views. In our publication[34] we reviewed the probable causes of the hardness of chromium and were fully cognizant of the importance of small grain size, but felt that the unusual hardness of chromium involved some new factors. Quoting from our paper, "The hardness of chromium is probably the result of three factors: oxide inclusions, small grain size, and internal stress, of which the first two factors are probably the most important. The effect of small grain size and internal stress in increasing the hardness of a metal is well known. . . ." On another page we stated: "The oxygen content of chromium is one of the most important factors affecting its hardness. The data show a definite trend of hardness with oxygen content, but no very precise relationship, as other factors besides oxygen content influence the hardness."

In our minds, the only matter which needs clarification is the relative importance of crystal size and of oxide dispersions in causing the abnormal hardness of chromium. We believe that the latter factor is the more important. The evidence of the recrystallization of chromium at 500°C, cited by the authors, shows that softening of chromium is accomplished by recrystallization, but it does not prove that other phenomena, such as the agglomeration of finely dispersed oxide, are not also taking place.

The authors object to the oxide theory on the basis of some of their photomicrographs, which apparently do not show the presence of agglomerated oxide in annealed chromium. Their conclusion is that the oxide particles which are visible under the microscope are the remains of the basic material which originally was present in the cracks in the chromium; and, therefore, the softening of chromium on annealing is the result of recrystallization and not of the agglomeration of finely dispersed oxide particles. However, photomicrographs taken by us and by others show that in chromium which has been annealed above 1200°C, oxide particles become visible which do not follow a crack pattern. Furthermore, the photomicrographs of the authors (Fig. 7 and 13) show a more liberal and haphazard sprinkling of particles than corresponds to the cracks in the original deposit (Fig. 1). The difficulty in observing the oxide particles in chromium annealed at lower temperatures indicates that they are of submicroscopic size, as is often true of the precipitated phase in age-hardened alloys.

However, the presence of dispersed oxide particles cannot be demonstrated by microscopic examination alone. The most reliable evidence is based on chemical examination. The material present in the cracks in chromium accounts for only about 10 per cent of the oxide present in a hard chromium deposit and, therefore, the remainder

[31] *Trans. Electrochem. Soc.*, **86**, 441 (1944).

[32] Proceedings 3rd International Conference on Electrodeposition, London (1947).

[33] National Bureau of Standards, Washington, D. C.

[34] *J. Research Nat. Bur. Standards*, **40**, 31 (1948).

must be more finely dispersed. Hence, the microscopic observation of the cracks in chromium, as annealing proceeds, has no bearing on the oxide theory. That the presence of dispersed oxide in chromium has no relation to the presence of cracks is further shown by the observation that chromium deposits which are free from cracks still contain oxide. The best evidence for the presence of agglomerated oxide in annealed chromium is the observation of Adcock, which we have confirmed, that after electrodeposited chromium has been annealed at 800°C, all the oxide dispersed in the chromium becomes insoluble in dilute hydrochloric acid and is left as a residue when the chromium is dissolved. Chromium, as deposited, does not leave a residue. More work will have to be done to determine the lowest temperature at which the agglomeration of oxide can be detected.

To clearly define the effect of recrystallization on the softening of chromium, the element of time must be studied. In how short a period of heating can recrystallization be detected? The authors heated their specimens for a period of 12 hours. However, the major part of the softening of chromium occurs within an hour or less, and, therefore, may not be attributed to recrystallization.

The authors have inferred that the volume changes which occur during the heating of chromium are related to the recrystallization. However, the volume changes which are known to occur during the recrystallization of metals are small, usually of the order of 0.1 per cent and this is insufficient to account for the changes of the order of 1 per cent or more which occur when chromium is heated. The expulsion of hydrogen, and not recrystallization, is probably responsible for a large part of the change in volume.

We also wish to comment on the manner in which the chromium specimens were annealed. This was done in air with the chromium still adhering to the basis metal. This raises the question as to whether oxygen may not have entered the cracks and deposited a coating of oxide on their surface. The heating of chromium, while still attached to a basis metal, results in the production of additional cracks in the chromium because of the initial contraction in the chromium deposit and because of the difference in the thermal expansion of the two metals. It would have been preferable to separate the chromium and heat it in sealed evacuated tubes. Specimens thus heated do not show an oxide film of $Cr_2O_3$.

CLOYD A. SNAVELY AND CHARLES L. FAUST: Dr. Brenner's comments clearly delineate the difference in opinion regarding the major factor contributing to the hardness of chromium plate.

It appears to us that even the most careful metallographic examination of a chromium-plate specimen annealed at 1200°C leaves doubt as to the nature and origin of the constituents revealed. Thus, the phase we have identified as chromium nitride has been obtained by some investigators, as shown by their photomicrographs, and thought by them to be ordinary, annealed chromium. The experiments described in the paper, involving examination of chromium plates treated through a range of temperatures, were planned to follow the changes occurring in the plate during heating so that no question remains as to the mode of formation of the final structure obtained at the highest annealing temperature. It is hoped that sufficient detail is shown in the photomicrographs to allow the reader to draw his own conclusions, independent of our discussion.

We have not been successful in producing chromium free from cracks from the chromic acid bath. True, deposits of so-called "low-contraction" chromium contain a minimum number of cracks but are cracked nevertheless. Regarding the insolubility of oxide in annealed chromium, we adhere to the interpretation of Cohen[35], who appears to have proved that the crack-filling inclusion films in chromium plate are acid soluble before heating and insoluble after heating. This does not argue for the oxide agglomeration theory.

Experiments described in the paper were planned to establish general principles. Once the principles which apply are known, the effects of given variations in experimental conditions can often be estimated. The generalizations for time-temperature relations in the annealing of metals are ably expounded elsewhere. In short, the higher the temperature, the shorter the time for recrystallization, other factors being equal.

The volume changes occurring during heating of chromium plate have been discussed in a previous paper[25]. The situation is greatly complicated by the origin of chromium plate as chromium hydride and the subsequent decomposition to body-centered cubic chromium and hydrogen. This complicated process involves a shrinkage in volume of over 15 per cent. Our interpretation is that this entire volume change is not completed until the metal is heated enough to relieve all internal stress and allow the chromium to assume its natural lattice parameter. The expulsion of hydrogen is a concurrent phenomenon and we do not care to comment on its relative importance at this time.

Careful inspection of the photomicrographs shows that most of the cracks in chromium plate do not communicate with the atmosphere. Cracks which form during heating and cooling of chromium plate on steel are always easily distinguishable from those caused by the aforementioned decomposition of chromium hydride.

PIERRE A. JACQUET[36] AND ADRIENNE R. WEILL[36]: In a recent paper[37], we investigated the connection between the surface character of a steel base and the structure of a chromium layer plated on it. Some of our results confirm those of C. A. Snavely and C. L. Faust.

The starting point of our work was the following: thick chromium plate on an electrolytically polished steel base, treated by the Hispano-Suiza electrolytic superfinishing process[38], is smoother, brighter, and probably adheres better than on the same steel base mechanically polished without further preparation. From these observations, practical developments are now in progress in France.

[35] Reference 6 in the paper.

[36] Ingénieur Contractuel des Constructions et Armes Navales, Paris, France.

[37] "Chrome Dur," p. 4, Fascicule 1949 du Centre du Chrome Dur, Paris (1949).

[38] R. MONDON, *Tech. moderne*, **38**, 281 (1946); **39**, 17 (1947); *Tech. Sci. Aéronautiques*, No. 4, 186 (1949).

Layers 6 to 40 microns thick deposited on a Ni-Cr-Mo steel, either mechanically or electrolytically polished, were examined under the microscope and by x-ray diffraction.

*Results of Micrographic Examinations*

External surfaces and sections of deposits were examined. In the case of sections, electrolytic polishing in an acetoperchloric acid mixture allows simultaneous polishing of steel and chromium[39]. Observations of sections show the link between the origin of the cracks and the defects of the base surface. These defects are either microgeometric (peaks and troughs) or structural. The electrolytic treatment suppresses microgeometric defects; this explains the reduced number of cracks observed in that case. Through the same finishing process some structural inhomogeneities also vanish, but the remaining ones are nucleating cracks. Fig. 1 and 2 show the typical appearance produced by the two different states of the steel base surface. A remarkable feature is the branching of the cracks throughout the chromium deposit which occurs when the steel base is mechanically polished, whereas in case of subsequent electrolytic treatment of the base only single cracks appear through the chromium layer. The reduced number of cracks explains the improved protection of steel against corrosion, as recently observed by Eilender and co-workers[40].

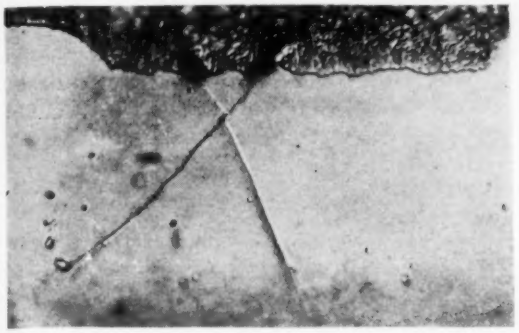

FIG. 1. Photomicrograph showing cross section of a 13-micron-thick chromium layer plated on a mechanically finished steel base. Vertical scale: 10 mm = 3$\mu$. Horizontal scale: 10 mm = 9$\mu$.

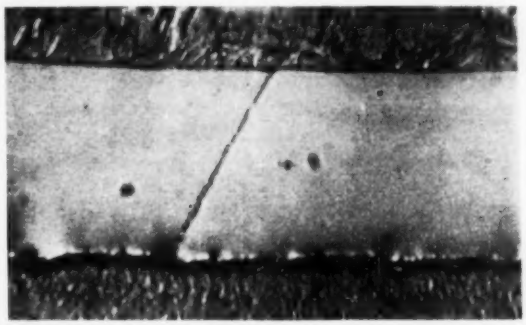

FIG. 2. Photomicrograph showing cross section of a 6-micron-thick chromium layer plated on an electrolytically polished steel base. Vertical scale: 10 mm = 2$\mu$. Horizontal scale: 10 mm = 4.5$\mu$.

Examination of the external surface of the plating after electrolytic polishing and anodic attack in 10 per cent chromic acid does not show any sign of grains on a microscopic scale. Nevertheless, the etching does not give identical patterns for the two types of plating (Fig. 3 and 4).

FIG. 3. Photomicrograph obtained after electrolytic polishing and anodic attack with 10 per cent chromic acid. Numerous cracks on the surface of Fig. 1 chromium deposit.

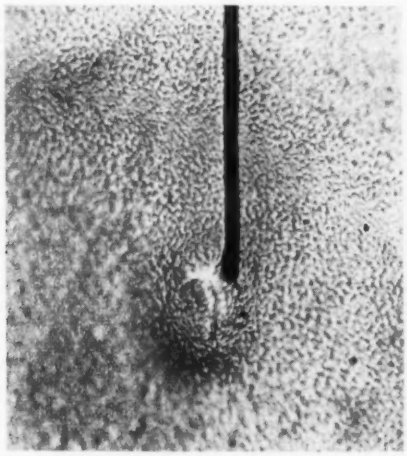

FIG. 4. Photomicrograph obtained after electrolytic polishing and anodic attack with 10 per cent chromic acid. Rare case of a crack seen on the surface of a 12-micron-thick layer plated on an electrolytically polished steel base.

*X-Ray Examinations*

Debye-Scherrer diagrams were obtained both by back-reflection and by grazing angle, using unfiltered chromium radiation. It can be seen, though the lines are broad, that

[39] P. A. JACQUET, *Compt. rend.*, **227**, 556 (1948); *Rev. mét.*, **46**, 214 (1949).

[40] *Metalloberfläche*, **3**, 32 (1949).

for the same thickness of deposit (12 microns), the parameter of both chromium and iron remains unchanged when the base is electrolytically polished (Fig. 5), whereas on a mechanically prepared steel an expansion of both lattices occurs (Fig. 6), roughly estimated as 2.5 to 3 per cent for iron and 1.5 to 2 per cent for chromium.

The lowest order Debye-Scherrer ring shows preferred orientation of the submicroscopic crystallites. This effect

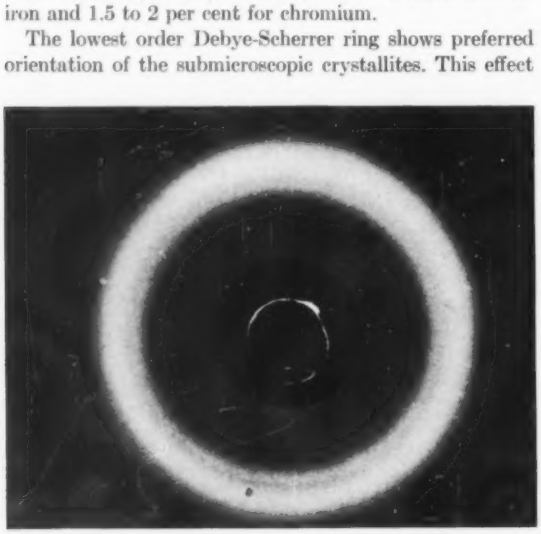

FIG. 5. Back reflection x-ray photograph of chromium deposits (unfiltered Cr radiation) on electrolytically polished steel base. Note the sharp gap between the inner steel ring and the outer chromium ring.

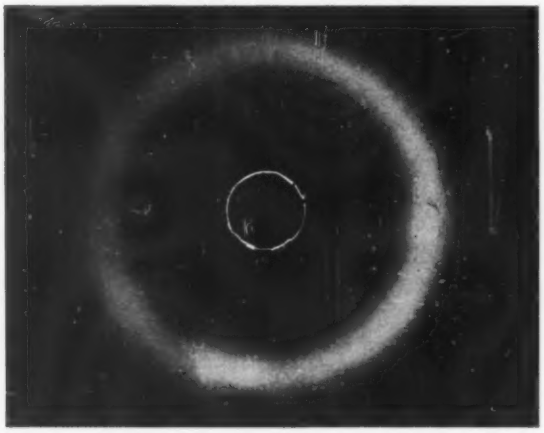

FIG. 6. Back reflection x-ray photograph of chromium deposits (unfiltered Cr radiation) on mechanically polished steel base. The two rings are much closer to each other.

is much stronger when the steel base has been electrolytically polished (Fig. 7 and 8); it is very strong when the chromium layer is only 8 microns thick, and becomes still stronger with increasing thickness of the deposit (Fig. 7*a* and 7*b*).

For a specimen polished in a phosphosulfuric acid bath under less favorable conditions to the production of a well-polished surface, intermediate results are obtained regarding the number of cracks as well as the preferred orientation (Fig. 9). For this specimen, however, no expansion of the iron or chromium lattice occurs, similar to a perfectly polished steel base.

*Conclusions*

It seems that smoothness of the steel base on a microscopic scale is necessary not only to reduce the number of cracks in the chromium deposit, but also to favor estab-

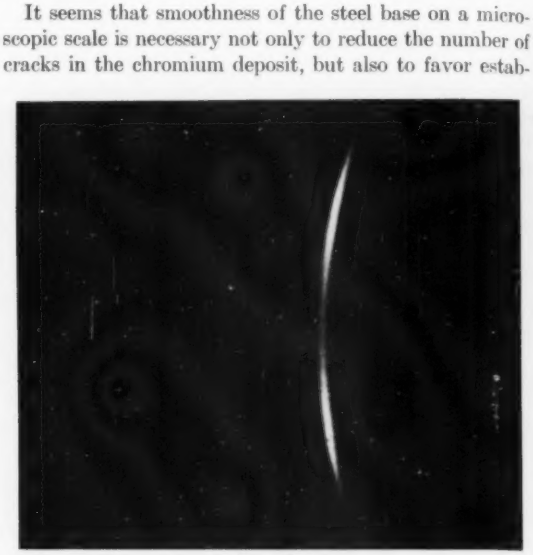

FIG. 7*a*

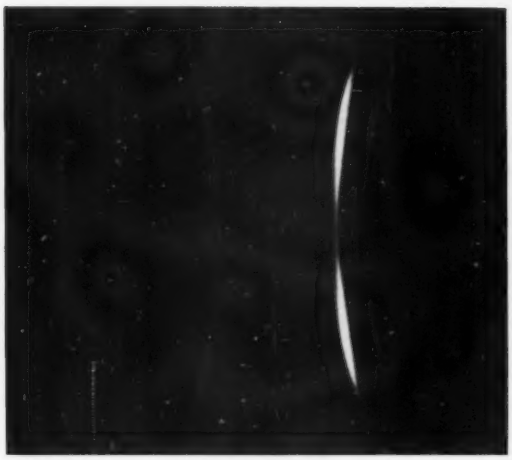

FIG. 7*b*

FIG. 7. Preferred orientation of chromium deposits, grazing angle x-ray photographs (unfiltered Cr radiation) on electrolytically polished steel base. (*a*) Strong orientation, thickness of Cr deposit: 8$\mu$. (*b*) Stronger orientation, thickness of Cr deposit: 12$\mu$.

lishing strong preferred orientation. On the other hand, the structural character of the base surface is predominant in maintaining lattice spacings of chromium and iron at their normal value. The structure of the steel surface presumably plays a part in cathodic hydrogen formation, absorption, and diffusion.

We assumed that thick chromium deposits possess two kinds of cracks: (1) those originating on micro-peaks and

structural defects of the steel surface, and (2) those due to internal stresses which develop in the layer.

Hume-Rothery and Wyllie[41] found that internal stresses are related to preferred orientation. When the crystallites are strongly oriented, internal stresses are less intense and vice versa. Therefore, the second type of cracks ought to be less numerous in a deposit plated on a very smooth

FIG. 8. Preferred orientation of chromium deposits, grazing angle x-ray photograph (unfiltered Cr radiation) on mechanically polished steel base. Not as much orientation as shown by Fig. 7.

FIG. 9. Preferred orientation of chromium deposits, grazing angle x-ray photograph (unfiltered Cr radiation) on imperfect electrolytically polished steel base. Not as much orientation as shown by Fig. 7.

surface. The same explanation accounts for the two patterns of cracks (either single or multiple) corresponding respectively to the two types of steel surface finishing.

The last point is connected with Rowe and Dance's observations[42]. According to the authors, fatigue cracks in a chromium-plated steel specimen appear in the steel at the bottom of the chromium cracks. It is clear from our results that the chromium cracks being nucleated by microgeometric roughness, or by structural inhomogeneity of the steel surface, a sort of notch effect might be present at these weak points.

[41] *Proc. Roy. Soc. London*, **A181,** 331 (1943).
[42] *Metal Progress*, **53,** 537 (1948).

## ANODE EFFECT IN AQUEOUS ELECTROLYSIS

**Herbert H. Kellogg** (pp. 133–142)

R. W. HERZER[43]: The author's experiments indicate that the anode effect in aqueous $H_2SO_4$ takes place when passage of current has heated the solution around the anode to a definite temperature. After the anode effect has started, the temperature of the anode (now enveloped in a vapor film) rises rapidly. It would be interesting to know whether, on cooling the apparatus, the anode effect is destroyed at exactly the same anode temperature at which the effect took place during the process of heating.

HERBERT. H. KELLOGG: In answer to Mr. Herzer's question, the anode temperature, the instant before anode effect starts, is 100°C (the boiling point of the electrolyte). The instant after anode effect has begun the anode temperature reaches a value well above 100°C. The same sequence is followed in reverse during the destruction of anode effect. Although exact measurements are difficult to make in this change-over region, I believe that the anode temperature just after anode effect has begun is the same as the temperature just before anode effect is destroyed.

DENNIS R. TURNER[44]: From what you have said, would it not be advisable to use a constant voltage power source to determine the exact potential of transition to the anode-effect region?

This may have already occurred to you. The glow discharges observed in the anodic and cathodic effects could be analyzed with a spectrograph to determine the nature of the material involved.

HERBERT H. KELLOGG: Mr. Turner's suggestion of the use of a constant-voltage power source, and spectrographic analyses of the anode glow are both excellent ideas, which also occurred to the author but were not acted upon.

H. H. UHLIG[45]: The electrical conductivity of thin films is apparently much greater than one calculates from data on dielectric breakdown. It is reported, for example, that thin films of oil are good electronic conductors when approaching a thickness of 10 microns or less. This fact is referred to in a survey by J. C. Henniker[46].

HERBERT H. KELLOGG: I want to thank Professor Uhlig for the reference on the conductivity of thin films. I believe that the major unsolved problem in connection with the anode effect is the nature of the electrical conduction in thin films of the electrolyte and through the gaseous film.

A. C. LOONAM[47]: Professor Kellogg is to be complimented for showing that the anode effect occurs in aqueous

[43] Aluminum Company of Canada, Montreal, Canada.
[44] Westinghouse Research Laboratories, East Pittsburgh, Pennsylvania.
[45] Department of Metallurgy, Massachusetts Institute of Technology, Cambridge, Massachusetts.
[46] *Revs. Modern Phys.*, **21,** 322 (1949).
[47] 70 East 45th Street, New York, New York.

solutions, thereby making its study possible at more convenient temperatures. He ascribes it principally to the so-called spheroidal condition, the effect observed when spitting on a hot stove. I wonder whether Professor Kellogg has tried the effects of adding to his solutions wetting agents and materials, such as flotation reagents, which increase the contact angle between water and metallic surfaces.

HERBERT H. KELLOGG: In answer to Mr. Loonam's question, it was my original plan to study in detail the effect of the wettability of the anode surface on anode effect. However, I was unable to find a conditioning agent which would render platinum nonwettable in strong acid or alkaline solution under the severe conditions existing in this experiment. I believe that nonwetting of the anode by the electrolyte will modify the anode effect. I hope to be able to show this in future work on anode effect in molten electrolysis."

## AN X-RAY METHOD FOR DETERMINING TIN COATING THICKNESS ON STEEL

**H. F. Beeghly** (pp. 152-157)

E. E. WICKER[18] AND G. E. PELLISSIER[19]: For several years, we have been interested in securing a rapid, accurate, nondestructive, physical method for measuring the coating thickness of tin on our tin plate product. The chemical and electrochemical stripping methods which have been in use up to this time have been destructive, time-consuming, and cannot easily be applied to production control on continuous tinning lines. None of the magnetic methods which has been conceived to date is sensitive enough to measure tin coatings of the thickness existing on commercial product. Following the fundamental work of H. Friedman and L. S. Birks, R. B. Gray, and A. Eisenstein on the x-ray diffraction measurement of thin films of one metal on another, referred to in the present paper, extensive work was carried out by D. S. Miller and K. G. Carroll at the United States Steel Corporation of Delaware Research Laboratory, Kearny, New Jersey, to investigate the applicability of the method to the measurement of tin coatings on steel. Several undesirable features inherent in the method were discovered which indicated that the method could not be made practical for control purposes. It was found that the coating thickness determinations were seriously affected by extraneous variables such as coarse grain size and/or preferred orientation, both in the tin coating and steel base, and interfering diffraction lines from Fe-Sn intermetallic compounds present in the alloy layer. Furthermore, the method was limited to the measurement of a very small area, and required extreme positional stability of the counting tube in order to insure measurement of the intensity maxima of the sharp diffraction peaks.

At this same time, it was found that the intensity of background radiation, which was believed to consist essentially of fluorescent radiation from the iron base, varied systematically with the coating thickness due to increased absorption with increasing thickness of the tin coating. A systematic study of this phenomenon was conducted at the United States Steel Research Laboratory, to determine whether this fluorescent method would be free of the objectionable features encountered in the diffraction method. This work demonstrated that the logarithm of the intensity of fluorescent radiation from the tin plate varied linearly with coating thickness, under the condition where there is no appreciable absorption of the primary x-ray beam by the coating, completely in conformity with the absorption theory. Furthermore, it was concluded that this fluorescent method is an accurate, reliable means of measuring the tin coating thickness of tin plate, and is adaptable to commercial control.

We have incorporated this fluorescence principle in a gauge designed for mill control purposes. The gauge consists mainly of a high-intensity x-ray tube, collimating systems, Geiger counter tube, and auxiliary circuits; the components are arranged on a rugged support in a fixed geometry, such that the angle between the specimen face and the axis of the counting tube provides optimum gauging sensitivity. The collimation systems are designed so that a four-square-inch area of tin plate is irradiated by the x-ray tube and is observed by the counting tube; this area of sample is customarily prescribed by tin plate consumers, and is used in the conventional chemical and electrochemical stripping methods. This area of a single measurement is large enough to average out the small-scale irregularities in coating thickness which exist on hot-dipped tin plate; these are of little practical importance. Although a single unit measures coating weight on only one side of tin plate at a time, two units can be employed to measure simultaneously the coating weight on both sides. The gauge may be applied equally well to static measurements on sheets, or to continuous measurements on moving strip. The range of tin coating weight which can be measured accurately extends from 0.0 to 2.80 lb/BB. The accuracy of measurement is ±2 per cent of the value obtained by the best chemical method, for an x-ray counting interval of 30 seconds; better accuracy can be achieved with longer counting times, since according to the statistical relation, the standard deviation of counting is equal to the square root of the total number of counts. It has been determined conclusively that the gauge measures total weight of tin in the coating, irrespective of the amount combined with iron as intermetallic compounds in the alloy layer. This is particularly significant for hot-dipped tin plate in which an appreciable portion of the total tin may exist in the combined form.

In several important respects, this gauge differs from the one described by the author. It is desirable that the primary x-ray beam be of sufficient intensity to excite strong fluorescence in the steel base, in order to provide high counting rates; this means that better accuracy can be achieved in a given time, or that for a prescribed accuracy the counting interval can be considerably shortened. We have accomplished this by utilizing a high-intensity tungsten-target x-ray tube. Although copper K-alpha radiation, such as the author used, excites fluorescent radiation in iron efficiently, the lower power-loading of the

[18] Carnegie-Illinois Steel Corporation Research Laboratory, Pittsburgh, Pennsylvania.

[19] Jones & Laughlin Steel Corporation, Pittsburgh, Pennsylvania.

target permitted in a copper tube adversely affects the maximum attainable intensity. Furthermore, we believe that the use of copper radiation is undesirable because of the considerable absorption of the primary beam in the tin coating upon entering the sample; the mass absorption coefficient of tin for copper K-alpha radiation is 265 cm² per gram, as compared to a mass absorption coefficient of 457 cm² per gram for the absorption of iron K-alpha radiation by tin. This means that the primary copper radiation is absorbed nearly as strongly upon entering the sample as the fluorescent iron radiation is absorbed by the tin upon emerging from the sample. This further decreases the amount of primary radiation available for the excitation of fluorescence in the steel.

In establishing the geometry of our gauge, we found that a small angle between the tin plate surface and the axis of the counter tube was necessary to obtain optimum sensitivity of measurement; this is contrary to the general recommendation made by the author. It is evident from the geometry of measurement, that the absorption for a coating of given thickness varies inversely as the size of the angle between the specimen surface and the axis of the counter. It is our experience that the surface imperfections normally encountered in commercial tin plate have only a minor effect on the measurement as compared to the loss of sensitivity which results from the use of a large angle.

We believe that the use of a rather large area of measurement, on the order of four square inches, is preferable to the use of a smaller area for two reasons; first, the measurement is thereby made comparable to those of the conventional chemical methods, and second, this average measurement smooths out local irregularities which are of no practical significance and yields a more useful result. We suspect that these local variations in coating thickness may explain the discrepancies between results of a standard method and of the x-ray method on hot-dipped tin plate reported in Table II of the paper.

In order to check on the stability of the calibration curve, and to permit adequate standardization, we feel that it is necessary to maintain a series of tin plate standards of various known coating weights, rather than to rely on a bare steel, zero-coating-weight standard.

It occurs to us that the semilogarithmic relationship plotted in Fig. 5 of the paper is inverted; according to the absorption equation, the logarithm of the transmitted intensity is a linear function of coating thickness, while the author has plotted logarithm of thickness as a linear function of transmitted intensity.

Patent coverage is being sought on the construction and operation of this fluorescent method of determining coating thickness.

K. G. Carroll[50]: The gauging of tin coatings on steel has been a perennial problem in the steel industry, and until recently the problem has defied approach by physical measurements.

Work done in this laboratory extending over several years is in general agreement with results of the author. We too have found that a diffraction method, depending upon absorption by the tin coating of an iron diffraction line, is not amenable to accurate gauging and that a method making use of fluorescence in the backing sheet is suitable for an accurate instrument, if sufficient precautions are taken. An arrangement used by the author, with a copper target source, has been found to be deficient for the heavier hot-dipped coatings, presumably because of the greater proportion of scattered copper characteristic radiation. It has been found advantageous to use radiation from an x-ray source more intense than that provided in the Philips spectrometer, and to avoid disturbing effects of tin fluorescence by using low tube voltages. Since the author is detecting iron characteristic radiation, it is difficult to understand why he used a nickel filter.

In order better to emphasize the fundamental absorption effect upon which thickness measurement depends, it would be preferable to reverse the scales on the author's Fig. 5, plotting logarithms of intensity against coating thickness; the resulting slope would then yield an effective absorption coefficient. For the data shown in Fig. 5, one finds a slope only 60 per cent of the theoretical absorption of incoming copper K-alpha radiation and outgoing iron K-alpha radiation. This indicates the presence of harder radiations, and suggests that disturbing influences are present which would tend to upset the linearity of the calibration curve. It has been our experience that a curve obtained under the conditions of the author's Fig. 5 fails to cover a wider range of coating thicknesses. Perhaps some of the scatter in experimental data on hot-dipped coatings (Table II) can be attributed to this cause, rather than to real variations in coating weight.

The author has reported only the results obtained using an arrangement in which the angle of incidence is equal to angle of emergence. We have found that it is not necessary to keep this condition for the purpose of measuring thickness and that greater flexibility and accuracy may be obtained by deviating from spectrometer geometry. Thus the apparatus may be arranged either for maximum sensitivity or maximum range of coating thicknesses by appropriate positioning of the specimens; by a suitable choice of angles it is possible to cover a 10 to 1 range in intensity with satisfactory accuracy for tin plate.

H. F. Beeghly: It is gratifying that Messrs. Wicker, Pellissier, and Carroll have reached conclusions which substantiate our work, namely that the variation of the secondary x-radiation from a steel base coated with tin is in accordance with the thickness of the tin coating; and that this variation can be made the basis for a dependable and rapid nondestructive method for measuring and controlling the thickness of tin applied to steel.

Messrs. Wicker and Pellissier raised a question about the advisability of measuring the thickness of tin on a small area. In our paper, the utilization of a commercial x-ray spectrometer for laboratory work was described. This apparatus is very satisfactory for measuring the coating thickness on small areas as, for example, on different portions of fabricated articles and for corrosion studies. In general, it is useful where the coating thickness of some small, specific area must be determined and constitutes the first satisfactory nondestructive method for this purpose. It thus provides a new tool for research on tin plate. At the same time, as was recognized by Messrs. Wicker and

[50] Research Laboratory, U. S. Steel Corporation, Kearny, New Jersey.

Pellissier, the x-ray method provides a valuable replacement for the conventional, destructive chemical method. For such applications, the conventional spectrometer may be used or a special unit may be constructed with which the average thickness of some larger predetermined area can be measured. The particular job will determine which type would be more valuable. A large area of measurement, as advocated by Messrs. Wicker and Pellissier, has a distinct disadvantage for some applications but is quite useful for others.

For the continuous indication and control of tin coating weights on the electrotinning line, however, a unit designed for this specific application is essential. In designing such a unit it is necessary to take into consideration the required speed of response and rugged nature of the service under plant conditions. Our experience has shown that use of copper K radiation in conjunction with a suitable circuit for measurement of the fluorescent radiation transmitted by the coating provides adequate intensity for this application and avoids the design difficulties inherent with use of harder, high intensity primary radiation and the Geiger counter method of radiation measurement suggested by Messrs. Wicker, Pellissier, and Carroll.

As indicated in Fig. 1 of my paper, the angle between the incident primary beam and the coating and between the axis of the pick-up tube and the coating may be varied and is not necessarily the same for all materials or operating conditions. This concurs with the suggestion of Dr. Carroll that the apparatus may be arranged either for maximum sensitivity or maximum range of coating thickness.

We prefer use of bare steel as a primary standard with use of tin coated coupons as secondary standards as indicated in our paper rather than to confine ourselves to a series of tin plate standards.

The relationship plotted in Fig. 5 of the paper is an empirical one and was plotted in inverted form in order that it not be confused with a plot of the absorption equation which applies strictly only for monochromatic radiation—a condition that is not necessarily true for this x-ray method.

Dr. Carroll wonders why a nickel filter was used before the counter tube. A filter is not an essential feature of the method; its principal function was to protect the counter tube from light.

The novel features of the method described in the paper are covered by United States Patent 2,521,772 assigned to Jones & Laughlin Steel Corporation.

## REACTIONS OF β-PINENE, III. ELECTROLYTIC OXIDATION

**James B. Redd and J. Erskine Hawkins** (pp. 178–182)

A. E. Remick[51]: Dr. Hawkins, in relation to your assertion that the chemical oxidation of β-pinene gave different products from electrochemical oxidation, I would like to know what oxidizing agents were used.

J. Erskine Hawkins: Chemical oxidizing agents which have been used include potassium permanganate, chromic acid, selenium dioxide, lead dioxide, oxygen, nitric acid, and others.

A. E. Remick: These are all two- or three-electron reagents. I would like to suggest that it might be found that one-electron oxidizing agents give the same products as obtained by electrochemical oxidation.

J. Erskine Hawkins: Thank you for the suggestion.

[51] Wayne University, Detroit, Michigan.